Mechanics of antigen extraction by B cells

Anita Kumari

UNIVERSITE PARIS DESCARTES

Spécialité Biologie interdisciplinaire
Ecole doctorale Frontières du Vivant

THESE DE DOCTORAT

Soutenue le 11Octobre 2017 par

Anita KUMARI

Pour obtenir le titre de
DOCTEUR EN SCIENCES
DE L'UNIVERSITE PARIS DESCARTES

Mechanics of antigen extraction by B cells

Mécanique de l'extraction de l'antigène par les cellules B

Jury :

Pavel TOLAR	Rapporteur
Pierre-Henri PUECH	Rapporteur
Claire HIVROZ	Examinateur
Martial BALLAND	Examinateur
Paolo PIEROBON	Examinateur
Ana-Maria LENNON DUMENIL	Directeur de thèse

To Vijay,

To Arun,

To my parents,

Acknowledgements

To jury members

First of all, my sincere thanks to the jury members who kindly accepted my invitation to evaluate my thesis work. Thanks to Dr Pavel Tolar and Dr Pierre-henri Puech for their time spent in reading my manuscript. Sincere thanks to Dr Claire Hivroz and Dr Martial Balland for reviewing my thesis work . Finally thank you all for being with me at my thesis defense and for the fine discussion we will have together.

To my incredible two bosses

Thank you Ana and Paolo for giving me the opportunity to work with you. Ana, thank you for always pushing me forward. I have learnt a lot from you in past 4 years, not only scientifically but also personally. Discussions with you have always been very inspiring and made us see things clearly. Paolo my "actual boss", we have walked this difficult yet adventures path of PhD together with our share of "the firsts". Me being your first PhD student, we have learned to understand each other in the process. You have been a cool boss and I learnt being always curious from you. Because of you I started to like physics (still scared of those equations though). In the end it comes down to only one word for both of you …..THANK you.

To STRAP team

I would like to thank the entire Lennon team for many exchanges, discussions, and hard work that have made my stay in the lab so enriching. I especially thank Pablo SAEZ, who taught me almost everything in the lab. Pablo I met you as a colleague, least I knew you would become a friend for life. Thank you would be an understatement on how you have helped me in not only my professional life but also listening to my endless blabbering. Thank you Danielle Lankar for helping me in my initial years in developing experiments and making me understands the infamous "Bilan", thank you for your valuable advices and always being so compassionate and available for doing the SEM experiments. Thank you to Isa, Pablo Vargas, Dorian, Marine, Odile, Violaine , Doriane, Zahraa, Camille, Margot, Judith, and Graciela for your unfailing support, for your availability, your advice, thank you for having been there in moments of doubt to re-

motivate me. I would like to specially thank Hélène for helping me towards the end in the writing phase; you are a saviour, thank you so much. Special mention to Andrea for listening to me so patiently throughout the last few months, in you I found another Chilean friend, thank you for being there in moment of despair. How can I not mention the "Buddha" Mathieu MAURIN for making me laugh all these years? Thank you Mathieu for just being you and making me look at the bigger picture always. Your advices have always been very helpful and you know it ;), thank you for everything.

To 5th Floor, U932, CRI

A big thank you to all the smiling people on the floor who made these past years so much fun. I would like to thank each one of you individually for creating a very nice environment on the floor. Special thanks to Matteo, Ester, FX, Ahmed, Cecile and rest of the team member. This would not be complete without the support of Silvia, who has been with me in thick and thins in these past years, thank you sister for just being yourself☺. I would like to add my sincere acknowledgements for the whole unit U932 for the annual feedback in the unit meeting and constantly creating a stimulating environment. Last but not at all the least I would like to thank Paris Descartes and Labex for funding me for my first 3 and last year respectively. I wouldn't be here without being associated to CRI so a big thank you to my wonderful doctoral school.

To my family and friends

I wouldn't have imagined being at this point in my life without the constant support of my family and my in-laws. I would like to thank my parents for always encouraging me to follow my dreams with special mention to my elder brother Vijay, whatever I am today is because of you bhai and forever I shall remain indebted to you. I would like to thank my sister Jyoti for her selfless love and for always believing in me. I would not be writing this acknowledgement without the support of my two pillars of strength Sandy and Anuj, thank you everyone…..cheers to life.

I came to France in 2011 and since than I made a family away from home here, who has made it living in Paris so much more worthwhile. Khushbu and Dev has not only made me feel at home but also always have given me the best advice be it personal or professional, you have always challenged me to become a better version of myself,

thank you guys for everything. Thank you Pooja and Sanjog for always being so positive and giving the best advices and making it all look so easy, you guys are an inspiration, thank you. I would like to mention my friends back home in India for always giving me courage in least expected times, thank you Sudi, Annu and Chaitanya, you guys are precious. In the end, I would like to thank you Arun for being the coolest husband ever and encouraging me to do this PhD at the first place and being so helpful throughout the journey of not only this thesis but life. You are the best possible thing happened to me, I love you.

Anita KUMARI

Abstract

B cells produce antibodies and are therefore essential effectors of adaptive immunity. *In vivo*, their activation is mostly triggered by the engagement of their B cell receptor (BCR) with antigens exposed at the surface of neighboring antigen presenting cells. This leads to formation of an immune synapse that coordinates the signaling and cytoskeleton rearrangement events that are essential for B cells to extract and process antigens. Two models have been proposed for extraction of surface-tethered antigens by B cells: (1) Membrane spreading followed by cell contraction and (2) direct mechanical pulling on BCR-antigen molecular complexes. According to the first model, specific recognition by the BCR of antigens bound to supported lipid bilayer leads to contraction of the actin cytoskeleton, transporting BCR-bound antigens towards the centre of the synapse. The second model arose from observations made using atomic force microscopy of antigens tethered to plasma membrane sheets, which suggest the actin based motor protein myosin II actively pulls on BCR-antigen complexes in clathrin coated pits. It has also been shown that antigens can be internalized via protease secretion at the synapse, but this pathway only activate if the mechanical pathway fails, typically on non-deformable antigen coated substrates.

In this study, we developed a method for extracting force patterns using antigen-coated substrate deformations for direct force visualization (traction force microscopy, TFM). We demonstrate the existence of global contractile forces at the periphery of the synapse and local pulling forces at its center. Peripheral contractile forces were dependent on the centripetal organization of myosin II, whereas central pulling forces were generated by F-actin protrusions formed in a myosin II-dependent manner. We observed collective pulsatile contractions, potentially underlying the organization of actin structures in the center of the synapse through intermittent myosin II activity. Our results thus propose a unified model for antigen extraction by B cells where myosin II is needed for global cell contractility as well as for antigen internalization through local regulation of actin dynamics. Importantly, the methods and model proposed here may be generalizable to other systems involving surface-tethered molecules, as this model might concern many endocytic processes *in vivo*.

Key words: B cells, Immune synapse, traction force, antigen extraction

Résume

Les lymphocytes B sont un des éléments essentiels de l'immunité adaptative de par leur fonction de production d'anticorps. In vivo, leur activation est principalement déclenchée par l'engagement de leur récepteur BCR (B cell receptor) associé à des antigènes présents à la surface des cellules voisines. Cette interaction conduit à la formation d'une synapse immunitaire qui coordonne les événements de réorganisation de la signalisation et du cytosquelette qui sont essentiels pour l'extraction et le traitement des antigènes par les lymphocytes B. Deux modèles ont été proposés pour l'extraction d'antigènes : (1) L'étalement des membranes suivie d'une contraction cellulaire et (2) l'extraction mécanique directe des complexes moléculaires BCR-antigène. Selon le premier modèle, la reconnaissance spécifique par le BCR des antigènes liés à la bicouche lipidique, conduit à la contraction du cytosquelette d'actine transportant les antigènes associés au BCR vers le centre de la synapse. Le deuxième modèle résulte d'observations effectuées à l'aide d'un microscope à force atomique, d'antigènes associés à la membrane plasmatique suggérant que la protéine motrice myosine II tire activement sur des complexes BCR-antigène dans des puits enduits de clathrine. Il a également été montré que les antigènes peuvent être internalisés via la sécrétion de protéase à la synapse, mais cette voie ne s'active que si la voie mécanique échoue, typiquement sur des substrats non déformables enduits d'antigènes.

Dans cette étude, nous avons développé une méthode pour extraire des modèles de force en utilisant des substrats déformables enduits d'antigènes pour la visualisation directe de la force (microscopie de force de traction, TFM). Nous démontrons l'existence de forces contractiles globales à la périphérie de la synapse et des forces d'attraction locales au centre. Les forces contractiles périphériques dépendent de l'organisation centripète de la myosine II, alors que les forces de traction centrales sont générées par des protubérances de F-actine formées de manière dépendante à la myosine II. Nous avons observé des contractions pulsatives et collectives, qui mettent potentiellement en évidence l'organisation de structures d'actine au centre de la

synapse par l'intermédiaire de l'activité de la myosine II par intermittence. Nos résultats proposent donc un modèle unifié pour l'extraction de l'antigène par les lymphocytes B, où la myosine II est nécessaire pour la contraction cellulaire globale ainsi que pour l'internalisation de l'antigène par la régulation locale de la dynamique de l'actine. Il est important de noter que les méthodes et le modèle proposés ici peuvent être généralisés à d'autres systèmes impliquant l'association de molécules associé à une surface pouvant concerner de nombreux processus d'endocytose in vivo.

Mots clés: cellules B, synapse immunitaire, force de traction, extraction antigénique

Table of contents

List of abbreviations

APCs	antigen-presenting cells
AFM	atomic force microscopy
Bcl-6	B-cell lymphoma 6 protein
BCR	B cell antigen receptor
Btk	Bruton's tyrosine kinase
BLNK	B cell linker protein
BFP	Biomembrane force protein
BSA	Bovine serum albumin
CD4/8/40/169	cluster of differentiation 4/8/40/169
Cdc42	cell division control protein 42
CLPs	common lymphoid progenotors
CCPs	clathrin coated pits
DAG	diacylglycerol
DNA	deoxyribonucleic acid
Erk1/2	extracellular signal-regulated kinases 1/2
ERM	ezrin, radixin, moesin
ELC	essential light chain
F-actin	filamentous actin
G-actin	globular actin
GCs	germinal centers
GFP	green fluorescent protein
GTP(ase)	guanosine triphosphate(ase)
HEL	
HSCs	

ICAM-1	intracellular adhesion molecule-1
Ig(H/L)	immunoglobulin (heavy/light chain)
Ii	invariant chain
IP3	inositol-1,4,5-triphosphate
ITAM	immunoreceptor tyrosine-based activation motif
KO	knock out
LAMP-1	lysosomal-associated membrane protein 1
LFA-1	lymphocyte function-associated antigen-1
MHC-I/II	class I/II major histocompatibility complex
MTOC	microtubule-organizing center
OVA	ovalbumin
PAA	poly acryl amide
PAMPs	pathogen-associated molecular patterns
PAX5	paired box 5
pH	power of hydrogen
PI3K	phosphoinositide 3-kinase
PIP2	phosphatidylinositol(4,5)-bisphosphate
PRRs	pattern recognition receptors
(m/si)RNA	(messenger/small interfering) ribonucleic acid
SCS	sub-capsular sinus
SHM	somatic hypermutation
(c/p/d)SMAC	(central/peripheral/distal) supramolecular activation cluster
hen egg lysozyme	TCR
hematopoietic stem cells	Tfh

V(D)J	follicular helper T cells
WASH	variable (diversity) joining
WT	Wiskott–Aldrich syndrome protein
WAVE	Wild type
	Wiskott-Aldrich syndrome protein family member 1
T cell receptor	

Figure Index

Introduction

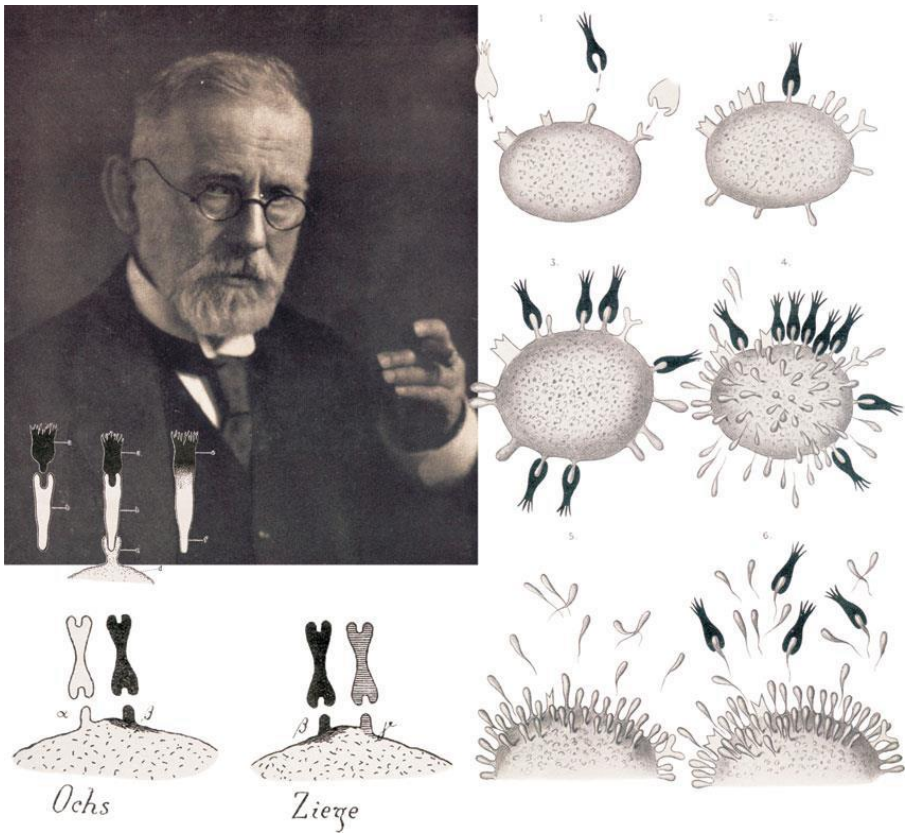

Figure 1 Ehlrlich's side-chain theory

Paul Ehlrich (1854 -1915), drawings of the formation and effector functions of antibodies according to the side-chain theory. Reproduced from (Kaufmann, 2008).

The immune system:

The system that our body has evolved to fight against microbial components is called immunity. History of immunology (the study of immunity) goes back to the 15th century when the first inoculation of smallpox was performed in China by Wan Quan, the paediatrician of Ming's family. Since then several factual observations show that exposure to a pathogen could lead to immunization. However, major advances were only made in the 19th century with Elie Metchnikoff and Paul Ehrlich explaining the mechanisms leading to efficient immune responses. Metchnikoff first demonstrated the process of phagocytosis by punching the small thorns in the starfish larvae and finding unusual white cells surrounding the thorns. He proposed the hypothesis that this could be the process by which bacteria were attacked and killed by white blood cells. At the same time, Paul Ehrlich was developing side chain theory, where he postulated that cell protoplasm contains special structures with chemical side chains to which toxins bind **(Figure 1).** New side chains replace old side chains in case the organism survives injury caused by toxins. Elie Metchnikoff and Paul Ehrlich shared the Nobel Prize in Physiology for their "work on immunity" in 1908 (Kaufmann, 2008). They had basically discovered the innate and adaptive immune systems.

I. **Innate immune system:** The innate immune system refers to nonspecific defence mechanisms that come into play immediately or within hours of microbial infection. These mechanisms include barriers such as skin and mucosa, chemical compounds circulating in the blood such as complement system molecules and phagocytes and innate lymphocytes that are recognized microbes, a process known as innate sensing. The innate immune response is triggered by the recognition of the chemical properties of antigens. Neutrophils (phagocytes) are a good example of innate immune system cells. Whereas, macrophages and dendritic cells work at the frontier between innate and adaptive immunity.

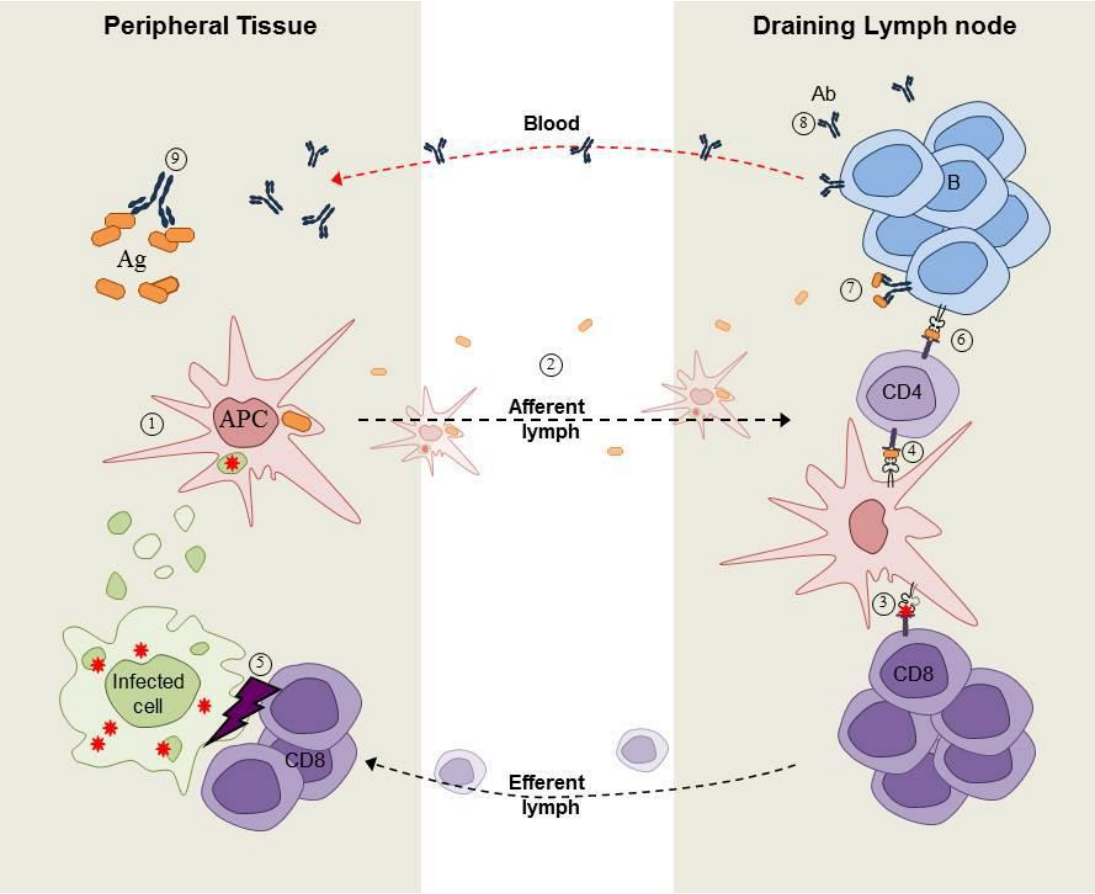

Figure 2. Overview of immune responses.

Antigen-presenting cells (APCs) that have internalized pathogens and/or infected cells ① leave peripheral tissues and reach, via the lymph, secondary lymphoid organs such as the spleen and lymph nodes ②. There, depending on its origin, the antigen will be presented to either CD8+ T cells ③ or CD4+ T cells ④. While CD8+ T cell activation results in the cytotoxicity-mediated killing of target cells ⑤, CD4+ T cells provide help ⑥ to antigen-stimulated B cells ⑦. B cell activation induces the production and secretion of antigen-specific antibodies ⑧ that recirculate through the blood to fight against pathogen within peripheral tissues ⑨. Ag=antigen, Ab=antibody [Picture credit: Dorian Obino]

II. **Adaptive immune system:** The adaptive immune system allows generating antigen-specific immune responses. It is more complex than the innate immune system as antigens must be specifically recognized and processed. First step of adaptive immune response is antigen uptake by dendritic cells in the peripheral system, soon after the uptake dendritic cells leave the periphery and travel through the lymph to reach secondary lymphoid organs such as lymph nodes, where they present processed antigen to antigen specific CD4+ or CD8+ T cells. While CD8+ T cell activation results in the cytotoxicity-mediated killing of target cells, CD4+ T cells provide help to launches the adaptive immune response that creates an army of immune cells specifically designed to attack the antigen **(Figure 2)**. Adaptive immunity also includes a "memory" that makes future responses against a specific antigen more efficient. Development, structure and function of B lymphocytes are detailed in next chapter.

B lymphocytes

B lymphocytes (B cells) are important cells of adaptive immune system and are essential for antibody production. For efficient antibody production, B cell needs to acquire antigens that are presented to them by neighbouring antigen presenting cells. B cells acquire antigen through their specific membrane receptors called B cell receptor (BCR). Following antigenic stimulation, B cells can process and present antigens in association with MHC class II molecules, thereby recruiting specific CD4+ T-cell help and stimulating B-cell proliferation and differentiation (Rock, Haber, Liano, Benacerraf, & Abbas, 1986). B cells can differentiate along two distinct pathways: they can either differentiate into extra follicular short lived plasma blasts, that are important for rapid antibody production and early protective immune responses, or they can enter into germinal centres (GC). There, they differentiate into long live plasma cells, which secrete high-affinity antibodies following affinity maturation*, or memory B cells, which confer long-lasting protection from secondary challenges (MacLennan, 1994)(Rajewsky, 1996). The process of B cell development, BCR signalling, antigen processing, presentation and internalization are detailed in following subparts.

***Affinity maturation:** Affinity maturation occurs on surface immunoglobulin of GC B cells. It is the process of high affinity antibody production by B cells which are activated by T follicular helper cells during the course of an immune response. With repeated exposures to the same antigen, B cells will produce antibodies with several log-fold higher affinities than in a primary response.

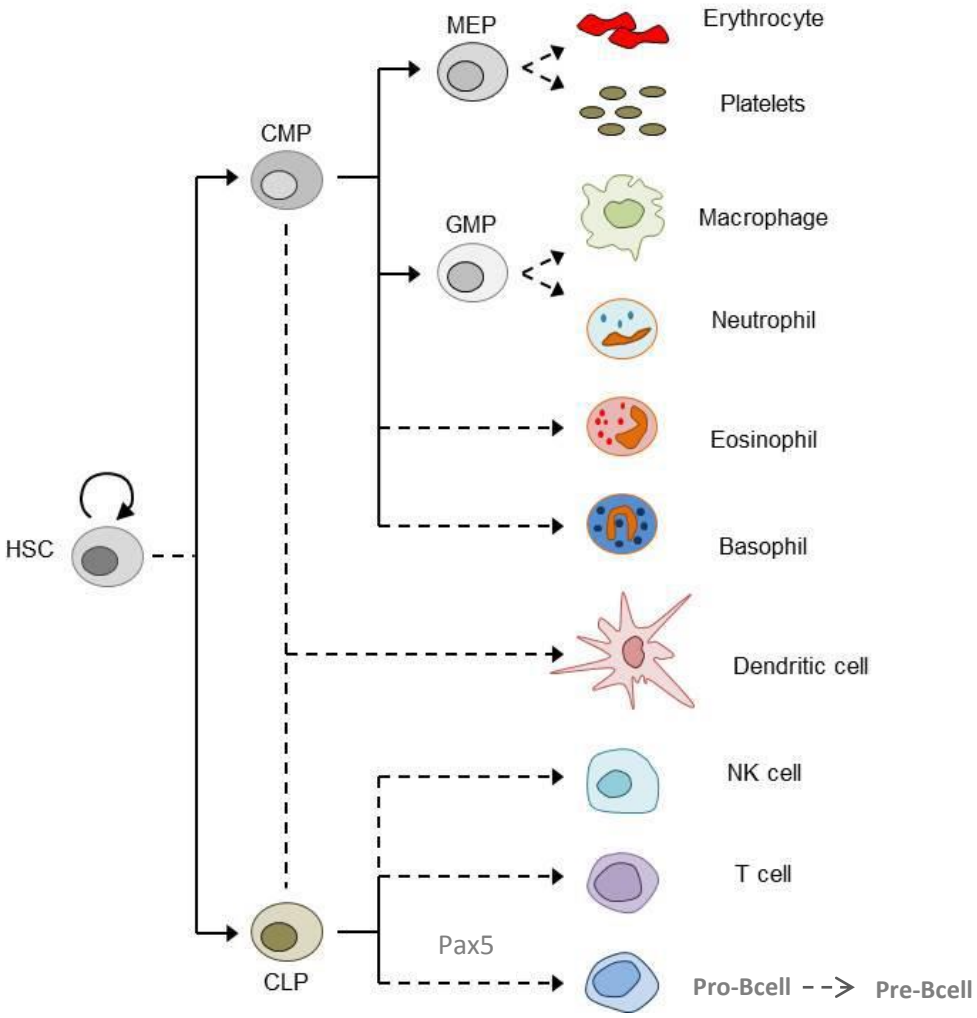

Figure 3. Overview of hematopoiesis.

HSC, hematopoietic stem cell; CMP, common myeloid progenitor; CLP, common lymphoid progenitor; MEP, megakaryocyte/erythroid progenitor; GMP, granulocyte-macrophage progenitor. Adapted from (Larsson & Karlsson, 2005)

I. B cell development

Development of B cells begins in the foetal liver and continues in the bone marrow. B cells differentiate from hematopoietic stem cells (Sub capsular sinus). Sub capsular sinus give rise to common lymphoid progenitors (CLPs) that can differentiate into either T or B lymphocytes depending on the upregulation of unique transcription factors such as PAX5 (Larsson & Karlsson, 2005). Upon upregulation of PAX5, CLPs irreversibly differentiate into Pro-B cell, which express Immunoglobulin (Ig)a and Igβ on their surface (Nutt et al., 1999). Pro-B cells become pre-B cells when they express membrane μ chains with surrogate light chains in the pre-BCR. Checkpoint at pre-B cell stage only selects cells with functional pre-BCRs. Further gene rearrangement in Light (L) chain leads to differentiation to immature B cells, which express mature-BCRs at their surface. Another round of selection eliminates self-reactive B cells. Selected B cells at this stage exit the bone marrow and enter the spleen and complete their maturation process and develop into mature B cells residing within B cell follicles (follicular B cells) or the spleen marginal zone (marginal zone B cells). At that stage, a pool of mature B cells egress from the spleen, gains access to the blood circulation and colonize lymph nodes surface (Nagasawa, 2006) (Nutt et al., 1999) **(Figure 3)**. Pro-B cells become pre-B cells when they express membrane μ chains with surrogate light chains in the pre-BCR. Checkpoint at pre-B cell stage only selects cells with functional pre-BCRs. Further gene rearrangement in Light (L) chain leads to differentiation to immature B cells, which express mature-BCRs at their surface. Another round of selection eliminates self-reactive B cells. Selected B cells at this stage exit the bone marrow and enter the spleen and complete their maturation process and develop into mature B cells residing within B cell follicles (follicular B cells) or the spleen marginal zone (marginal zone B cells). At that stage, a pool of mature B cells egress from the spleen, gains access to the blood circulation and colonize lymph nodes (Nagasawa, 2006).

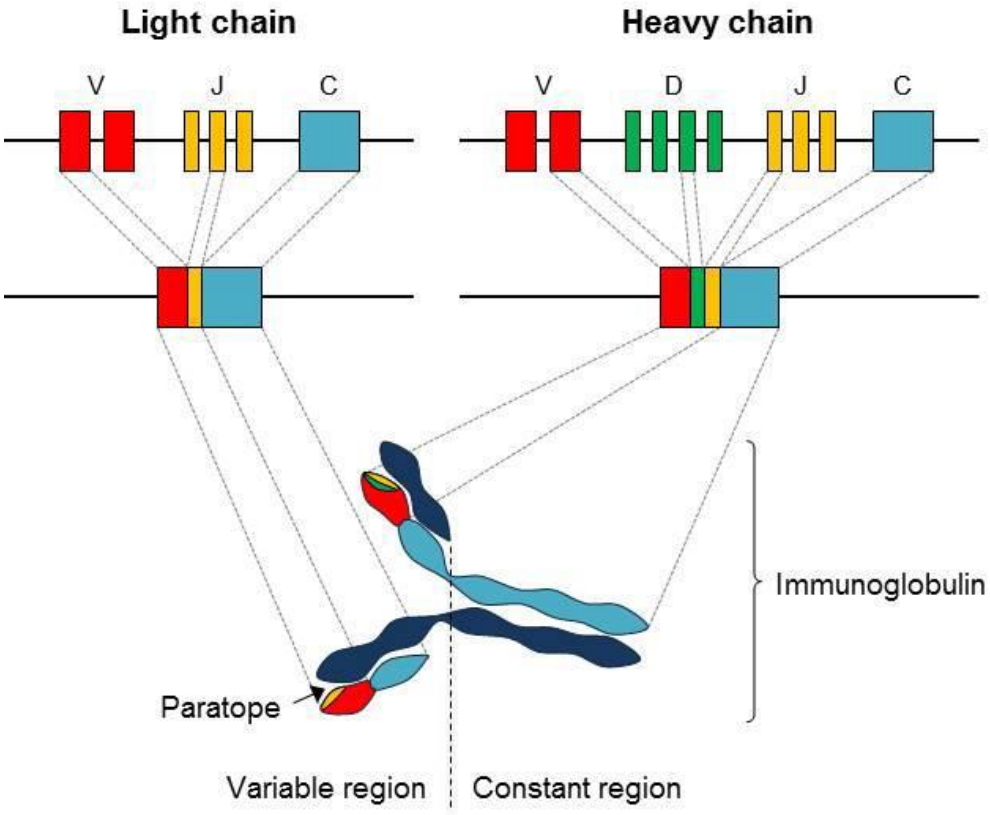

Figure 4. Structure and assembly of immunoglobulins

Immunoglobulins are composed of two light chains associated with two heavy chains. These chains are generated by an unique combination of rearranged coding sequences, divided in variable (V), diversity (D) and joining (J) segments through a process called V(D)J recombination. [Picture credit: Dorian Obino]

II. Structure of the B cell receptor

The BCR consists of an antigen binding transmembrane immunoglobulin (mIg) facing the extracellular environment. The BCR is composed of two parts: (1) a membrane-bound antigen-binding immunoglobulin (mIg) molecule of one isotype (IgD, IgM, IgA, IgG, or IgE), (2) two transmembrane polypeptides, Iga and Igβ, containing immunoreceptor tyrosine activation motifs (ITAMs), which enable the transmission of intracellular signalling. As all immunoglobulins (Igs), the BCR can be subdivided into two main regions: at the N-terminus, the variable region is formed of two paratopes involved in antigen binding, whereas the C-terminus part of the protein corresponds to the constant region and defines the isotype (IgM, IgD, IgA, IgE or IgGs) and function of Igs **(Figure 4).**

Immunoglobulins are large Y shaped proteins composed of two light chains associated with two heavy chains. These chains are generated by an unique combination of rearranged coding sequences, divided in variable (V), diversity (D) and joining (J) segments through a process called V(D)J recombination. During the lifetime of a B cell, immunoglobulin loci undergo several genetic rearrangements to generate mature BCR. The first recombination event occurs between one D and one J gene segment of the heavy chain locus that deletes any DNA between these two gene segments. This D-J recombination is followed by the joining of one V gene segment, from a region upstream of the newly formed DJ complex, forming a rearranged VDJ gene segment. All other gene segments between V and D segments are now deleted from the cell's genome. This rearranged VDJ segment then associates with the constant region of IgH (Immunoglobulin heavy chain) to form the Pre-BCR. Undergoing allelic exclusion, Pre-B cell rearranges V_L and J_L segment of IgL (Immunoglobulin light chain) gene locus to form a mature BCR with a unique variable region. At this stage, autoreactive B cells are subsequently eliminated, and the remaining B cells start to express both IgM and IgD (Metzger, Metzger, Ling, Hurst, & Van Cleave, 1992)

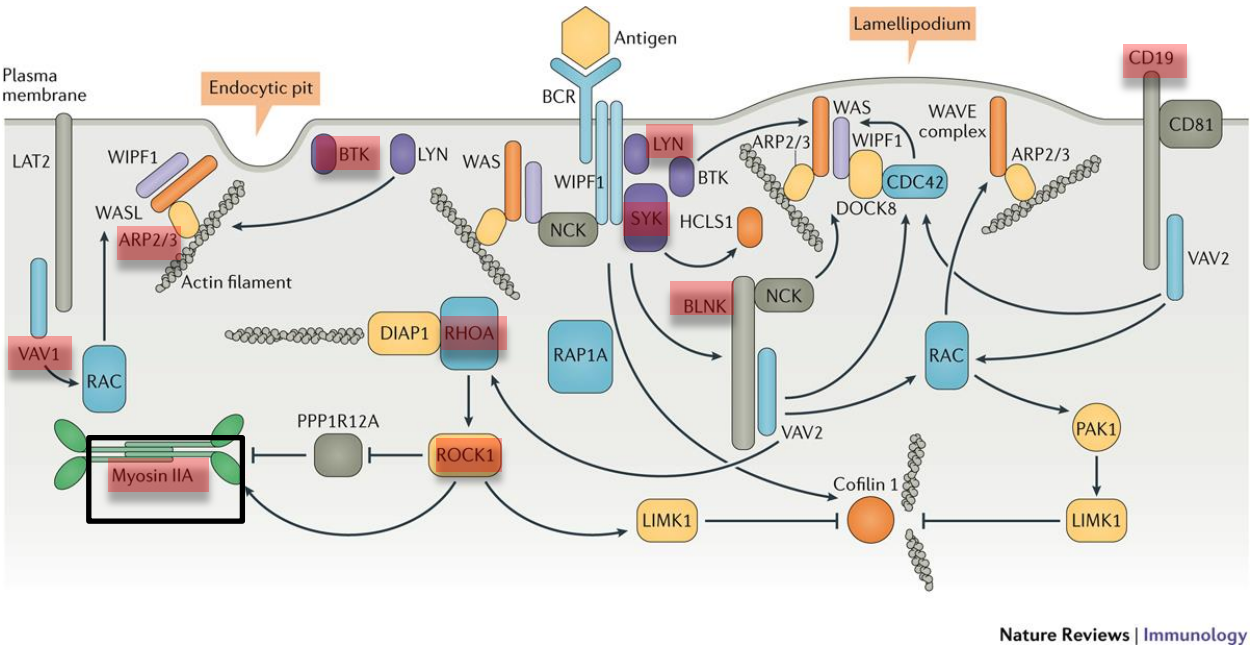

Figure 5 . B cell receptor signalling to the cytoskeleton

Adapted from (Tolar, 2017).

III. BCR signalling

As mentioned above, BCR is composed of membrane immunoglobulin (mIg) molecules and associated with Igα and Igβ heterodimers. The mIg subunits bind antigen, resulting in receptor aggregation, while the α/β subunits transduce signals to the cell interior. BCR activation induces activation of Lyn, a Src family kinase which phosphorylates the ITAMs and this in turn leads to phosphorylation of Syk, Btk and Vav. This initiates intracellular calcium release and the generation of secondary messengers e.g inositol-1.4.5-triphosphate (IP3) and diacylglycerol (DAG) (Tolar, Sohn, & Pierce, 2008)(Cambier, Pleiman, & Clark, 1994).

Although receptor aggregation is required for BCR signalling, it is not sufficient to elicit B cell activation. B cells needs to amplify these aggregation by spreading the membrane around the antigen presenting cell (Fleire et al., 2006) leading to actin remodelling. Spreading of B cell has been directly linked to BCR signalling, which depends on the BCR-associated tyrosine kinases Lyn and Syk, phosphorylation of the adaptor CD19, and recruitment of cytoplasmic proteins BLNK, PLCγ2, and Vav (Weber et al., 2008), (Depoil et al., 2009) **(Figure 5).** These molecules form a protein complex associated with the BCR that activates signalling pathways responsible for actin remodelling. Plasma membrane changes shape upon activation via dephosphorylation of Ezrin-Radixin-Moesin (ERM), these proteins influence the organization and integrity of BCR microclusters (Treanor, Depoil, Bruckbauer, & Batista, 2011). Activation of Vav stimulates actin polymerization through activation of Rac and the Arp 2/3 complex. Actin polymerization drives extension of the membrane edge and generation of lamellipodia (Arana et al., 2008)(Depoil et al., 2009)(Weber et al., 2008) and endocytic pits. RhoA activates actin polymerization and stimulates myosin II contractility through Rock1 activity (Saci & Carpenter, 2005).

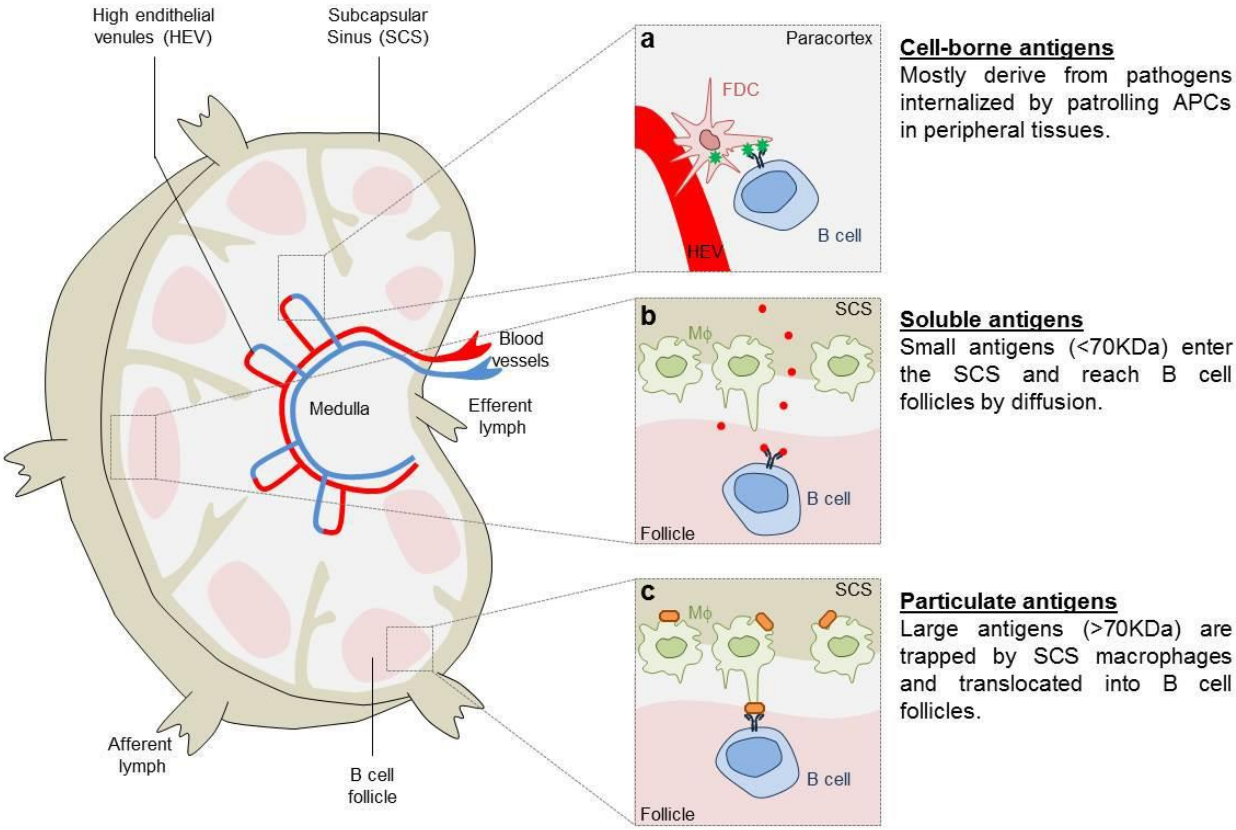

Figure 6. Antigen encounter by B cells.

Depending on their nature and origin, antigens follow different routes to be presented to B cells. Pathogen-derived antigens generated within antigen-presenting cells (APCs) are presented to B cells in areas close to high endothelial venules (**a**). Small soluble antigens reach B cell follicles by diffusion where they encounter antigen-specific B cells (**b**). In contrast, large/particulate antigens reaching the sub-capsular sinus of lymph nodes are trapped at the surface of specialized macrophages (SCS CD169+ macrophages), translocated within B cell follicles and presented to antigen-specific B cells in their native form (unprocessed antigens) (**c**). Adapted from (Batista & Harwood, 2009) [Picture Credit Dorian Obino]

IV. Antigen encounter by B cell

B cells are not migratory cells that patrol the body in search of antigen like T cells or dendritic cells. They reside in the follicles of secondary lymphoid organs where they encounter specific antigens. Antigens residing in the peripheral tissues can be taken up by sub-capsular macrophage or dendritic cells that transport them towards lymph node or directly present them to B cell (Qi et al., 2006). Antigens may also reach draining lymph nodes passively, through the lymph or the blood circulation, where B cells encounter them by different means that are detailed below **(Figure 6).**

i. Encounter via macrophage or dendritic cells

Follicular dendritic cells have been described to acquire and present antigens to B cells (Suzuki, Grigorova, Phan, Kelly, & Cyster, 2009) as well as medullary macrophages, which acquire opsonized antigens. However, these cells were not required to initiate B cell responses in a model of influenza virus infection, which rather relies on dendritic cells presenting in the medullary sinus (Gonzalez et al., 2010)**(Figure 6a)**.

ii. Encounter with soluble antigen

Antigen smaller than 70 KDa are considered as soluble antigen. Afferent lymph vessels supply antigen to the lymph node and soluble antigen can be detected within minutes of subcutaneous administration (Nossal, Abbot, Mitchell, & Lummus, 1968). In1980, Farr. A. et al. identified small pores (0.1-1 µm) in the region of sub-capsular sinuses by electron microscopy **(Figure 6b).** These pores might allow small soluble antigens to enter the lymph node through the afferent vessels and get direct access to B cells.

iii. Antigens immobilized on cell membranes

Large antigens (greater than 70 kDa) remain trapped at the sub capsular sinus (SCS) floor site where CD169+ macrophages have been shown to capture and transfer them to follicular B cells (Carrasco & Batista, 2006)(Junt et al., 2007)**(Figure 6c)**. How antigens are transferred from the SCS to B cell follicles is unclear. Two routes have been suggested: first, the sub-capsular CD169+ macrophages that display a poor phagocytic capacity recycle antigens and expose them in their native form at the cell surface. Second, antigens that are immobilized at the surface of CD169+ macrophages could

be translocated from the SCS to B cell follicles through macrophage protrusions (Martinez-Pomares & Gordon, 2007). In all stated cases, antigens are presented to B cells triggering the internalization of antigen-BCR complexes into endo-lysosomal compartments. This leads to the processing of the antigen and the generation of antigenic peptides that will be loaded onto MHC-II molecules for further presentation to primed CD4+ T cells.

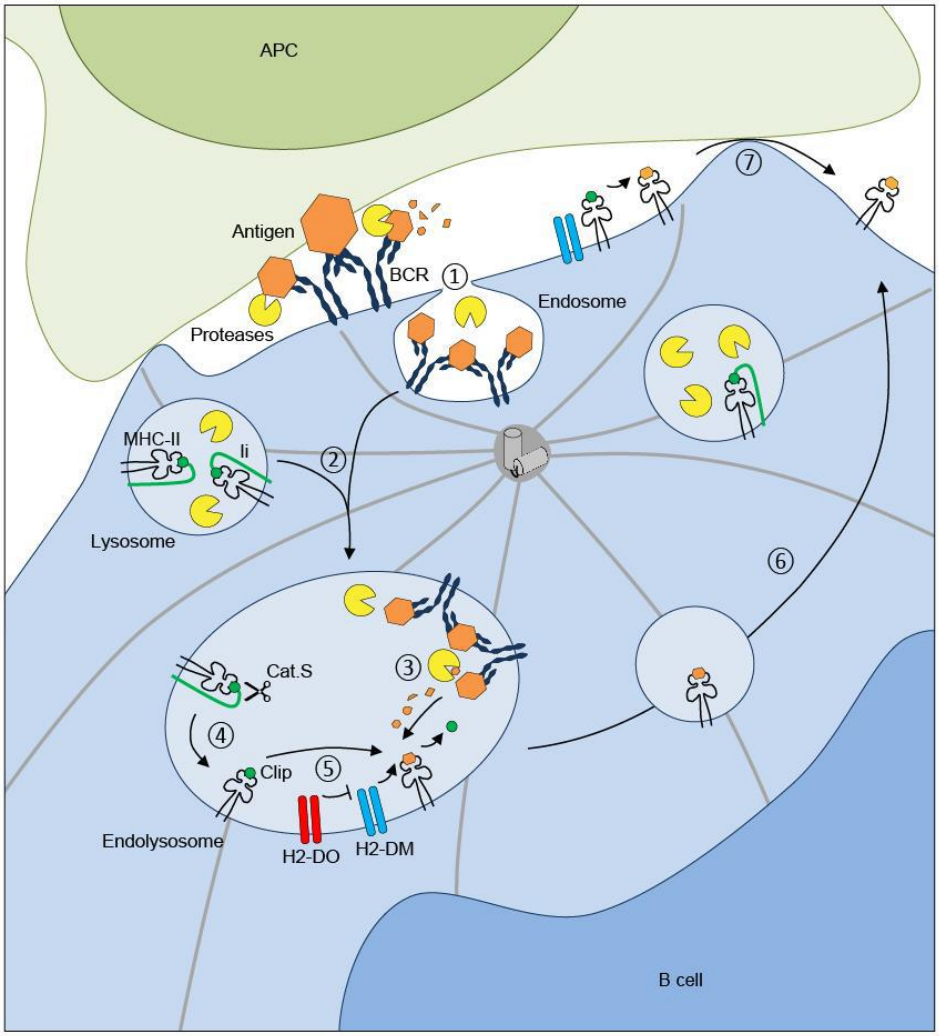

Figure 7. Antigen processing by B cells:

BCR cross-linking by antigens induces the internalization of BCR antigen complexes within B cell–endosomes ①. Endolysosomes that are formed by the fusion ② of antigen containing endosomes with lysosomes that carry MHC-II molecules allow the efficient processing of antigens ③. In the same compartment, Cathepsin S (Cat.S) cleaves the invariant chain (Ii) resulting in MHC-II–CLIP complex formation ④. Finally, H2-DM molecules promote the exchange between CLIP and antigenic peptides for them to be loaded onto MHC-II molecules ⑤. The catalysis of CLIP released by H2-DM is regulated by another non-classical MHC-II molecule, H2-DO. Peptide–MHC-II complexes are exported to the B-cell surface ⑥. Of note antigenic peptides might also be generated within the synaptic space where they are directly loaded onto MHC-II molecules at the cell surface ⑦. Adapted from (Obino & Lennon-Duménil, 2014)

V. Antigen processing by B cells

For the production of high affinity antibodies by B cells, it is essential that internalized antigen is processed and loaded on to MHC-II molecules to eventually present to primed CD4+ T cells. This step is known as T-cell/B-cell cooperation and is pivotal for the ultimate formation of GC and production of high-affinity antibodies by B cells (Mitchison, 2004).

BCR cross-linking by antigens induces the internalization of BCR-antigen complexes and polarization of MTOC to the BCR–antigen interaction zone, allowing the local recruitment of lysosomes. Antigens undergo limited proteolysis in order to preserve T-cell epitopes from excessive degradation (Delamarre, Pack, Chang, Mellman, & Trombetta, 2005) that was also shown to facilitate the arrival of antigen–BCR complexes into MHC-II endo lysosomes through its interaction with the cytosolic tail of invariant chain (Ii) (Vascotto et al., 2007). To prevent the premature binding of endogenous peptides and MHC-II molecules, Ii gets associates to MHC-II molecules during biogenesis in the endoplasmic reticulum. Once in endo-lysosomes Cathepsin S cleaves the Ii (Bakke & Dobberstein, 1990), (Lotteau et al., 1990), (Roche & Cresswell, 1991) **(Figure 7)** .This ultimately leads to the generation of the Ii CLIP fragment that occupies the MHC class II peptide-binding groove. Non-classical MHC-II molecule "H2-DM" catalyses the exchange between antigen-peptide complex and CLIP, this catalysis is regulated by another non-classical MHC-II molecule called "H2-DO" (Driessen et al., 1999)(Riese et al., 1996). H2-DO knockout B cells were found to exhibit increased amount of MHC-II peptide complexes and compete wild-type B cells for the entry to GCs. Finally, Peptide–MHC-II complexes are exported to the B-cell surface for further presentation to primed CD4+ T cells. Remarkably, antigen processing and peptide loading onto MHC class II molecules can also directly take place at the B-cell surface, where H2-DM molecules are also found(Lisa K. Denzin & Cresswell, 1995),(L K Denzin, Sant'Angelo, Hammond, Surman, & Cresswell, 1997).

VI. Antibody production

After antigen internalization and processing, a pool of B cells differentiates into short-lived plasmablasts producing antibodies with relatively low affinity (Cunningham et al., 2007), another pool migrates towards T cell boundary and receive signals from helper T cells to differentiate into T follicular helper cells (Reif et al., 2002)(Okada et al., 2005). This T-B cooperation is required for B cells to be fully activated, proliferate, and form GCs (Mitchison, 2004).

During the GC reaction, while proliferating, antigen-activated B cells undergo affinity maturation through a process named somatic hyper mutation (SHM). This results in the introduction of point-mutations within the V (D) J segment of immunoglobulin variable regions leading to changes in the affinity of the BCR for its cognate antigen. Here, affinity refers to the strength with which the epitope binds to an individual antigen-binding site on the antibody. High affinity antibodies bind quickly to the antigen with a stronger bond whereas low affinity antibodies bind weakly to the antigen and often do not detect efficiently the antigen. Following selection of B cells with higher affinity for the antigen, they go through immunoglobulin class switch recombination , leading to the generation of different classes of high-affinity Igs (De Silva & Klein, 2015). Following successive rounds of the GC reaction, selected class switched B cells* differentiate into either plasma cells, which produce antigen-specific high affinity antibodies, or memory B cells (Allen et al., 2007), (MacLennan, 1994).

*** Class Switch:** the mechanism that changes the antibody production of B cells from one type to another, e.g. B cells switch from the isotype IgM to the isotype IgG. During class switch recombination the constant region portion of the antibody-heavy chain is changed, but the variable region of the heavy chain remains the same; thus, class switching does not affect antigen specificity. Since variable regions do not change, class switching does not affect antigen specificity. Instead, the antibody retains affinity for the same antigens, but can interact with different effector molecules.

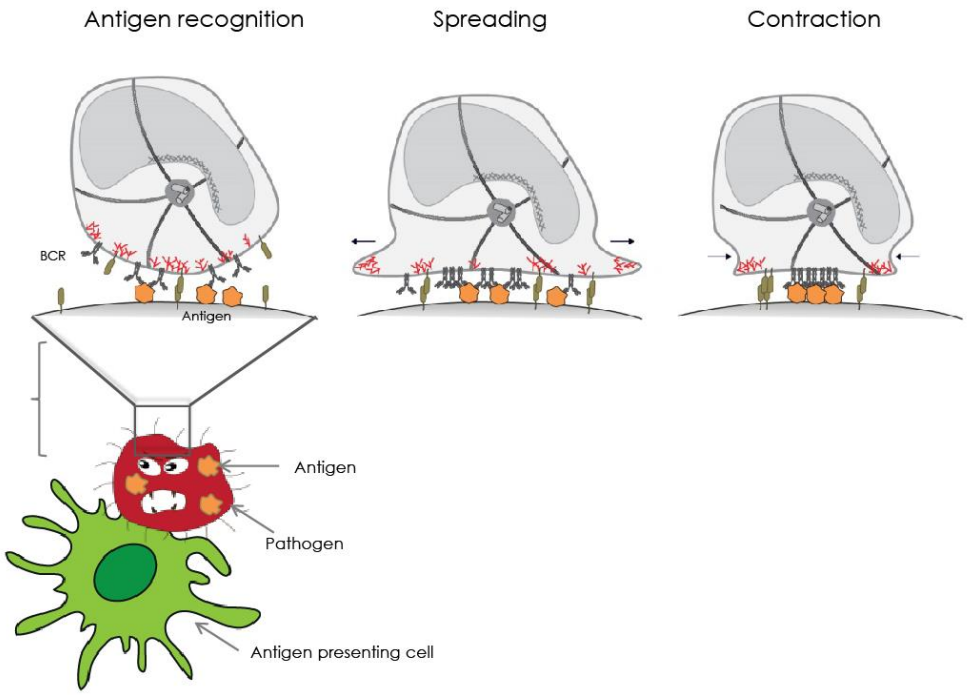

Figure 8. B lymphocytes form an immunological synapse when acquiring antigen in vivo:

Upon antigen recognition , B cells starts to spread around antigen presenting cell , soon after reaching the maximum spreading, it starts to contract and gather antigen in the center to eventually internalize it.

B cell immune synapse

Immune synapse is an interface between the APC and lymphocytes similar to the neurological synapse. It was discovered by Abraham Kupfer at the National Jewish Medical and Research Centre in Denver. The term immune synapse was coined by Michael Dustin at NYU. Where he coined the term in context of T and B cell interaction, where B cell act as an APC. In this thesis, immune synapse between APC and B cell is detailed.

Formation of B cell immune synapse is essential for antigen recognition. In order to efficiently acquire antigen, B cell first spread around the APC to gather maximum amount of antigen and then starts to contract to eventually pull off the antigen from the surface of APC **(Figure 8)**. The acto-myosin cytoskeleton plays a central role in each of these steps that are detailed in subsequent sections. In the first section I will describe role of actin and myosin in antigen and the different extraction pathways, B cell spreading and contractions. I will also describe most common biophysical techniques to measure forces: in particular traction force microscopy that will be used through this entire thesis.

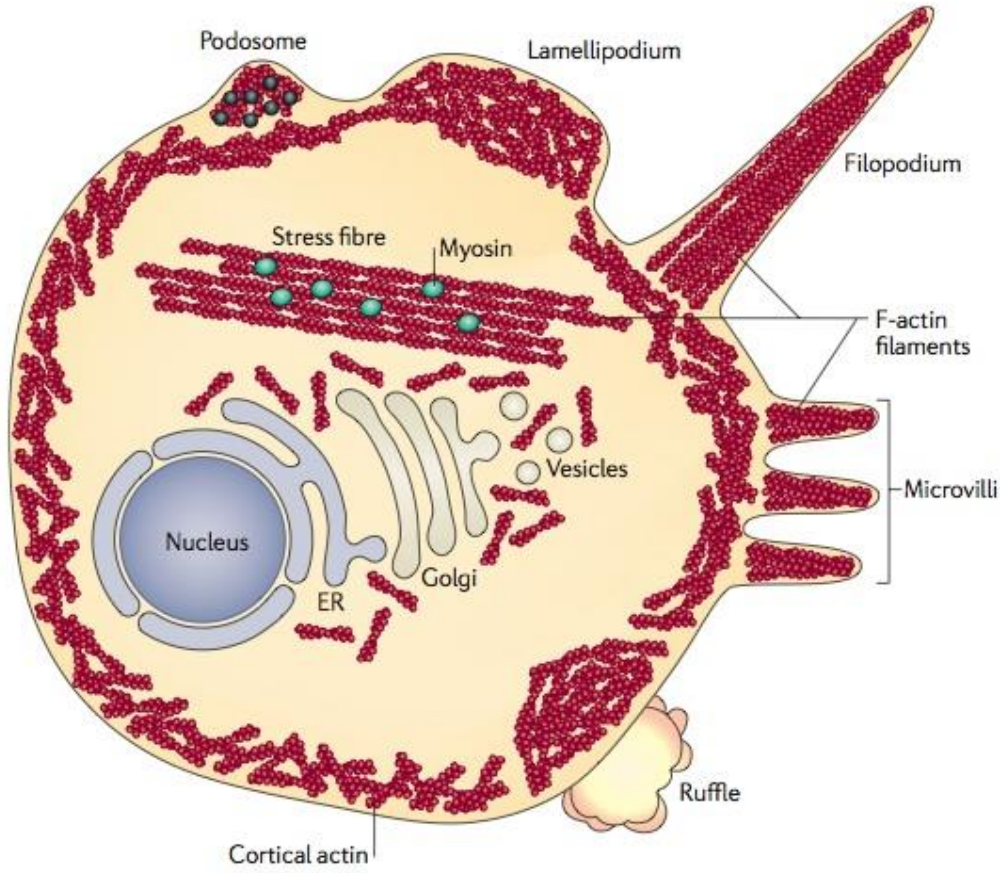

Figure 9. Actin cytosketon structure: showing lamellipodium , filopodium, microvilli, podosomes [http://jonlieffmd.com/blog/virus-tricks-manipulate-the-cytoskeleton].

Actin and Myosin:
Two core component of B cell cytoskeleton

The cytoskeleton is a highly interconnected structure, which regulates cell shape, cell division and movement. In eukaryotic cells, the cytoskeleton is mainly composed of three structures: microfilaments made of actin, intermediate filaments and microtubules (Wickstead & Gull, 2011). Of note, it is now well admitted that proteins belonging to the septin family form the fourth component of the cytoskeleton (reviewed in (Mostowy & Cossart, 2012)).

I. Actin Cytoskeleton

Actin is the major cytoskeletal protein, which polymerizes to form actin filaments. Actin filaments are made up of thin, flexible fibers approximately 7 nm in diameter that can be cross-linked together to form different actin structures. In1942 , actin was first isolated from muscle cells (Needham, 1942) in which it constitutes approximately 20% of total cell protein. Although actin was initially thought to be uniquely involved in muscle contraction, it is now known to be an extremely abundant protein (typically 5 to 10% of total protein) in all types of eukaryotic cells.

Actin monomers are called globules. These higher-order structures form bundles or three-dimensional networks with the properties of semisolid gels. The assembly and disassembly of actin filaments, their crosslinking into bundles and networks, and their association with other cell structures (such as the plasma membrane) are regulated by a variety of actin-binding proteins, which are critical components of the actin cytoskeleton. Branched networks form lamellipodia **(Figure 9)** that helps the cell to propel itself on a surface. Parallel actin filament networks helps in membrane protrusions, called filipodia. Myosin II can connect two parallel actin fibres to make stress fibres. Actin not only provides mechanical support, determines cell shape, and allows movement of the cell surface but also help in several endocytic internalization processes described in subsequent sections.

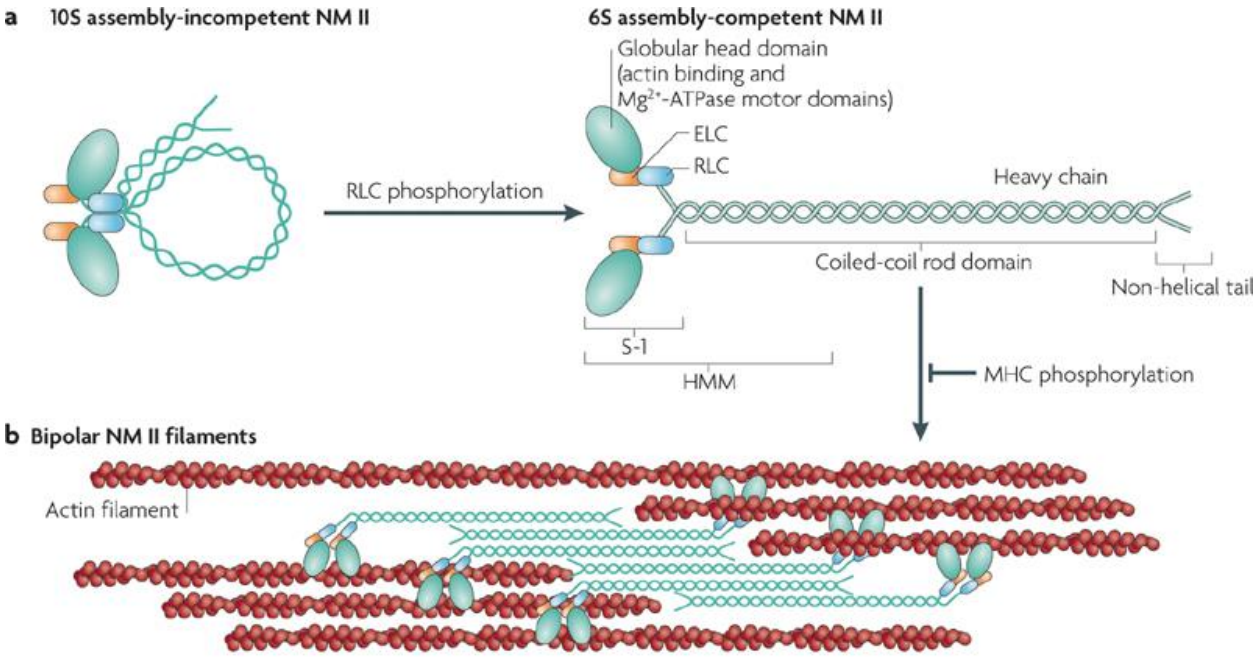

Figure 10. Domain structure of Myosin II

(a)The subunit and domain structure of non-muscle myosin II (NM II), which forms a dimer through interactions between the alpha-helical coiled-coil rod domains. The globular head domain contains the actin-binding regions and the enzymatic Mg2+-ATPase motor domains. The essential light chains (ELCs) and the regulatory light chains (RLCs) bind to the heavy chains at the lever arms that link the head and rod domains. In the absence of RLC phosphorylation, NM II forms a compact molecule through a head to tail interaction. This results in an assembly-incompetent form (10S; left) that is unable to associate with other NM II dimers. On RLC phosphorylation, the 10S structure unfolds and becomes an assembly-competent form (6S). S-1 is a fragment of NM II that contains the motor domain and neck but lacks the rod domain and is unable to dimerize. Heavy meromyosin (HMM) is a fragment that contains the motor domain, neck and enough of the rod to effect dimerization. (b) NM II molecules assemble into bipolar filaments through interactions between their rod domains. These filaments bind to actin through their head domains and the ATPase activity of the head enables a conformational change that moves actin filaments in an anti-parallel manner(Vicente-Manzanares, Ma, Adelstein, & Horwitz, 2009)

II. Myosin II cytoskeleton

Myosins constitute a superfamily of motor proteins that play important parts in several cellular processes that require force and translocation. Most myosins belong to class II and, together with actin, make up the major contractile proteins. Thus, myosin II is the conventional motor protein involved in cardiac, skeletal and smooth muscle contraction. It is made up of two heavy chains. The N terminus of the heavy chain has a globular head domain, that binds to actin head domain and have the catalytic sites where energy is generated by ATP hydrolysis. The C-terminus tail domain has a coiled coil morphology that holds the two heavy chains together. The intermediate regulatory neck domain makes the angle between the neck and tail domain described in **(Figure 10)**. Myosin II molecules that resemble their muscle counterparts, with respect to both structure and function, are also present in all non-muscle eukaryotic cells (Clark, Langeslag, Figdor, & van Leeuwen, 2007)and (Conti & Adelstein, 2008). Like muscle myosin II, non-muscle myosin IIA (NM II) molecules are comprised of three pairs of peptides: two heavy chains of 230 KDa, two 20 KDa regulatory light chains (RLCs) that regulate NM II activity and two 17 KDa essential light chains (ELCs) that stabilize the heavy chain structure. Although these myosins are referred to as 'non-muscle' myosin II to distinguish them from their muscle counterparts, they are also present in muscle cells, where they have distinct functions during skeletal muscle development and differentiation, as well as in the maintenance of tension in smooth muscle (Vicente-Manzanares et al., 2009).

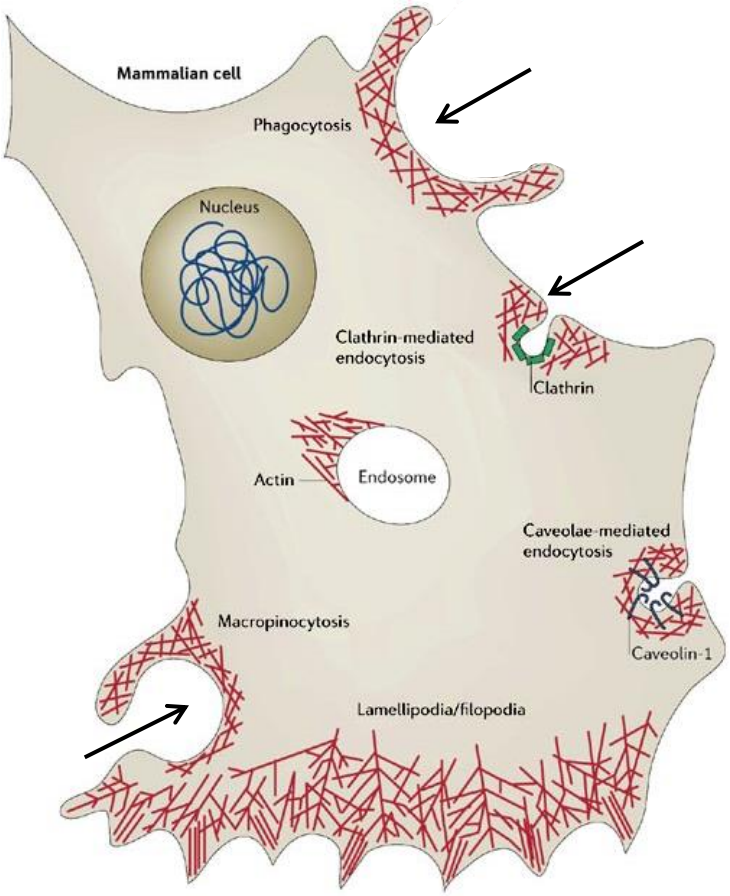

Figure 11. The dynamic polymerization of actin filaments:

Actin filament (red) is involved in different processes that reshape or move cellular membranes. These processes include different forms of endocytic uptake at the plasma membrane — that is, clathrin-mediated, macropinocytosis and phagocytosis in mammalian cells. The protrusion of lamellipodia and filopodia in migrating mammalian cells is dependent on actin polymerization (Kaksonen, Toret, & Drubin, 2006), arrows indicating actin cytoskeleton organization in phagocytosis, macropinocytosis and clathrin mediated endocytosis .

Antigen extraction by B cells

I. Endocytosis

Internalization of extracellular fluid/particles represents an important path of entry within cells and particularly applies to cells of the immune system. Actin remodelling underneath the plasma membrane leads to the formation of membrane protrusions that are essential for the initiation of the internalization process. As most of the important chemical substances are large polar molecules that cannot pass through plasma and cell membrane by itself, they need to be transported , endocytosis is a form of active transport in which a cell transports molecules (such as proteins) into the cell by engulfing them. Reshaping of plasma membrane and actin polymerization plays a central role in different forms of endocytic internalization — for example phagocytosis, micro and macro-pinocytosis, and clathrin-mediated endocytosis.

***Phagocytosis*:** Phagocytosis was discovered by Elie Metchnikoff. It is an internalization process of harmful foreign particles such as bacteria, dead or dying cells by phagocytes. Dendritic cells, macrophages, mast cells are example of professional phagocytes. In general phagocytosis is induced by specific surface receptors within the cell, named pattern recognition receptors (PRRs), which recognize pathogen-associated molecular patterns (PAMPs), a class of molecules that are broadly shared by pathogens but distinguishable from host molecules **(Figure 11).**The size of a phagocytic particle goes up to several micrometers (Champion, Walker, & Mitragotri, 2008)

***Micropinocytosis/Macropinocytosis*:** Pinocytosis is defined as the drinking up by cells in greek language. We can define pinocytosis as the taking up of fluid into a cell of by invagination of the plasma membrane, which is then pinched off, resulting in small vesicles in the cytoplasm. When cells uptake molecules of less than 0.1 μm diameter, the process is named micropinocytosis and for the particles greater than 0.5 μm it is termed macropinocytosis. Macropinocytosis is the primary form of internalization in dendritic cells. No receptor is required for the initiation of micro and micropinocytosis **(Figure 11)**.

***Clathrin-mediated endocytosis*:** is a type of receptor mediated endocytosis involving production of small (approx. 100 nm in diameter) vesicles that have a morphologically characteristic coat made up of the cytosolic protein clathrin. Clathrin-coated vesicles (CCVs) are found in virtually all cells and form domains of the plasma membrane termed clathrin-coated pits (Marsh & McMahon, 1999)**(Figure 11).**

i. B cell antigen internalization

Clathrin mediated endocytosis is the principle type of antigen internalization in B cells (Natkanski et al., 2013)(Stoddart et al., 2005). Natkanski et al., showed that knocking down clathrin leads to substantial reduction of internalization of both soluble and membrane presented antigens. Clathrin colocalize with most of internalized antigen clusters. They also showed that although actin polymerization and clathrin coated pits (CCPs) formation are essential for antigen internalization, they are not sufficient for extraction of membrane antigens in B cell synapse. They addressed the role of myosin II contractility in the invagination of BCR microclusters, which occurs before the formation of the CCPs. Formation of CCPs alone does not generate the forces required for endocytosis of membrane-attached antigens. However, DNA-based tension sensor measurements (detailed in next section) showed that B cell exert force of 10 pN to extract one antigen molecule and with the help of repetitive pulling on the BCR-antigen bond with the help of myosin II, B cells are able to extract antigens that have a stronger bond (Wan et al., 2015). Apart from mechanical extraction, there's also enzymatic extraction through lysosomal proteases that polarize towards the synapse and cleaves the bond between antigen and APC (Yuseff et al., 2011). However recently it has been shown enzymatic extraction is used by B cell only on the substrate that cannot be mechanically deformed. Interestingly, once the mechanical way is activated the secretion of proteases is impaired (Spillane & Tolar, 2016). Even after all the recent progress in the field of B cell antigen internalization, a global picture of what types of forces are involved in antigen internalization is missing.

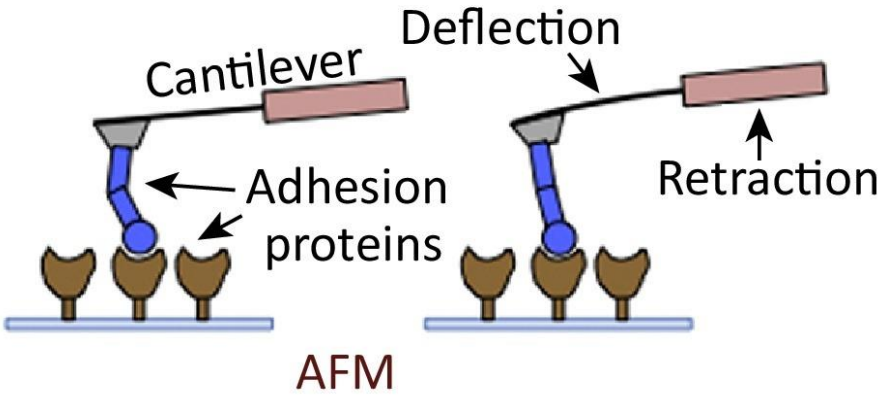

Figure 12. Atomic force microscopy :

(AFM) to measure bond strength as a function of applied force. (Basu & Huse, 2016)

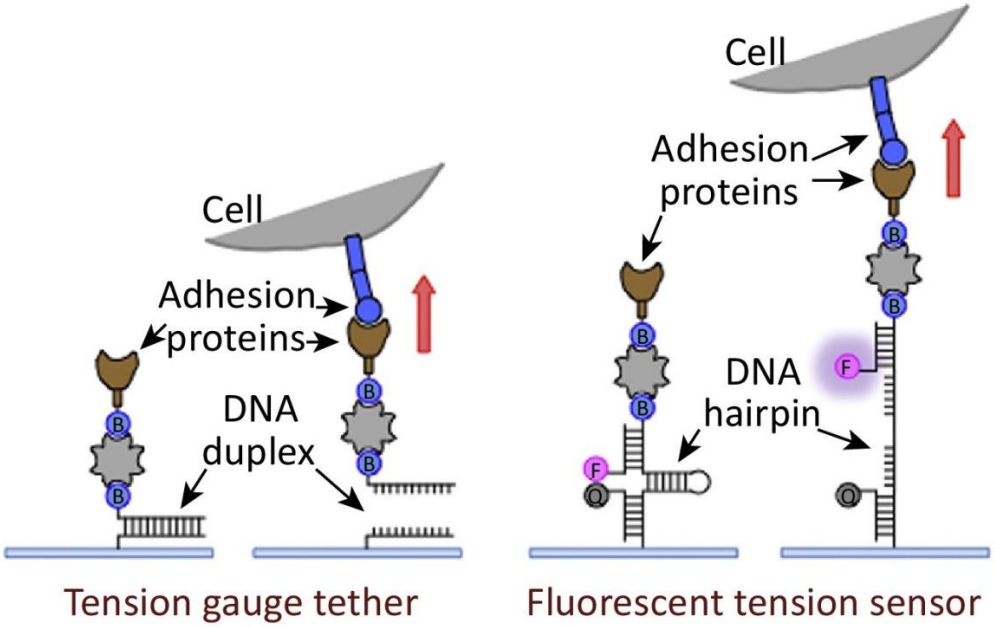

Figure 13.DNA-based tension gauge:

DNA based tension gauge tethers remain attached to the surface unless a sufficient force is applied to rupture Watson–Crick base pairing. Right, a DNA hairpin coupled to a fluorophore (F) and quencher (Q) is used to generate a tension probe that fluoresces upon application of a threshold force. (Basu & Huse, 2016).

II. Techniques used in measurement of antigen extraction forces

Immune-synapse undergoes continuous architectural changes, these changes are the result of forces produced inside the cells and is transmitted through receptors, membrane, or integrins to the neighbouring cells. Immune synapse is not only a platform for chemical dialogues but also for mechanical ones. Our understanding of immune synapse mechanics relies on methods designed to measure synaptic forces between single cells such as AFM (Atomic force microscopy), DNA based force sensors, Traction force microscopy (TFM) and Micro-pillars that are described in the following sections (Basu & Huse, 2016).

i. Atomic Force Microscopy:

In this approach, a cell or molecule of interest is attached to a flexible cantilever and then brought into contact with a glass surface coated with target cells or cognate ligands **(Figure 12)**. With atomic force microscopy one can measure adhesive forces up to molecular level between cells. Forces are measured by monitoring the negative deflection of the cantilever as it is withdrawn away from the surface (Basu & Huse, 2016). Although this technique is reliable to measure intermolecular forces, for inter cellular forces it is not always easy to interpret data and get rid of experimental artefacts.

ii. DNA based force sensors

This approach relies on molecular tension gauges containing DNA duplexes linked to stimulatory ligands (Wang & Ha, 2013). Suitable force exertion on the ligand will rupture the duplex, detaching the ligand from the surface. The strength of the duplex depends on its length, degree of base pairing, GC content, and junction point with the protein ligand **(Figure 13)** (e.g., the center or the end of the strand). Because mechanosensitive receptors, like integrins, only signal effectively under tension, they will be activated only by tension gauge tethers that are strong enough to withstand the associated pulling forces. Hence, by measuring signalling responses on a panel of different TGT surfaces, one can establish the force threshold required for receptor activation (Wan et al., 2015)and (Wang & Ha, 2013).

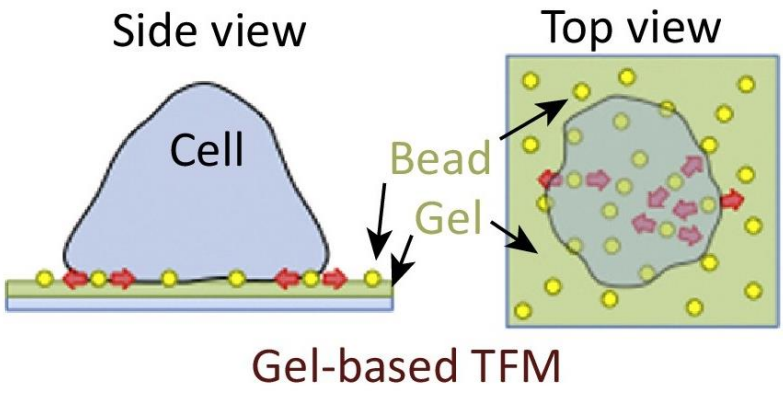

Figure 14. Gel-based TFM:

Force exertion is determined from the movements of beads embedded in the gel matrix. (Basu et al., 2016)

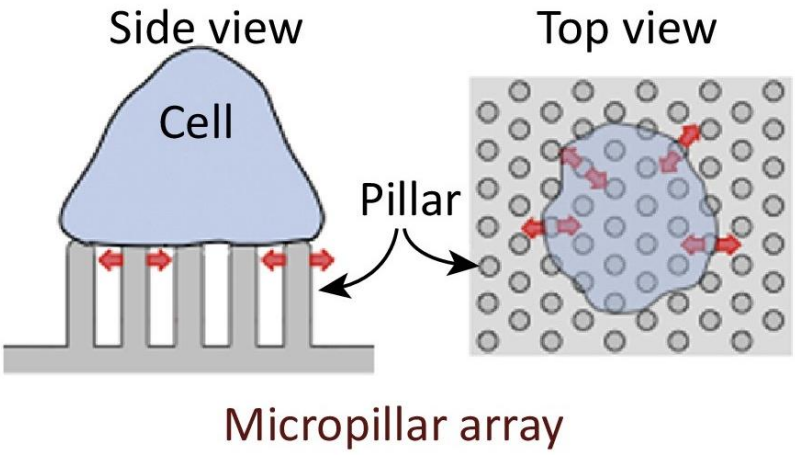

Figure 15. Micropillars:

Cells are imaged on an array of flexible micropillars, allowing applied forces to be calculated from pillar deflection (Basu & Huse, 2016).

iii. Traction Force Microscopy:

TFM is a technique for measurement of force based on the deformation of the elastic substrate on which the force is exerted (Harris, Wild, & Stopak, 1980). In this approach, small fluorescent beads are embedded on the top surface of a polyacrylamide hydrogel substrate bearing ligands (Dembo & Wang, 1999). This technique is generally used to measure forces developed during adhesion. Displacement observed in TFM is always measured by comparing each image to a non-stressed reference image. Cells form a contact structure with the deformable substrate (hydrogel), they distort the hydrogel, thereby moving the beads. The displacement field obtained by bead movement is used to obtain the force (inversion of the problem) (Butler, Tolić-Nørrelykke, Fabry, & Fredberg, 2002),(Mandal, Wang, Vitiello, Orellana, & Balland, 2014). The inversion of the problem is done in Fourier space by interpolating the data. Stress maps obtained reveal not only the magnitude and direction of applied forces but also their spatial distribution within the contact structure **(Figure 14)** (Basu & Huse, 2016). This technique has been generally used for bigger cells (≈100-120 µm) then lymphocytes with many beads underneath the cells to have precise force measurement (down to a single focal adhesion). We adapted this technique to use on B cell (≈5-7 µm) force measurement by optimizing the rigidity of the gel, number of beads and algorithm to measure forces, which are explained in the material and method section.

iv. Micropillars

This approach is a version of TFM in which the hydrogel substrate is replaced by a hexagonal array of PDMS micro pillars coated with stimulatory ligands (Bashour et al., 2014). Lymphocytes form immune synapse like contacts with the pillar tops and move them as they exert force against the surface. Each pillar deflection can be converted into a force measurement based on the height, width, and composition of the pillars. The micro pillar method provides enhanced spatial resolution relative to gel- based TFM because pillars (i) can be spaced within 1 µm of one another and (ii) they move independently of their neighbours (Basu & Huse, 2016) **(Figure 15)**. Limitation of this would arise when using small cells like B cells (5-7 µm), which can easily leak into the pillar gaps.

III. Biomechanics of B cell antigen extraction

Immune cells probe their environment and their function replies on extraction and sensing the tissue that makes them constantly influenced by cellular mechanics. B cells also have been shown to have varying degree of activation based on the stiffness of the antigen presenting substrates (Wan et al., 2013). Antigens presented on stiff substrates, promote BCR signalling more efficiently with the generation of higher forces on the BCR, than to the antigens presented on softer substrates, which limit tension. Conversely, precise measurements using DNA tension sensors have revealed that the BCR-antigen bond is poorly responsive when the tension on the BCR is below 20 pN, but responds better to tensions between 20 pN and 40 pN, and reaches a maximum responsiveness to tensions above 40 pN (Wan et al., 2015). The low forces are probably generated in a myosin independent manner, whereas the high forces require myosin contractility. Even in the absence of the mechanosensitive activation of signalling, mechanical forces have strong effects on membrane receptor–ligand complexes by changing the rate of their dissociation.

Most protein–protein bonds are slip bonds, for which stability decreases when pulling forces are applied. In special cases, pulling can induce conformational changes within the proteins and somehow stabilize the bond. These types of bond, termed catch bond, have been observed in various adhesion receptors, such as integrins, and also in the T cell receptors (TCR) (B. Liu, Chen, Evavold, & Zhu, 2014) but this has not yet been proved in B cells. In B cells, it has been proposed that pulling on the antigen-bound BCR against resistance from the APC contributes to affinity discrimination by B cells because bonds with low-affinity antigens, but not high-affinity antigens, rupture before inducing a biological response(Natkanski et al., 2013). This is particularly important for affinity-dependent extraction of antigens, in which bonds need to sustain extraction forces before antigens are endocytosed by the B cell. The mechanical extraction of antigen provides an advantage for high-affinity B cells during antibody responses (Tolar, 2017).

Thus, mechanical aspects of B cell synapse emerges as a pivotal feature regulating the B cell immune synapse formation, activation, and eventually antigen extraction. More on cellular mechanics and its role in different cells and systems are mentioned in discussion.

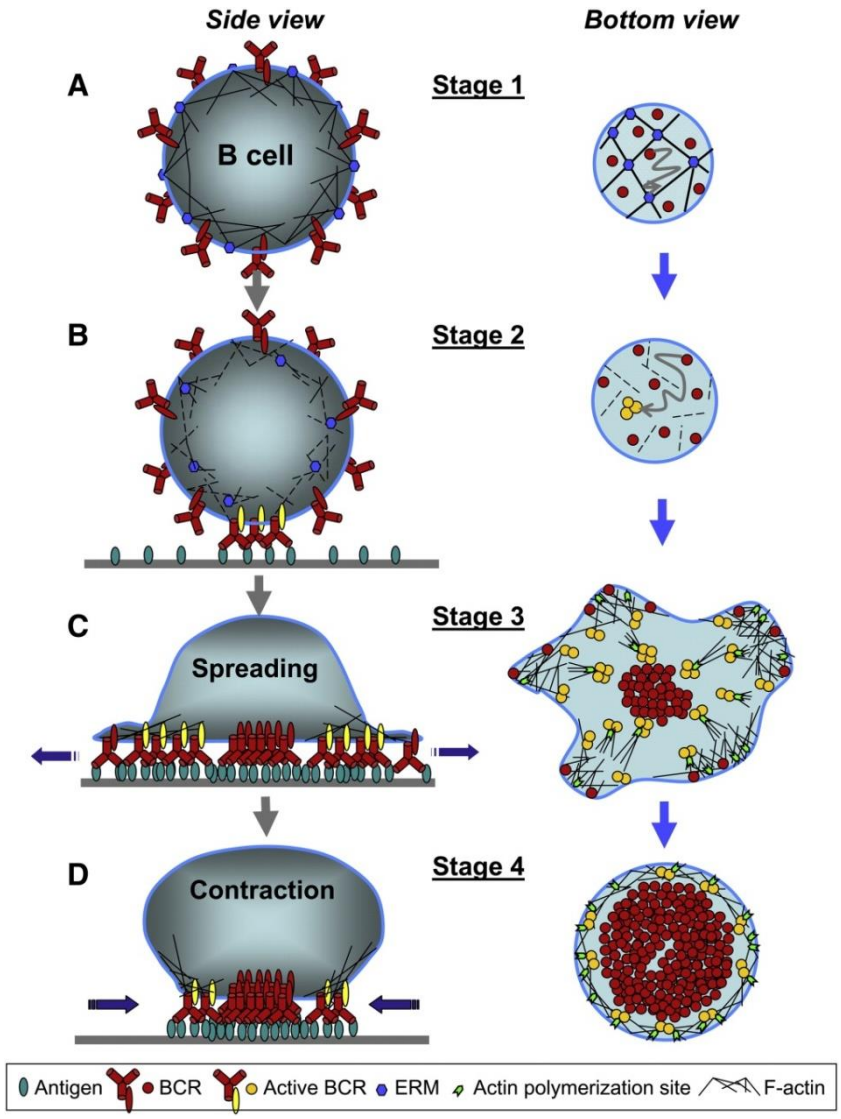

Figure 16. The coordination of BCR and actin dynamics during signalling activation:

Stage 1: In resting B cells, surface BCRs and BCR nanoclusters have a relatively limited lateral mobility, which is constrained by the cortical actin network tethered to the plasma membrane by the interaction of ERM proteins with membrane anchored proteins. (B) Stage 2: In response to the binding of membrane-associated antigen, the lateral mobility of BCRs is transiently increased, which is concurrent with the detachment of the cortical actin from the plasma membrane and a transient actin disassembly. This is followed by receptor immobilization and the formation of small clusters, triggering signalling activation. (C) Stage 3: B cell spreading on antigen-associated membrane increases the number and sizes of BCR clusters as the signalling level rises. Actin polymerizes and is accumulated at the leading edge of the spreading membrane and at BCR microclusters. (D) Stage 4: BCR microclusters merge into a central cluster at one pole of the cell while the B cell contracts. The actin cytoskeleton reorganizes away from BCR clusters to the outer rim of the BCR central cluster. The signalling activity of BCRs in the central cluster is reduced. (Song, Liu, & Upadhyaya, 2014)

B cell spreading and BCR clustering

Dynamic changes in the actin cytoskeleton upon immune synapse formation induces B cell spreading, which helps to promote the gathering and extraction of membrane-tethered antigens. BCR activation is triggered by receptor clustering that induces receptor phosphorylation and signalling cascades (Tolar, Sohn, & Pierce, 2005). During signalling activation, occurrence of BCR clustering can be temporally described in four stages on rigid but fluid surface like supported lipid bilayer:

1. In the first stage BCRs exist in nano-clusters that have limited lateral mobility, an average diffusion coefficient of IgM-based BCR in naïve primary B cells of ~0.03 $\mu m^2/s$ (Tolar, Hanna, Krueger, & Pierce, 2009),(Treanor et al., 2010) **(Figure 16A)**.
2. In the second stage in response to the binding of antigen, the lateral mobility of BCRs transiently increases (~0.05 $\mu m^2/s$ for membrane-associated antigen), enabling interactions between BCRs and their nano-clusters to lead to the formation of microclusters (Fleire et al., 2006) (Treanor et al., 2010), (Treanor et al., 2011)**(Figure 16B)**.
3. In the third stage, the B cell spreads on antigen-associated membrane (Fleire et al., 2006), thereby driving the formation of more BCR microclusters. Newly formed BCR microclusters move centripetally to one pole of the cells or to the center of the cell surface contact zone, recruiting more BCRs and apparently colliding with each other along the way (Tolar et al., 2009)**(Figure 16C)**
4. In the final stage, BCR microclusters merge together, resulting in the formation of a central cluster either at one pole of the cell (for soluble antigen) or in the center of the B cell contact zone (Carrasco, Fleire, Cameron, Dustin, & Batista, 2004) and (Tolar et al., 2009)**(Figure 16D)**.

Actin polymerization at the membrane edge generates lamellipodia, the contact of lamellipodia with the antigen presenting cell is followed by integrin (LFA-1 and VLA-4) mediated adhesion, which stabilizes the synapse and contributes to the synaptic architecture (Carrasco & Batista, 2006)(Carrasco et al., 2004). Soon after actin reorganization, lamellipodial extensions proceed through cycle of protrusion and retraction (Tolar et al., 2009). It has been shown in fibroblasts that these protrusions are driven by actin polymerization at the leading edge of the cell, while the retractions are mediated by the non-muscle Myosin IIa pulling from the back of the lamellipodia (Giannone et al., 2017). Actin polymerization at the edges generates forces perpendicular to the edge of the synapse that initiate the centripetal BCR movements (Fleire et al., 2006)(Song et al., 2014). During the last stage of BCR clustering, the levels of F-actin diminish in the centre of the B cell contact zone as B cells contract and BCR microclusters merge into a central cluster (Song et al., 2014). To conclude, B cells spread around antigen-associated membranes and start the formation of microclusters. These microclusters move centripetally and fuse into a big central cluster.

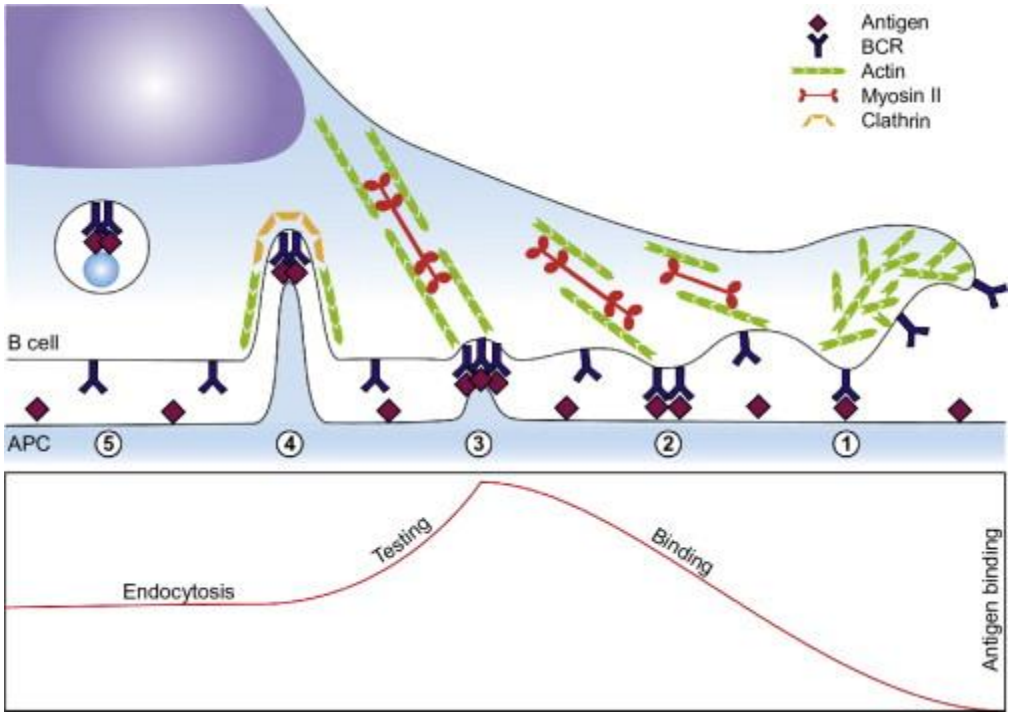

Figure 17. Mechanics of BCR binding at the B-cell synapse:

Schematic depiction of the B-cell synapse (top) and the amount of local antigen binding (bottom). (1) BCR signalling in lamellipodia stimulates actin polymerization, protrusion of the leading edge, and pushing of the B cell membrane into contact with the APC. Binding is limited by the incomplete alignment of the B-cell membrane with the APC. (2) BCR microclusters are transported by actin flow and by myosin IIa contractions toward the center of the contact. Binding is promoted by alignment of the synaptic membranes and by BCR clustering. (3) Myosin IIa pulls on the microclusters and invaginates the B-cell membrane. The forces trigger accelerated dissociation. (4) Formation of clathrin-coated pits (CCPs) generates additional actin polymerization and eventual endocytosis of the antigen. (5) Forces are terminated and endocytosis reads the final number of antigens bound to the BCR . (Tolar & Spillane, 2014)

B cell contractile phase

B cell spreading is short lived and contractions starts already after 2-3 minutes (Fleire et al., 2006). Spreading pushes B cell membranes to contact antigen coated surface but initial binding of B cell membrane and antigen coated surface is limited because they are not completely aligned to be pulled back together **(Figure 17-1)**. Membrane alignment is reinforced by the actin flow and myosin II contractility, which helps transporting BCR microclusters towards the centre of the synapse **(Figure 17-2)**. During the contractile phase, myosin activity builds up and continues to pull on antigen microclusters creating local, unsynchronized invaginations throughout the synapse (Natkanski et al., 2013) **(Figure 17-3)**. Invaginations appear to be initiated by actin polymerization together with recruitment of myosin II. Myosin very quickly clears from the proximity of microclusters, while F-actin remains associated to them. How myosin II pulls microclusters inward is yet to be understood. What is known so far is that myosin II is very dynamic at the B-cell synapse, which results from the phosphorylation of the myosin II regulatory light chain (Vascotto et al., 2007). Myosin II contractility at the B cell synapse and potential involvement of Rock1 suggests that myosin II is activated by the canonical pathway downstream of RhoA. RhoA has been reported to be activated upon BCR engagement (Saci & Carpenter, 2005) and is required for B-cell development (Zhang, Zhou, Lang, & Guo, 2012). Myosin II thus plays an important role in B cell activation, although the pathways that activate RhoA are not fully understood. Once microclusters have been pulled towards the centre of the synapse, formation of clathrin-coated pits (CCPs) generates additional actin polymerization and eventual endocytosis of the antigen (Natkanski et al., 2013). Natkanski et al., showed that knocking down clathrin leads to substantial reduction of internalization of both soluble and membrane presented antigen-BCR complexes **(Figure 17-4)**. Upon CCP formation, forces are terminated and endocytosis reads the final number of antigens bound to the BCR **(Figure 17-5)** (Tolar & Spillane, 2014).

Thesis objective

Non-muscular myosin II is an actin-based molecular motor responsible for contraction of the actin network and stress-fiber tension in the context of cell adhesion. The first antigen internalization model of membrane spreading and contraction(Fleire et al., 2006) as described in the introduction did not directly involve myosin II, but this protein was subsequently found to be responsible for the contraction phase, through the generation of an actin flow (C. Liu, Miller, Orlowski, et al., 2012), (C. Liu, Miller, Sharma, et al., 2012). In the second mode showing pulling of BCR-antigen complexes (Natkanski et al., 2013) where myosin II was implicated in the internalization of individual BCR-Ag complexes (Natkanski et al., 2013).This second model provides a molecular explanation, but the link between the molecular and macroscopic scales remains unclear.

The main goal of my thesis was to (1) measure forces at B cell immune synapse using a physiological antigen presenting surface and (2) to understand their origin and involvement in antigen extraction, ultimately to be able to bridge the scales between the two models mentioned above.

Results

Mechanics and force patterning in antigen extraction by B cells

Abstract: B cells are the cells that produce antibodies and are therefore essential effectors of adaptive immunity. *In vivo*, their activation is mostly triggered by the engagement of their B cell receptor (BCR) with antigens exposed at the surface of neighboring antigen presenting cells. This leads to formation of an immune synapse that coordinates the signaling and cytoskeleton rearrangement events that are essential for B cells to extract and process antigens. Two models have been proposed for extraction of surface-tethered antigens by B cells: (1) Membrane spreading followed by cell contraction and (2) direct mechanical pulling on BCR-antigen molecular complexes. In this study, we developed a method for extracting force patterns using antigen-coated substrate deformations for direct force visualization (traction force microscopy, TFM). Results obtained are described below.

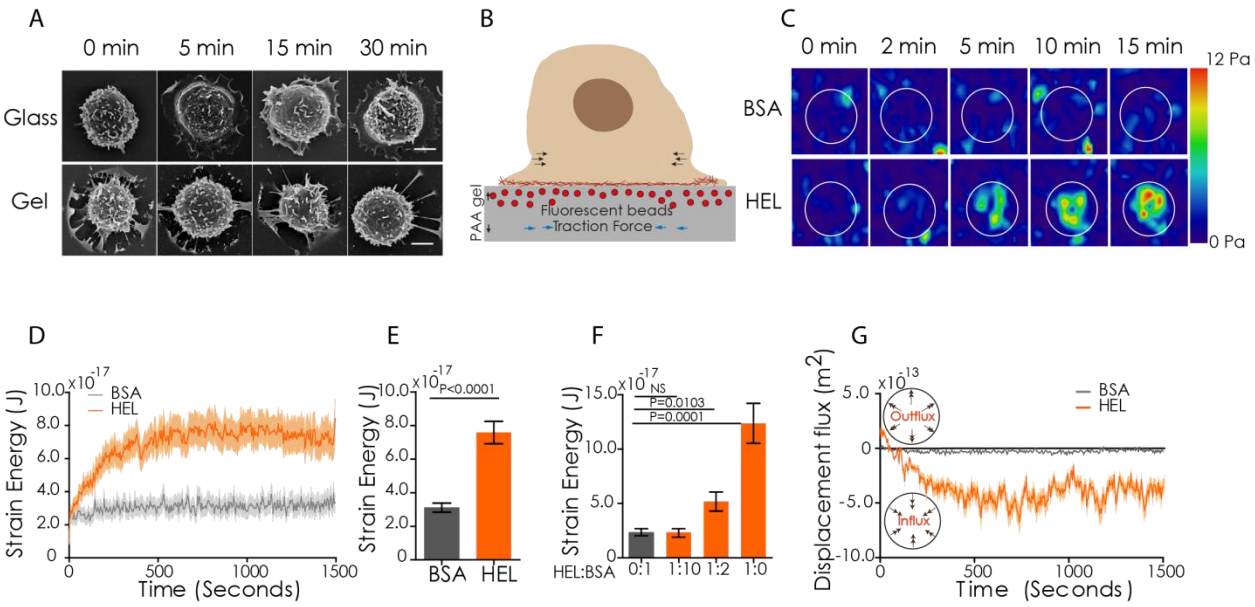

Figure 18. B cells show antigen specific traction forces on PAA gels:

(A)Scanning electron microscopy of fixed B lymphocytes on HEL coated glass and polyacrylamide gels, scale bar is 2µm (B) Cartoon showing B cell plated on antigen coated PAA gel containing fiducial markers. (C) Representative force map images for HEL and BSA condition (D) Graph representing average energy profile for HEL and BSA conditions, Error bars represent Mean±SEM (n=65 for HEL and n=35 for BSA, 5 independent experiments , 5 mice). (E) Summary statistics of HEL and BSA, error bar represents Mean±SEM (n=65 for HEL and n=35 for BSA, 5 independent experiments, 5 mice), Mann Whitney test was performed for statistical analysis. (F) Graph representing concentration dependent decrease in strain energy, error bars representing Mean±SEM (n=10-15 , 3 independent experiments, 3 mice), Mann Whitney test was performed for statistical analysis.(G) Displacement flux showing the direction of displacement over time in HEL and BSA condition (n=65 for HEL and n=35 for BSA, 5 independent experiments, 5 mice).

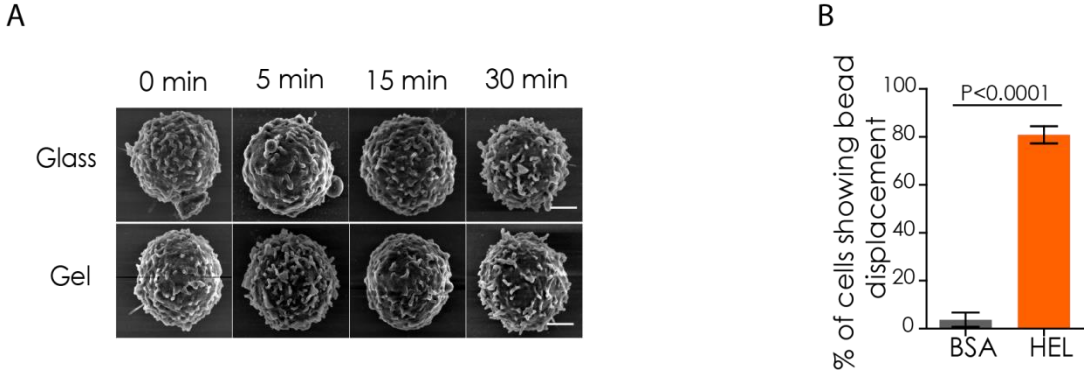

Figure 19: B cells exert BCR-antigen specific traction force on PAA gels:

(A) Scanning electron microscopy of fixed B cells on BSA coated glass and polyacrylamide gels, scale bar is 2µm. (B) Graph representing percentage of B cells showing bead displacement in HEL and control BSA condition, error bars represents mean±SEM, Mann Whitney test was performed for statistical analysis.

I. B cells exert measurable forces at the immune synapse

We used traction force microscopy (TFM) on polyacrylamide (PAA) gels to analyze the spatiotemporal distribution of forces at the B-cell synapse. We plated primary naive B cells purified from the spleen of MD4 transgenic mice expressing a hen egg lysozyme (HEL)-specific BCR. We coated the gels with the specific antigen (HEL) or with BSA as a negative control. A rigidity of 500 Pa was selected, as this matches the physiological rigidity of macrophages, the cells typically responsible for antigen presentation in lymph nodes (Bufi et al., 2015). Surprisingly, no B-cell spreading was observed on 500 Pa gels whereas such spreading was clearly visible on antigen–coated glasses **(Figure 18A and 19A).** We performed force measurements on gels containing fluorescent beads as fiducial markers, by time-resolved Fourier transform traction force microscopy **(Figure 18B)** (Sabass, Gardel, Waterman, & Schwarz, 2008). We observed the arrival of cells on the substrate in order to determine the initial contact time. No forces were observable on gels with a rigidity exceeding 500 Pa, probably because the movements in such conditions would be too small to be detected. Shear stress was of the order of 15 Pa, with peaks at 40 Pa. Interestingly, such movements were almost totally absent on BSA–coated gels: only 10% of the cells on such gels responded, versus 90% of the cells on HEL–coated gels **(Figure 18C and 19B)**.

We compared the behavior of B cells at the various time points, by calculating the energy involved in this process (as the sum of the local forces times the displacement in the same direction). Strain energy analyses showed that there was a growth phase lasting about 10 min, followed by a plateau **(Figure 19D and 19E)**. The energy of the plateau displayed almost linear dose dependence **(Figure 19F)**. We investigated whether the forces exerted by B cells were directed mostly inward or outward, by calculating the flux of a 2D deformation field through cell boundaries **(Figure 19G)**. These fluxes were mostly negative, even in the rare cells exerting measurable forces on BSA-coated gels. We conclude that B cells exert increasingly contractile pulling forces on substrates of physiological rigidity in an antigen dose-dependent manner.

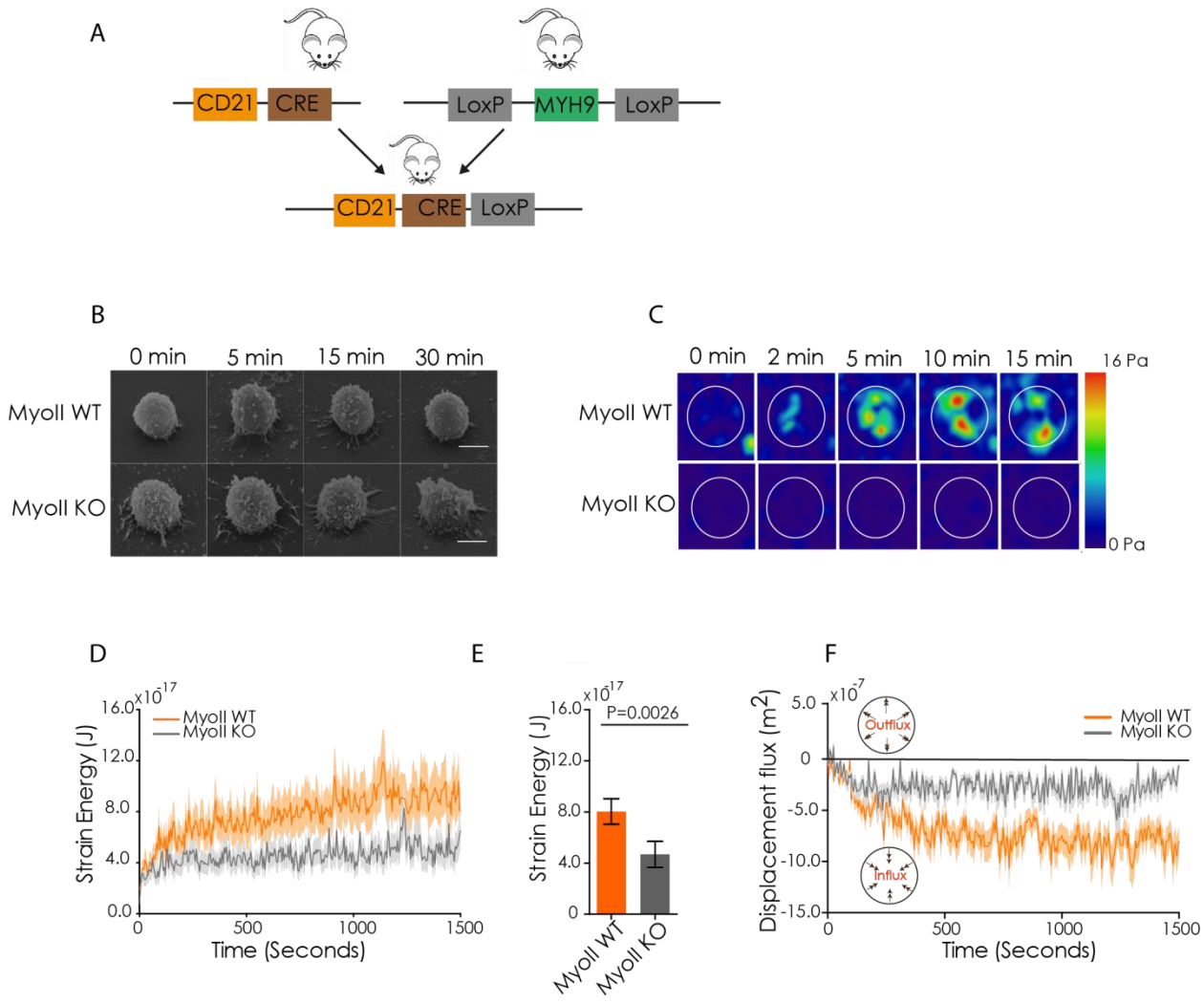

Figure 20. Myosin II is essential for force generation by B cells:

(A) Genetic approach used to ablate Myosin IIA specifically in B cells. (B) Scanning electron microscopy of fixed B lymphocytes in Myosin IIA knock out and wild type condition. scale bar is 5µm (C) Representative force map images for MyoII KO and MyoII WT condition. (D) Graph representing average energy profile for HEL and BSA conditions, Error bars represent Mean±SEM (n=23, 4 independent experiments, 4 mice). (E) Summary statistics of MyoII KO and MyoII WT , error bar represent Mean±SEM (n=23, 4 independent experiments, 4 mice), Mann Whitney test was performed for statistical analysis. (F) Displacement flux showing the direction of displacement over time in MyoII KO and MyoIIWT condition (n=23, 4 independent experiments, 4 mice).

II. Forces at the immune synapse are myosin II dependent

In typical traction force microscopy experiments, contractile forces are exerted on the substrate via focal adhesions. However, this is not the case for B cells, which do not form such adhesive structures. Myosin II was found to be involved in the internalization of the BCR-bound antigen and (more importantly) in generation of the force used by the cell to discriminate between low and high-affinity antigens (Natkanski et al., 2013). We thus investigated the potential role of myosin II in force generation, using conditional knockout mice for myosin IIA, the principal isoform of myosin II expressed in mouse B cells. These mice were generated by crossing mice bearing the MYH9 floxed allele with mice expressing the Cre recombinase under control of the CD21 promoter **(Figure 20A, 21A)**, and are referred to hereafter as myosin II KO mice. B cells extracted from MD4-Myosin II KO mice spread less on the gel but had larger numbers of protrusions around the cell body than those from wild-type mice **(Figure 20B)**, consistent with impaired actin protrusion retraction in the absence of myosin II. Myosin II KO cells exerted considerably less force (or contractile energy) than WT cells **(Figure 20C)**. About 30% of myosin II KO cells responded, albeit less strongly than WT B cells, accounting for the slightly higher mean values than for the BSA control **(Figure 20D and 20E)**. Measurable forces detected in myosin II KO cells were contractile, as shown by the field fluxes in **(Figure 20F)**. Similar results were obtained when inhibiting myosin II with para-nitro-blebbistatin **(Figure 21B)**. Thus, both genetic and pharmacological approaches show that the traction forces exerted at the B cell synapse depend on myosin II.

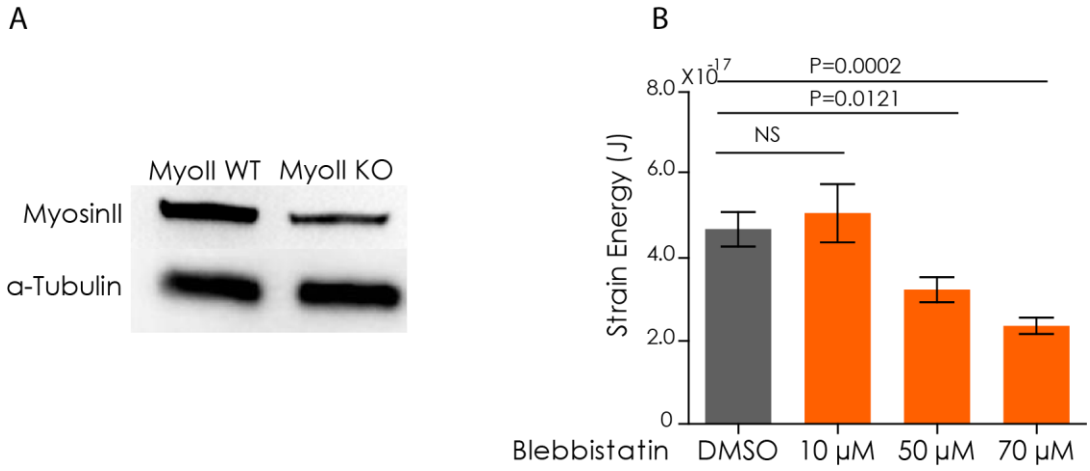

Figure 21: Inhibiting myosin II with blebbistatin reduces traction forces in a dose dependent manner:

(A) Western blot analysis of the efficiency of Myosin II knock out, a- tubulin was used as loading control. (B) Graph representing concentration dependent decrease in strain energy of blebbistatin treated B cells, error bars representing Mean±SEM (n=10-15, 3 independent experiments, 3 mice), Mann Whitney test was performed for statistical analysis.

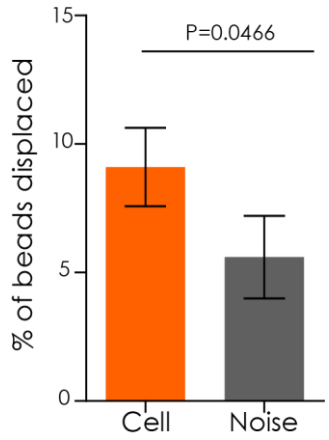

Figure 22: Non-coordinated displacements are not resulting from gel deterioration:

Graph representing percentage of bead displaced on removing the cells after the experiments, Mean±SEM (n=15), Mann Whitney test was performed for statistical analysis.

III. The immune synapse displays specific force patterns

As mentioned above, TFM experiments are classically used to measure forces transmitted by cell focal adhesions, the movements of a single bead being accompanied by the movements of neighboring beads. Indeed, the algorithm for force calculation from bead displacement is based on two hypotheses that (1) the forces are transmitted in two dimensions only and (2) gels are linearly elastic (modeled with Boussineq Green's function). We found that a few beads did not display movements parallel to the one of their neighbors, as it would be expected from a force field displaying decay as the inverse of the distance from the application point. There are two possible reasons for this: (1) the gel may be altered by the cell, irreversibly changing its elastic properties or (2) the forces exerted by B cells may have a component along the Z axis in addition to their shear component. In this case, the classical 2D inversion algorithm is not applicable. We tested the first hypothesis, by detaching the cells at the end of TFM experiments (30 min after plating) and measuring the percentage of beads displaying at least one movement during recording and that had returned to their original position (with a margin of error of 50 nm). We compared this analysis with another performed on a region devoid of cells, as defocusing, bleaching or illumination might generate apparent noise. This analysis showed the vast majority of beads returned to original position upon cell detachment indicating that the elastic properties have not been altered by B cells **(Figure 22)**. We conclude that non-coordinated displacement is an intrinsic property of the system, suggesting that it results from bead movements in Z axis.

We investigated the nature of the forces measured further, by splitting the pool of beads into two groups based on the correlation of the directions of displacement vectors within neighbors, within a range of 1µm **(Figure 23A)**. For each frame, we split the beads in two groups: coordinated ($r>0.5$) and non-coordinated ($r<0.5$), being the correlation coefficient. Each group was analyzed independently, by interpolating the displacement field to obtain two independent force fields, from which strain energies were calculated.

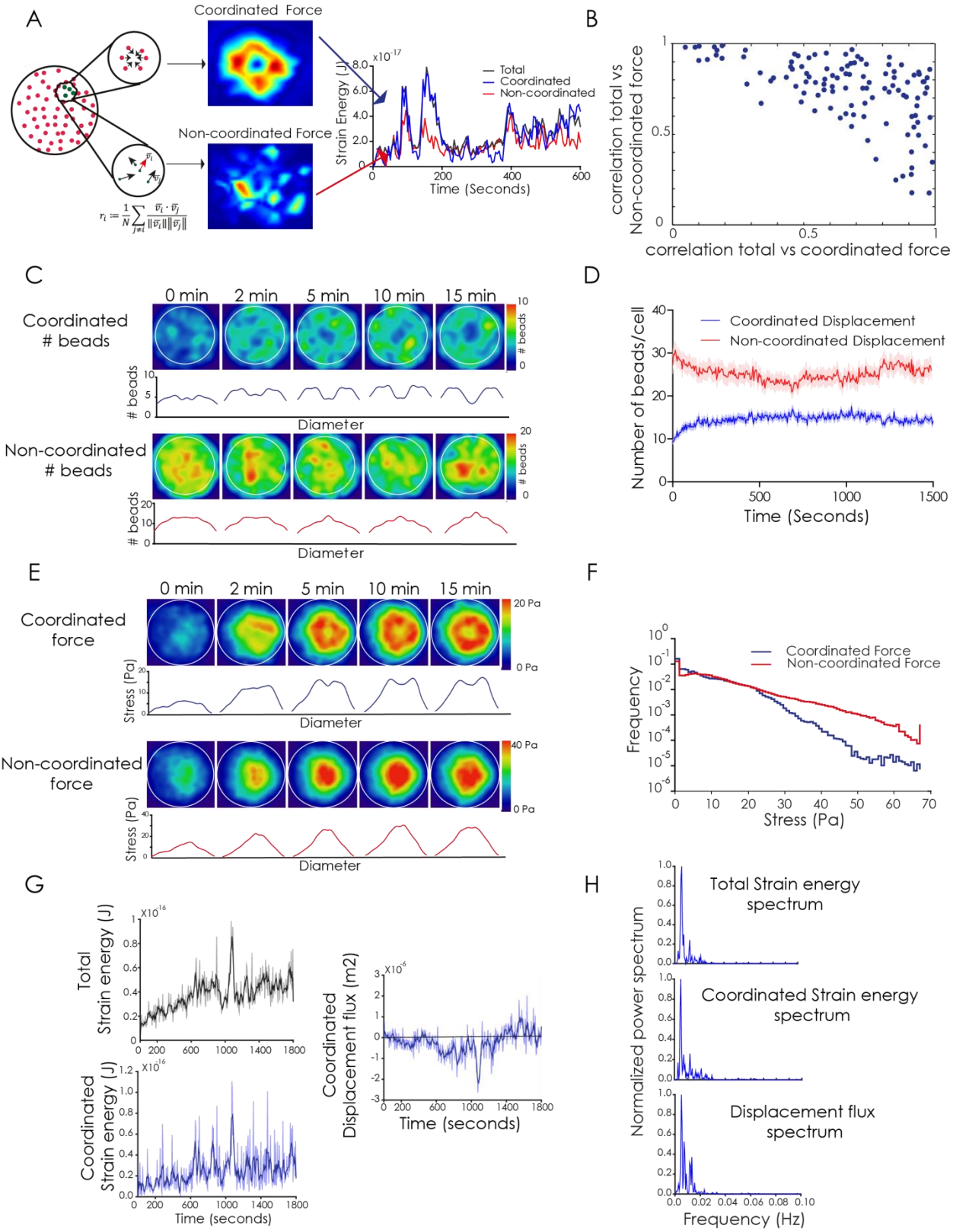
A
Coordinated Force
Non-coordinated Force
Strain Energy (J)
Total
Coordinated
Non-coordinated
Time (Seconds)
B
correlation total vs Non-coordinated force
correlation total vs coordinated force
C
0 min
2 min
5 min
10 min
15 min
Coordinated # beads
Non-coordinated # beads
beads
Diameter
D
Coordinated Displacement
Non-coordinated Displacement
Number of beads/cell
Time (Seconds)
E
Coordinated force
Non-coordinated force
20 Pa
0 Pa
40 Pa
Stress (Pa)
Diameter
F
Coordinated Force
Non-coordinated Force
Frequency
Stress (Pa)
G
Total Strain energy (J)
Coordinated Strain energy (J)
Coordinated Displacement flux (m2)
Time (seconds)
H
Total Strain energy spectrum
Coordinated Strain energy spectrum
Displacement flux spectrum
Normalized power spectrum
Frequency (Hz)

All cells display both force components, in various proportions, at each time point. We identified the cells with the most coordinated forces, by calculating the coefficients for the correlations between total energy and coordinated energy and between total energy and non-coordinated energy **(Figure 23B)**. The cells on the left of the dot plot are those with markedly coordinated forces. Density maps and relative radial scans **(Figure 23C)** revealed a distinct separation into two pools, within as little as two minutes of contact. The beads displaying coordinated movement were located at the periphery of the synapse (about 2 μm from the center), whereas the non-coordinated pool was located at the center of the synapse. The number of beads moving in a coordinated manner increased with time, reaching a plateau about two to three minutes after initial contact and the number of beads moving in a non-coordinated manner decreased **(Figure 23D)**.

Calculation of coordinated and non-coordinated displacements and forces for each cell at each time point showed that coordinated forces operated at the periphery and were organized centripetally. In contrast, non-coordinated forces were generally located in the center and oriented randomly **(Figure 23E).**

The global distribution of force magnitudes into a non-coordinated component (each pixel) displayed a single exponential decay pattern **(Figure 23F)**, whereas the coordinated component displayed a two-scale decay pattern, consistent with the presence of a small but measurable pool of high-stress peaks. Noise was distributed similarly to the non-coordinated component (data not shown). The presence of rare, but strong stress is, therefore, a signature of the coordinated component. We conclude that within 2 minutes from the contact, cells build up a centripetal contractile stress, with rare peaks at 40Pa, accompanied by a central disordered field of forces.

In terms of dynamics, the coordinated component of the strain energy and flux (displacements or forces) contained peaks correlated with isolated global contractions **(Figure 23G)**. After detrending and smoothing, the spectrum obtained for flux displayed Gaussian-like behavior, with a maximum highlighting the presence of a characteristic time scale. In signals with prevalent coordinated forces, these peaks are clearly identifiable, with a typical time of 167±7s **(Figure 23H)**. Non-coordinated forces yielded

Figure 23. Two components of forces:

(A) Scheme showing two pools of forces, coordinated shows a peripheral ring at the peaks whereas non-coordinated is randomly distributed. (B) Distribution of each cell in the profile shows correlation of total forces to coordinated force and non-coordinated forces respectively. (C) Mean bead distribution in coordinated and non-coordinated type of forces (n=100 cells). Graph represents the radial profile of the density map obtained by average spatial distribution of the beads by resizing all cells and interpolating each bead with a Gaussian kernel. (D) Graph representing number of beads per cell over time in coordinated and non-coordinated type of forces. Error bars represent Mean±SEM. (E) Mean force density map ,obtained by resizing and averaging over all cells in coordinated and non-coordinated type of forces (n=37) (F)graph showing distribution of magnitude of forces in coordinated and non-coordinated components. (G)Graph showing dynamic peaks in total and coordinated strain energy, displacement flux of coordinated component showing inward centripetal displacements. (H) Detrended and smooth spectrum of total energy, coordinated energy and displacement flux showing the peaks.

individual peaks that could be linked to single-bead movements. In conclusion, nearest-neighbor correlations between the displacement vectors of the beads revealed that most B cells exert two types of force: peripheral coordinated and central non-coordinated forces. The peripheral forces displayed pulsatile contractions at intervals of about 2.5 min.

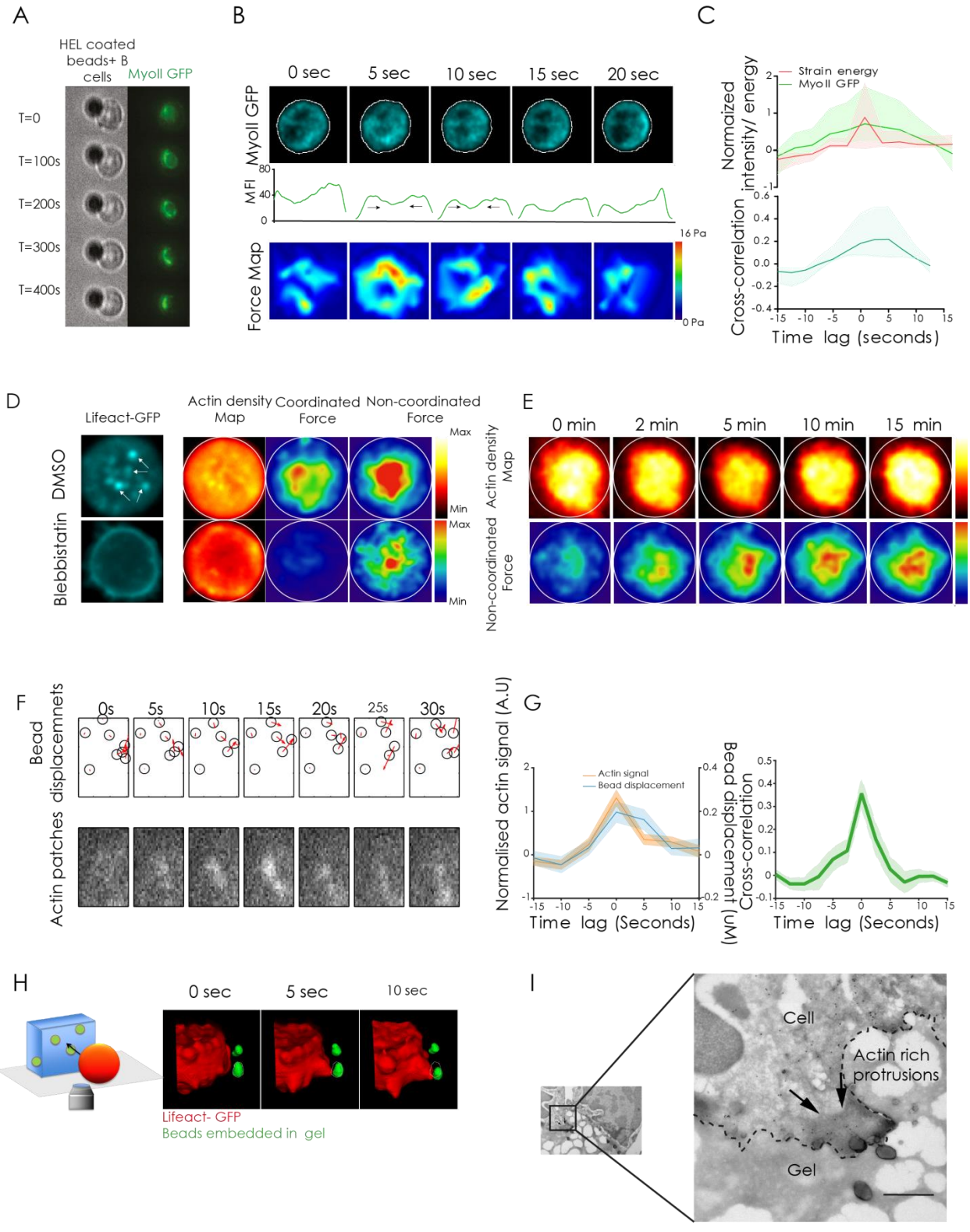
A
HEL coated beads+ B cells
MyoII GFP
T=0
T=100s
T=200s
T=300s
T=400s
B
0 sec
5 sec
10 sec
15 sec
20 sec
MyoII GFP
MFI
80
40
0
16 Pa
Force Map
0 Pa
C
Strain energy
MyoII GFP
Normaized intensity/ energy
Cross-correlation
Time lag (seconds)
D
Lifeact-GFP
Actin density Map
Coordinated Force
Non-coordinated Force
DMSO
Blebbistatin
Max
Min
Max
Min
Actin density Map
Non-coordinated Force
E
0 min
2 min
5 min
10 min
15 min
F
Bead displacemnets
0s
5s
10s
15s
20s
25s
30s
Actin patches
G
Normalised actin signal (A.U)
Actin signal
Bead displacement
Time lag (Seconds)
Bead displacement (uM)
Cross-correlation
Time lag (Seconds)
H
0 sec
5 sec
10 sec
Lifeact- GFP
Beads embedded in gel
I
Cell
Actin rich protrusions
Gel

IV. Actin and myosin II patterns at the synapse follow force patterns

Does myosin II generate both coordinated and non-coordinated forces? To answer this question we monitored the dynamics of myosin II GFP at the synapse forming between the cell and the antigen-coated gel. We found that myosin II accumulate at the synapse plane, consistent with experiments in which antigens were presented to B cells on trapped beads from the side **(Figure 24A)**. Observations of single cells on gels showed that the collective contractions described in previous result section corresponded to collective pulsing of the myosin accumulated in concentric rings **(Figure 24B)**. This feature became even more evident when the results were averaged over 40 peaks **(Figure 24C)**. Cross-correlation analysis showed that myosin II peaks preceded force peaks by at least five seconds **(Figure 24C)**, suggesting that the motor protein is directly involved.

Analysis of Lifeact-GFP dynamics revealed the presence of patches of actin at the center of the synapse **(Figure 24D)**. These central actin structures did not form in the absence of myosin II activity **(Figure 24D)**. In addition, central non-coordinated forces generally followed the same pattern as dynamic actin microclusters **(Figure 24E)**. Strong non-coordinated forces were found apposed to actin patches and these two observations were correlated over time **(Figure 24F)**. These findings suggest that actin patches are responsible for the strongest non-shear forces that we classified as non-coordinated forces (**Figure 24G)**. Given the resolution of the system, it was not possible to monitor the 3D movements of the beads. However, we observed protrusions associated with bead movement on antigen-coated gel pieces presented laterally to B cells **(Figure 24H)**. The presence of these actin-enriched protrusions was further confirmed by electron microscopy **(Figure 24I)**. We conclude that, at the cell-gel interface, the peripheral centripetal organization of forces is regulated by collective contractions of actomyosin, with central structures mostly associate to actin protrusions but dependent on the myosin II.

Figure 24.Myosin II and actin dynamics follow force pattern:

(A) Time-lapse images showing myosin II accumulation at the synapse formed between antigen coated bead and primary B cell. (B) Time-lapse image showing dynamics of myosin II and corresponding force, graph represents line scan across the cell, arrowhead points to contraction. (C) Graph represents average of different peaks (n=40) and cross correlation between strain energy and myosin II peak intensity. (D) Left, single cell showing actin patches in the centre of the cell which are lost in case of blebbistatin treated cells. Right, Mean actin distribution, mean coordinated and mean non-coordinated force in control and blebbistatin treated B cells (n=12). (E) Mean actin distribution over time correlates with mean non-coordinated force distribution. (F) Time-lapse images showing simultaneous appearance of actin patches and bead displacements, arrowhead showing direction of displacement. (G) Graph representing correlation between actin patch appearance and bead displacement. (H) Protrusions associated with bead movement (green) on antigen coated gels pieces presented laterally to B cell (red). (I) Electron microscopy image showing actin protrusions through PAA gel. (scale bar 0.2 μM).

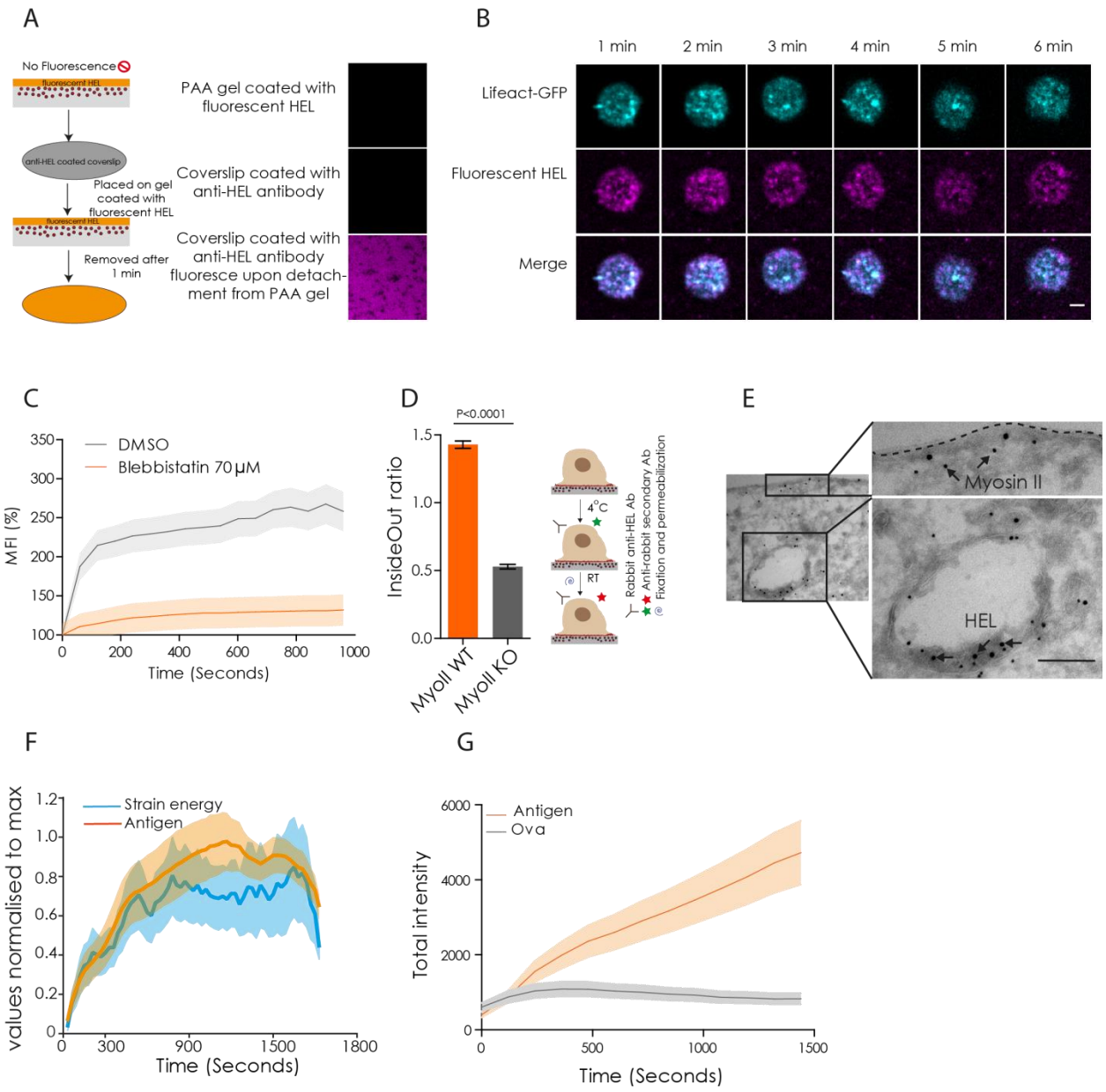

Figure 25. Antigen Internalization:

(A) Scheme showing stripping experiments. (B) Time-lapse of Lifeact GFP and fluorescent HEL. Scale bar is 2 µm (C) Graph showing antigen gathering over time in control and blebbistatin treated cells. Error bars showing Mean±SEM (n=15 DMSO, n=9 Blebbistatin). (D) Graph representing the ratio of internalized to outside antigen in Myosin II KO and WT B cells. Error bars showing Mean±SEM (n=29 Myosin II WT, n=21, Myosin II KO, 3 independent experiments, Mann Whitney test was performed for statistical analysis. (E) Scanning electron microscopy images showing internalized antigens and its proximity to myosin II (scale bar 0.2µM). (F)Graph representing profile of strain energy and antigen gathering. (G) Graph showing specific increase in the intensity of antigen overtime upon B cell contact as compared to unspecific Ova. Error bars represent Mean±SEM (n=67Antigen, n=67 Ova, 2 independent experiments).

V. Antigen internalization is dependent on the action of actomyosin

We next investigated whether force organization at the synapse regulates site of antigen extraction. We coated our gels with fluorescently labeled antigens. No fluorescence signal was detected for HEL-AF455 attached to the gel surface, although immunolabelling revealed the presence of the protein. We hypothesized that this might result from quenching of AF555 by the gel. Consistent with this hypothesis, we found HEL-AF555 signal was detected on detaching it from the gel **(Figure 25A)**. This unexpected observation provided us with a robust system to measure HEL detachment at the B cell synapse and its dependency on myosin II.

Detached antigen clusters colocalize with the actin patches described above were observed **(Figure 25B)**. Monitoring of antigen detachment in time showed that antigen extraction progressively increased in control cells, suggesting a gradual detachment of antigen starting as soon as B cells contact with the gel surface and slowing down three minutes after contact. Extraction was slower three minutes after contact. Antigen detachment was impaired in the absence of myosin activity **(Figure 25C)**. Inside-out experiments, based on the differential staining of HEL within and outside cells, showed that antigens were not only detached from the substrate, but also internalized within B cells **(Figure 25D)**. This finding was confirmed by TEM **(Figure 25E)**, which further revealed presence of myosin II on the cytosolic face of the cell containing internalized antigens.

To assess specificity of antigen internalization, we coat gels with a 1:1 mix of fluorescent HEL and ovalbumin, which is not recognized by the BCR of MD4 cells. Only HEL extraction was observed, suggesting that only molecules associated to the BCR are being internalized **(Figure 25F)**.

We next assessed the impact of myosin II *in vivo*. The number of B cells in lymph nodes did not differ significantly between myosin II KO and WT mice **(Figure 26A)**. However, upon immunization, smaller numbers of germinal center B cells were detected in myosin II KO mice **(Figure 26B)**. Histological analyses of the spleen showed the germinal center cells to be fewer in number and more disorganized in myosin II KO mice **(Figure 26C)**.

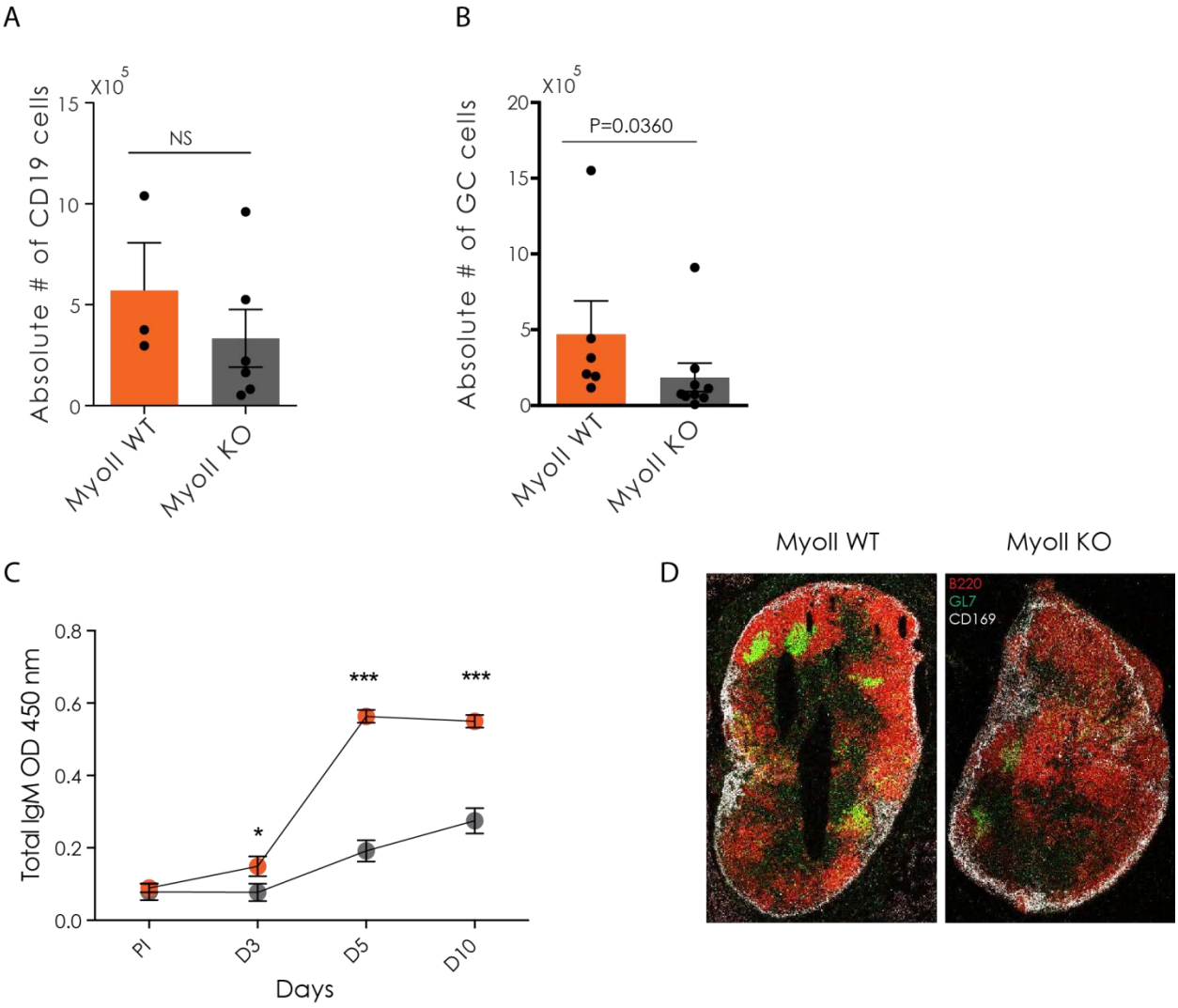

Figure 26. *In-vivo* antibody production:

(A)Graph representing absolute number of CD19 positive B cells in myosin II WT and KO mice , each dot represents one mice, from 3 independent experiments ,error bars represents mean±SEM, Mann Whitney test was performed for statistical analysis. (B) Graph representing absolute number of GC B cells in myosin II WT and KO mice, each dot represents one mice, from 3 independent experiments, error bars represents mean±SEM, Mann Whitney test was performed for statistical analysis. (C) Graph representing IgM antibody production over different days in myosin II WT and KO mice,from 3 independent experiments ,error bars represents mean±SEM, Mann Whitney test was performed for statistical analysis. (D) Histology image of spleen showing scattered GC B cells in myosin II KO mice.

Myosin II KO mice also displayed lower levels of antibody production upon immunization **(Figure 26D)**. In conclusion, we observed a strong correlation between forces and antigen internalization in vitro, which translated into a smaller capacity to mount immune responses in KO mice.

Altogether our results suggest that global B cell contractility mediated by myosin II leads to the formation of actin patches that generate non-coordinated forces responsible for the internalization of BCR ligands.

Discussion

In this work, we analyzed the spatio-temporal distribution of forces at the B cell immune synapse by using antigen – coated substrate deformation that allow direct force visualization (TFM) . We uncovered the existence of both global contractile forces at the periphery of the synapse and of local pulling forces at the center of the synapse. Peripheral contractile forces depend on centripetal organization of myosin II whereas central pulling forces are generated by F-actin protrusions that form in a Myosin II-dependent manner. Interestingly we observed collective pulsatile myosin II dependent contractions that, we suggest, are responsible for the organization of the actin structures at the center of the synapse. We further highlight the involvement of acto-myosin contractility in force generation and antigen extraction as well as in B lymphocyte response and antibody production *in vivo*. The methods and model we built might be generalizable to other systems where molecules are surface-tethered. We propose that Myosin II dependent forces may generally be involved in the endocytosis of immobilized ligands by a variety of cell types *in vivo*.

In this section I will discuss the results presented, few preliminary results and future perspectives of this work.

Cytoskeleton: Main player in B cell antigen extraction

I. Actin at the centre stage for B cell antigen gathering

Similar to us several groups (Batista et al., 2001) (Natkanski et al., 2013) have observed that antigen is detached from substrate despite the fact that the bond with the substrate (covalent) is stronger than the BCR-ag one. The most plausible explanation is that the detachment (prior to internalization) occurs in though multimerisation of BCRs that can yield higher stress. Additional mechanisms could include catch-bonds and 3D conformational change as discussed in the introduction section.

In antigen gathering experiments, antigen accumulation curves are different from energy curves **(Figure 25F)**. In particular a plateau is never reached, antigen is gathered linearly during the adhesion phase and continues to be accumulated more slowly in the plateau phase of the traction energy curve. This suggests that in the first phase of antigen gathering, BCR engagement is dominated by their diffusion while forces grow with the number of BCR engaged and amount of antigens detached. Cells continue to pull even when the plateau of traction forces has been reached. In the plateau, BCRs reaching the synapse and binding antigens are recruited at the periphery of the cell. Thus although BCR interact with antigen, internalization is happening on a slower time scale. We stop most of our observations after 15-20 minutes because of antigen/fluorophore degradation or segregation into subcellular acidic compartments. In contrast to Natkanski et al., we show co-localization of actin with antigens but not with myosin II. However, as antigens are not visible until they detach from the gel, we cannot exclude that myosin II is initially recruited at the site of antigen internalization.

II. Actin structure at B cell immune synapse resemble podosomes

In B cells, podosome/ invadosome-like structures have not yet been described. However, in our work we show small yet dynamic actin structures in the center of the cells forming in a myosin II dependent manner **(Figure 24C)**. Electron microscopy images **(Figure 24I)** also demonstrated actin rich protrusions at the gel-cell interface. It has been shown in macrophages that podosomes are mechanosensing and could help in sensing stiffness of the substrate, in addition they also have pushing activity to exert protrusive forces (Labernadie et al. 2010). In T cells, robust actin polymerization at the synapse upon stimulation is well known. Actin flows centripetally in a retrograde manner, eventually disassembling near the center (Yi, Wu, Crites, & Hammer, 2012). This centripetal flow of acto-myosin is accompanied by contractile activity of Myosin II, which stabilizes the actin network and maintains radial symmetry (Yi et al., 2012) and (Babich et al., 2012). Recently the group of Michael Dustin showed the presence of two pools of dynamic actin filaments at the immune synapse. In addition to the peripheral pool, actin polymerization also occurs in smaller actin foci structures that are closely associated with newly formed TCR microclusters (Kumari et al., 2015). Function of these actin foci is to support calcium ion signalling through stabilization of PLCγ recruitment and phosphorylation. However, similar actin structures are shown to resemble podosomes or invadosomes that have been found at the T cell-APC interface (Sage et al., 2012). In line with these findings, we could hypothesise that the actin structures could be mechanosensing protrusive podosomes. However, more experiments are needed to characterize these actin structures at B cell synapse as real podosomes using immunofluorescence by staining for actin regulators like WASP, Arp2/3 and integrin associated proteins such as paxillin, talin and vinculin.

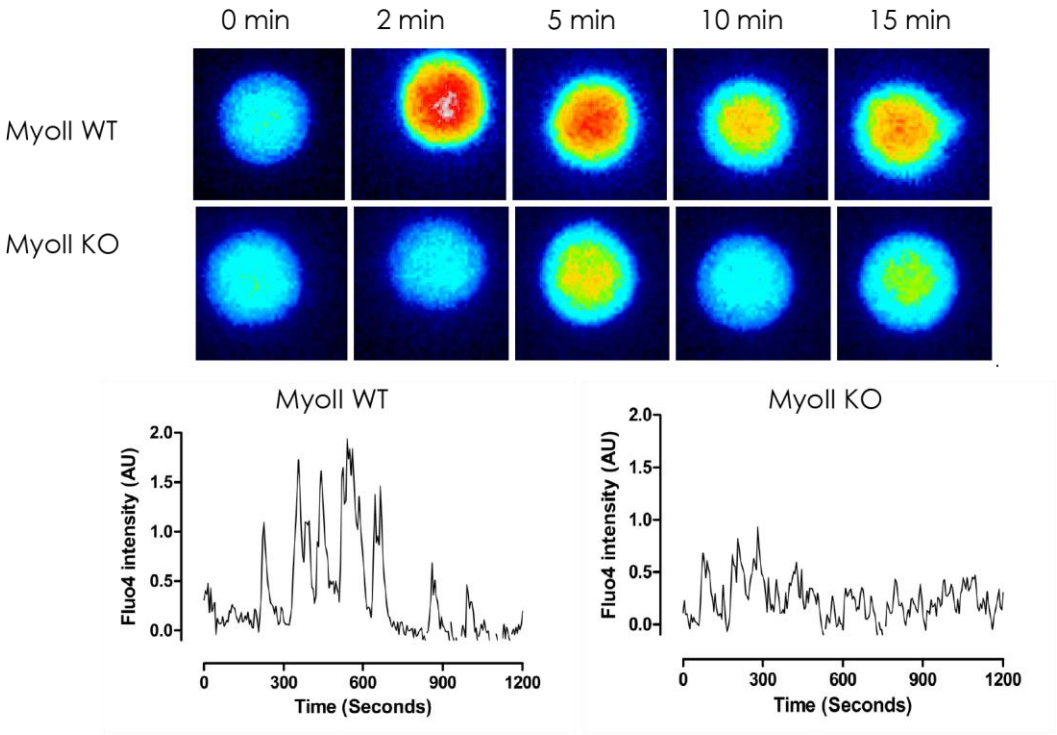

Figure 27. Calcium signalling in myosin II KO B cells:

Time- lapse montage showing Ca^{2+} oscillations in MyoII WT and KO B cells, Graph representing the profile of oscillations over time.

III. Calcium signalling in Myosin II knock out B cells

As we have discussed in the introduction, actin cytoskeleton play an important role in each step of immune synapse formation starting from B cell spreading to antigen internalization. Calcium (Ca^{2+}) signalling plays a crucial role in both B cell activation and acto-myosin contractility. Upon engagement of the BCR, the intracellular Ca^{2+} concentration increases promoting the activation of various signalling cascades including signalling via PLCγ2, Btk and BLNK (Weber et al., 2008). It is known that the activity of the actin severing protein cofilin depends directly on PLCγ, linking BCR-induced cytoplasmic Ca2+ mobilization to actin cytoskeleton reorganization and B cell spreading (Maus et al., 2013). In addition, there is evidence showing that Ca2+ signalling regulates myosin II activity in different cells (Solanes et al., 2014). Local Ca^{2+} pulses activate myosin light chain kinases (MLCK), which subsequently phosphorylates myosin light chain and triggers myosin contraction(F. C. Tsai & Meyer, 2012)(F.-C. Tsai, Kuo, Chang, & Tsai, 2015).Whether myosin II activity alters Ca^{2+} dynamics is however less clear.

Interestingly, in a preliminary experiment, we found that myosin II WT and KO B cells showed few or no Ca^{2+} oscillations upon interaction with nonspecific BSA-coated PAA gel, but both cell types exhibited increased Ca^{2+} dynamics upon interaction with BCR-specific HEL-coated PAA gel. As expected, Myosin II KO B cells showed fewer Ca^{2+} oscillation frequencies as compared to WT cells **(Figure 27)**. Diminished frequency of oscillations in myosin II KO B cells might be due to impaired signal that fails to reinforce in the absence of myosin II.

It is known that the affinity between MLCK and calcium modulating protein (calmodulin) is extremely high (Kasturi, Vasulka, & Johnson, 1993). Therefore, a slight increase of local Ca^{2+} concentration is sufficient to induce significant activation of MLCK and subsequent contraction of myosin II (F.-C. Tsai et al., 2015). Keeping these findings and our preliminary results in mind we propose that the absence of forces in myosin II KO B cells are due to reduced myosin II contractions that fails to reinforce in absence of Ca^{2+} signal. We could further investigate this by monitoring the calcium oscillations while inhibiting myosin II with blebbistatin in a dose dependent manner.

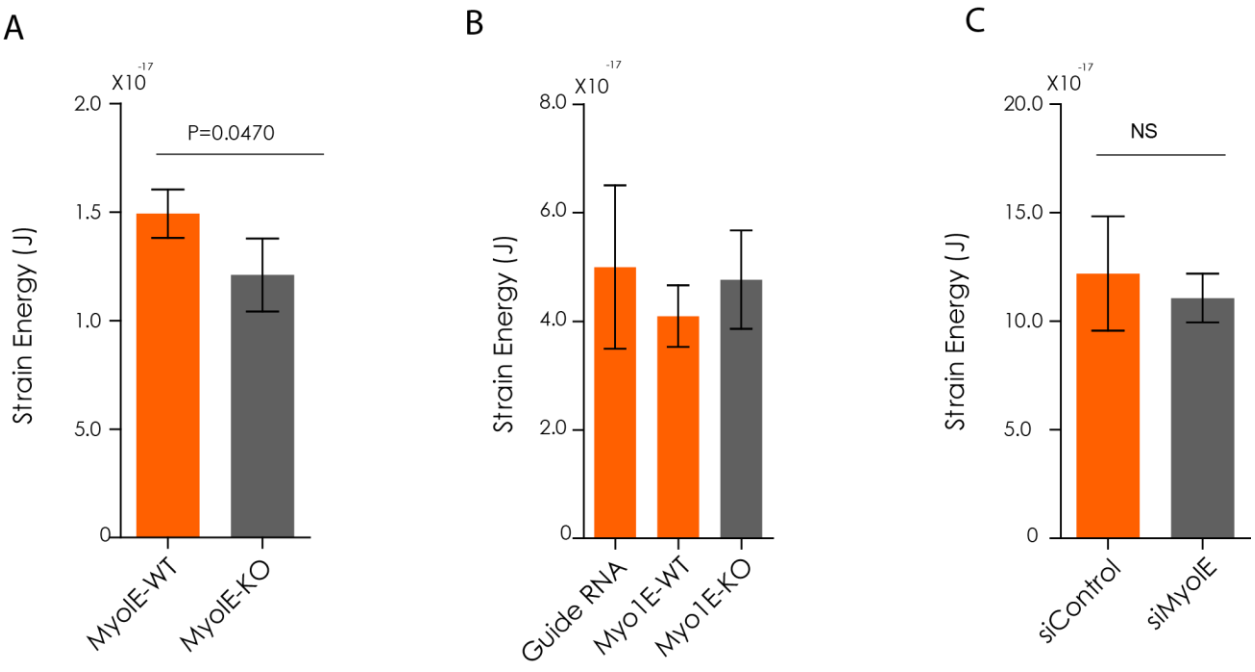

Figure 28. Myosin 1E traction force at B cell immune synapse:

(A) Graph showing comparison in strain energy of Myo1E WT and KO B cells, error bars represent mean±SEM (n=25 for WT and n=28 for KO, from 3 independent experiments), Mann Whitney test was performed for statistical analysis (B) Graph showing comparison in strain energy of crisper-cas9 induced silencing of Myo1E KO and B cells, error bars represent mean±SEM (n=13 for gRNA, n=20 for WT and n=22 for KO, from 3 independent experiments), (C) Graph showing comparison in strain energy of siRNA induced silencing of Myo1E KO and B cells, error bars represent mean±SEM (n=17 for siControl and n=22 for siMyo1E, from 3 independent experiments), Mann Whitney test was performed for statistical analysis.

IV. Role of class 1 myosin in B cell mechanics

This work provides insight into the role of myosin II in B cell mechanics. We showed the existence of two pools of forces: global contractile forces at the periphery of the synapse and local pulling forces at the centre of the synapse. Peripheral contractile forces depend on centripetal organization of Myosin II whereas central pulling forces are generated by F-actin protrusions that form in a Myosin II-dependent manner. In addition to myosin II, the lab has also been working on myosin class 1 motor protein such as Myosin 1E. Main function of the class 1 myosin motor proteins is to connect the actin cytoskeleton to cell membrane (P. Gupta, Martin, Knö Lker, Nihalani, & Sinha, 2017). Given the key roles played by myosin 1E in membrane reorganization and cytoskeleton in B cell synapse, during the end of my PhD, using my expertise to study force generation I have established collaboration with another member of the lab who was interested in evaluating force generation in B cells lacking Myo1E at B cell immune synapse. Myosin 1E is an actin based motor protein expressed in all cells. They are single headed, short tail motor proteins. There is evidence suggesting role of myosin 1E in coordinating membrane movements and actin associated forces (Yu and Bement, 2007). In fibroblasts, myosin 1E has been shown to be recruited to the sites of clathrin-mediated endocytosis together with actin. Depletion of myosin 1E caused reduced endocytosis and delayed transferrin trafficking to perinuclear region (Cheng, Grassart, & Drubin, 2012).

Very little is known on the role of myosin 1E in B cell activation, signalling and mechanics. In our lab laboratory, TIRF imaging has revealed that myosin 1E knock down (KD) B cells displayed more lysosomal recruitment and accelerated actin ring formation at the immune synapse when plated on antigen coated glass coverslips. These cells also had increased calcium oscillations. In characterizing the traction forces exerted by myosin 1E KD and KO) B cells, we used myosin 1E KO/KD B cells obtained with different approaches such as genetically knocking out the gene **(Figure 28A)**, by knocking down B cells using CRISPR-Cas9 technology **(Figure 28B)** and using siRNA technique **(Figure 28C)**. To our surprise, preliminary results show no difference between the forces exerted by myosin 1E WT and KD/KO B cells.

These results suggests that myosin 1E KD cells display increased antigen extraction, which might result from enhanced lysosomal recruitment and protease secretion rather than from increased mechanical extraction.

Physiological role of force patterns

In this work we unify two models of antigen extraction as described in results section. We developed a method to extract patterns of forces and discovered the existence of both global contractile forces at the periphery of the synapse and of local pulling forces at the centre of the synapse. Peripheral contractile forces depend on centripetal organization of Myosin II whereas central pulling forces are generated by F-actin protrusions that form in a Myosin II-dependent manner. Interestingly we observe collective pulsatile contractions that, we suggest, are responsible for the organization of the actin structures in the centre as a result of intermittent Myosin II action and in shaping a contractile peripheral pattern.

We also evidence for the first the existence of coordinated vs non-coordinated forces at the immune synapse. The pulsatile contractions observed in the coordinated component of the forces are a reminiscence of the acto-myosin flow observed in cells plated on planar lipid bilayers (Liu et al., 2012) and might allow accumulating actin, myosin and BCRs at the center of the synapse to create the critical actin structures needed for antigen internalization. Periodic contractions are not observed on lipid bilayers which might be due to the fluidity of the lipid bilayer.

We observed that a concentric pattern is therefore established via an intermittent flow generated by actomyosin contraction. This is reminiscent to what is described in (Maiuri et al., 2015), where a continuous flow of actin is required to establish a gradient of polarity cues. In our case, an intermittent flow of myosin II and actin instead of a continuous one is sufficient to create and sustain. This is due to the fact that the relevant molecules for the internalization are attached to cell membrane; hence their diffusion time (and the one necessary to destroy a pattern) is relatively long, larger than several minutes which correspond to the scale of the pulsations observed. Consistently with this hypothesis, when myosin II is inhibited, actin remains confined in the peripheral region of the synapse. Acto-myosin contractions are therefore essential to gather the machinery for the internalization towards the centre of the synapse.

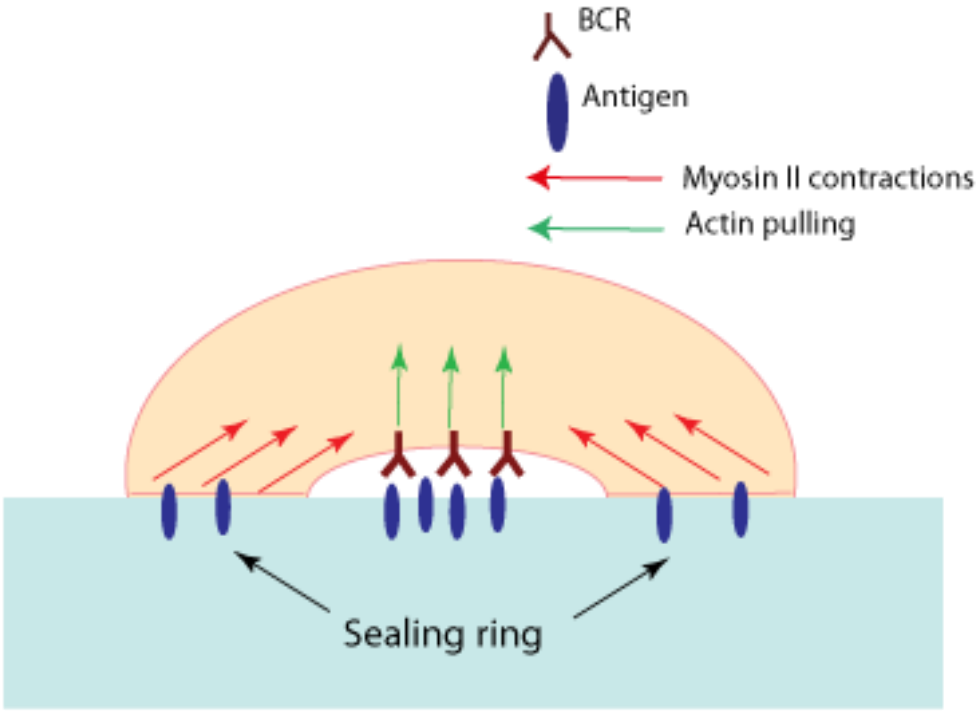

Figure 29. Schematics of the proposed model :

BCR-antigen engagement facilitates formation of acto-myosin sealing ring that would help in isolating the immune synapse from the environmental noise. Myosin II contractions at the periphery allow the formation of actin structures in the centre, that will eventually pull the antigen inside.

Note that this adds a role to the myosin II motor but does not contradict the model presented by (Natkanski et al., 2013). The interesting patterning of forces we highlight in our work raises the question not only of its origin but also of its role. The affinity discrimination model proposed by Tolar et al., relies on molecular interactions measured by DNA-force sensors or AFM measurements on the BCR-ligand system. Discrimination in terms of affinity would therefore be subjected to strong noise. The two antigens used in (Natkanski et al., 2013)to check affinity discrimination (NP and NIP) have a difference of about 1000 times. However, when rephrased in terms of difference in energy barrier at equilibrium this translates in a 2kT difference. This indicates that the difference in the barrier is almost at the thermal noise level and that could be easily overcome by application of external forces. This would imply that even a weak mechanical noise could disturb the affinity discrimination mechanism. One way for the cell to work around this problem is to protect the synapse from this external noise, lymphocytes form thick ring of acto-myosin at the periphery which effectively seal the synapse. Actin based invaginations than extract the antigen within this sealed synapse in a myosin II dependent manner **(Figure 29).** Similar organization has been known in Osteoclasts**,** these cells are responsible for physiological bone reabsorption. For efficient reabsorption, they organize their most prominent actin structures (podosomes) in to a big cloud around the bone forming lacunae (a hollow structure) and releasing proteasomes to degrade mineralized bone (Georgess, Machuca-gayet, Blangy, & Jurdic, 2014). With this analogy, we could conclude that acto-myosin cytoskeleton forms thick ring around the synapse which sustains because of the peripheral global forces and with help from central local non-coordinated forces, actin forms invadosomes/podosomes like structures to extract the antigen. Thus, both global coordinated and local non-coordinated forces play in harmony to efficiently extract antigens.

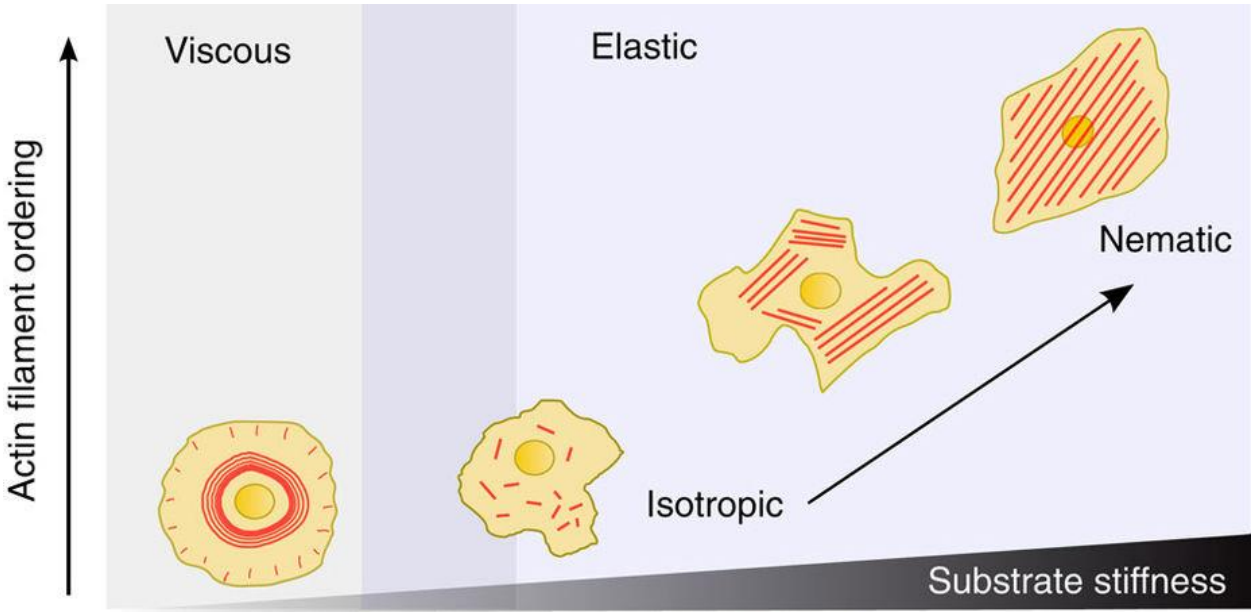

Figure 30. Cell spreading depends on substrate stiffness:

As the substrate stiffness increases, the large-scale order of actin filament alignment also increases. On soft substrates, actin cytoskeleton shows viscous behaviour, whereas on stiff substrates it shows elastic behaviour. On stiff substrates, as the stiffness increases, the cytoskeleton undergoes an isotropic to nematic phase transition (M. Gupta et al., 2015)

B cell spreading on physiological substrate

Different experimental systems have been developed as surrogate antigen presenting cells to study the immune synapse *ex vivo*: polystyrene beads (Yuseff et al., 2011), supported lipid bilayers (Fleire et al., 2006), plasma membrane sheets (Natkanski et al., 2013) and antigen coated cells (Batista, Iber, & Neuberger, 2001). It has been shown on supported lipid bilayers that the immune synapse is formed of a set of concentric patterns where molecules and cytoskeletal components are partitioned: a distal supra-molecular antigen cluster (dSMAC) with an actin ring, a peripheral one (pSMAC) where adhesion molecules concentrate and a central one (cSMAC) where the antigen is ultimately gathered (Grakoui et al., 1999)(Fleire et al., 2006). Based on this structure and on the observation that B cells spread on antigen-coated substrate an antigen extraction model was proposed on surrogate substrate: upon specific antigen recognition by the BCR, B cells spread and contract, transporting the BCR bound antigen towards the center. In 2006, the group of Dennis Disher showed that spreading in mesenchymal stem cells is related to mechanosensing by showing that cell spreading on deformable substrates increases with increasing stiffness (Engler, Sen, Sweeney, & Discher, 2006). In our experimental system where we use PAA gel of physiological rigidity (Bufi et al., 2015), we found that B cells could not spread on soft substrate as compared to glass **(Figure 18A)**. This difference between soft and stiff could be due to different acto-myosin organization on these two substrates. In fact, It has been shown in fibroblasts, as substrate stiffness increases, the large-scale order of actin filament alignment also increases. On soft substrates, actin cytoskeleton shows viscous behaviour, whereas on stiff substrates it shows elastic behaviour. On stiff substrates, as stiffness increases, the cytoskeleton undergoes an isotropic to nematic phase transition **(Figure 30)** (M. Gupta et al., 2015). Hence, we explain the fact that we do not see either flow of actin nor highly organized ring like structures is due to the fact that on a soft substrate the cytoskeleton has a different behavior (more elastic) than on a hard (albeit fluid) one.

Role of clathrin in force generation at B cell immune synapse

Following engagement of the antigen receptor, the BCR can be observed in clathrin-coated pits and vesicles, suggesting a clathrin-mediated route of internalization (Stoddart et al., 2005), (Brown & Song, 2001), (Natkanski et al., 2013). As the process of endocytosis is coupled with acto-myosin activity, it is natural to think that clathrin could play a role in the generation of scission forces. Recently it has been shown in epithelial breast cancer cells that clathrin coated structures not only help in endocytosis but also provide dynamic anchoring to collagen fibers by wrapping around them and eventual pinching off which allow the cells to cope up with high tensions across the protrusions (Elkhatib et al., 2017). In line with this study, we started exploring effects of clathrin on B cell traction forces. Preliminary data showed that B cells from clathrin knock mice have higher forces as compared to wild types cells. Further experiments are required to state anything concretely. Higher forces in clathrin knock out mice could result from the failure in scission, which induce frustrated loop of contractile events.

Mechanics at the immune synapse

T and B lymphocytes share many features in the processes that govern immune synapse formation and mechanics. In T cells, TFM measurements are shown to be driven majorly by actin polymerisation whereas myosin II only contributes in the early phase of stimulation and is not required for the maintenance of force at later time points (Hui, Balagopalan, Samelson, & Upadhyaya, 2014). The group of Arpita Upadhyaya found that traction forces in T cells were mostly concentrated at the periphery. Forces exerted in the central actin rich region were slightly higher than the peripheral region similar to what we have observed in our work. They also show that upon inhibition of myosin II, actin dynamics remain intact indicating that myosin IIA does not play a significant role in maintaining actin flow in T cells. This in strong discrepancy with our results highlighting that myosin II is strictly required for traction force measurement and antigen extraction by B cells, stressing once more on the difference between the two types of lymphocytes, the main difference being that TCR does not have to be internalized, while BCR does.

I. Mechanosensing in B and T lymphocytes

Range of immune responses is dictated by exchange of information between T and B lymphocytes with their APCs. Immune synapse in both B and T cells act as a signaling platform where both exocytotic and endocytotic events take place (reviewed in (Yuseff, Lankar, & Lennon-Duménil, 2009), (Obino & Lennon-Duménil, 2014). As we have mentioned in the introduction, immune synapse undergoes continuous architectural changes. These architectural changes induce mechanical stimulation thus, in both B and T cells, mechanosensitive* receptors such as antigen receptors and integrin receptors are essential for flow of information in the lymphocytes.

***Mechanosensing** is defined as the responsivity to mechanical stimuli at the cellular level or below

i. Mechanosensing via antigen receptors:

The fact that antigen receptors are mechanosensitive has become increasingly evident over the last few years. In 2012, Judokusumo, E. et al. demonstrated that the presentation of stimulatory ligands to T cells on stiff surface (100-200 KPa) elicit higher intracellular signalling than softer ones (Judokusumo, Tabdanov, Kumari, Dustin, & Kam, 2012). Similar experiments have been performed on B cells as we have mentioned in introduction (Wan et al., 2013), (Zeng et al., 2015). These work demonstrated that both T cells and B cells are sensitive to the physical disposition of antigen.

APC–antigen receptor interactions initiate adaptive immune responses, but the mechanism of how such interactions under force induce signalling is not completely understood. T cell receptors have shown to exhibit catch bond behaviour with its ligand, where bond lifetime is prolonged by force (Liu B. et al., 2014). Liu et al., used BFP approach to investigate the dependence of kinetics on force by controlling the force and the timing of T-cell–APC contact/separation. Similar to T cells, there are indications that B cells too function as a catch bond receptor. For example group of Wanli Liu has shown at single molecule level using DNA-based tension gauge tethers that when B cell pull against their ligand, a specific force range is required for optimal signal transduction (Wan et al., 2015)

ii. Mechanosensing via integrins:

The integrin family of proteins consists of alpha (α) and beta (β) subtypes each containing a long, stalk like extracellular domain, a transmembrane helix, and a short intracellular tail (Luo, Carman, & Springer, 2007). Integrin proteins are among the best-characterized mechanosensitive receptors that function mechanically, by attaching the cell cytoskeleton to the extracellular matrix (ECM), and biochemically, by sensing whether adhesion has occurred. The binding to the adhesion ligand via integrins rely heavily on its conformation. In the resting state, integrins maintain a bent, low-affinity architecture in which the ligand-binding site points toward the base of the integrin stalk.

Activating signalling pathways from within the cell can relieve this inhibitory conformation in an 'inside-out' fashion by assembling specific protein complexes on the cytoplasmic tails of the a and βchains.

In T cells, lymphocyte function-associated antigen 1(LFA-1) is a predominant integrin within the Immune synapse, which is critical both for strong adhesion to the APC and for transducing costimulatory signals that contribute to lymphocyte activation. On supported lipid bilayers, It engages with an intercellular adhesion molecule ICAM-1 on the target cell surface during initial cell spreading. Ligand-bound LFA-1 molecules are then trafficked toward the center of the immune synapse by retrograde F-actin flow, where they merge into the pSMAC.

Group of Jannice Burkhardt showed that different form of integrins occupy different regions of the immune synapse. High affinity integrin conformations localize in the center. They also showed inhibition of acto-myosin cytoskeleton reduces the accumulation of LFA-1 showing integrin activation at the immune synapse depends on force imposed by cytoskeletal dynamics (Comrie, Babich, & Burkhardt, 2015). Although we have not addressed integrin mediated forces in our work, further studies would be interesting to explore the role of integrins and answer the withstanding question of how cell uses antigen both to adhere and internalize it.

Concluding remarks

In this work, we analyzed the spatio-temporal distribution of forces at the B cell immune synapse by using antigen-coated substrate deformation that allows direct force visualization (TFM). We uncovered the existence of both global contractile forces at the periphery of the synapse and of local pulling forces at the center of the synapse. We give therefore a unifying explanation of the role of myosin II in the context of efficient antigen extraction. We show peripheral contractile forces depend on centripetal organization of Myosin II whereas central pulling forces are generated by F-actin protrusions that form in a myosin II-dependent manner. Interestingly we observed collective pulsatile myosin II dependent contractions that, we suggest, are responsible for the organization of the actin structures at the center of the synapse. We further highlight the involvement of acto-myosin contractility in force generation and antigen extraction as well as in B lymphocyte response and antibody production *in vivo*. The methods and model we built might be generalizable to other systems where molecules are surface-tethered. We propose that Myosin II dependent forces may generally be involved in the endocytosis of immobilized ligands by a variety of cell types *in vivo*.

Although with this work we bring new pieces in the puzzle of B cell mechanics by highlighting two pools of forces, further work is needed to characterize these forces in an exhaustive manner. Coordinated component is well described but measurement of the non-coordinated component was limited in our setup as using gel degrades the point spread function of the microscope. The best way to do these experiments would be using a different objective with better working distance like water immersion objectives. It would be of particular interest to better characterize and measure non-coordinated forces by using 3D traction force microscopy (Franck, Maskarinec, Tirrell, & Ravichandran, 2011). Finally, one of the most interesting effects we observe in our antigen presenting system is pulsatile events. That put the spotlight on withstanding questions which remain to be answered that are: Will one see the pulsatile dynamics of Myosin II dependent coordinated forces in between two actual cells? Are these pulsatile force dynamics present in vivo? The answers to these questions represent the next challenges to be addressed.

Material and Methods

Mice and cells: Mice with a conditional deletion of myosin II in B cells were generated by backcrossing mice carrying a floxed myosin II allele *(MyosinIIflox/flox)* (Jacobelli et al., 2010) with mice expressing the Cre recombinase under the control of the CD21 promoter *(CD21 cre$^{+/-}$)*. Mice expressing the hen egg lysozyme (HEL)–specific MD4 receptor were also crossed with mice carrying a floxed myosin II allele. Mice were crossed at an age of eight to 10 weeks, and Cre^{-} littermates were used as WT controls. The transgenic MD4, Lifeact GFP and myosin II-GFP mouse lines have been described elsewhere(Riedl et al., 2008), (Goodnow et al., 1988)). This resulted in all the desired genetic combinations being obtained in the C57BL/B6 background, and the corresponding breeding controls were systematically used. The experiments were performed on 8 to 10 week-old male or female mice. Animal care conformed strictly to European and French national regulations for the protection of vertebrate animals used for experimental and other scientific purposes (Directive 2010/63; French Decree 2013-118). Mature spleen B cells were purified with the MACS kit (130-090-862). B cells were cultured (Yuseff, M. I. *et al*., 2011) in CLICK medium (RPMI 1640—GlutaMax-I supplemented with 10% fetal calf serum, 1% penicillin–streptomycin, 0.1% □-mercaptoethanol and 2% sodium pyruvate).

Antibodies and reagents: The following reagents were used: 100 µg/ml HEL (Sigma), 100 µg/ml BSA (Euromedex), 40% polyacrylamide (Biorad), 2% bis-poylacrylamide (Biorad), 3-aminopropyltrimethoxysilane (Sigma), 0.2 µm Alexa647 Fluospheres (Thermo Fisher, F8807), Sigmacote (Sigmacote), ammonium persulfate (Sigma), TEMED (ICN Biomedicals), Sulfo-SANPAH (Thermo Fisher), and the Alexa555 protein labeling kit (A30007, Molecular Probes). For drug treatments, we used para-nitro blebbistatin (Optopharma). The following antibodies were used: rabbit anti-HEL (Abcam,1/100), human anti-GFP (Institut Curie, 1/200), Alexa Fluor 647-conjugated anti-phalloidin (Thermo Fisher, 1/200), anti-myosin IIA heavy chain (Covance, 1/500), Alexa Fluor 488-conjugated goat anti rabbit IgG(Life Technologies, 1/200), Alexa Fluor 488-conjugated goat anti-human IgG (Life Technologies,1/200).

Inhibitors: Cells were incubated with 70 µM para-nitro blebbistatin (Optopharma) for 40 minutes at 37°C in RPMI media before the experiments, unless otherwise stated.

Live cell microscopy: Fluorodishes containing gels were placed under a microscope focused on the plane of beads. In total, $1x10^5$ B cells were added to the plate (time 0), and images were acquired over time. Images were acquired at 37°C, under an atmosphere containing 5% CO_2, with an inverted spinning disk confocal microscope (Roper/Nikon) equipped with a 60X (1.4 numerical aperture (NA)) oil immersion objective and a CoolSNAP HQ2 camera. Images were acquired in the synaptic plane, at five-second intervals.

Preparation of polyacrylamide gel substrates: PAA were produced in 35-mm FD35 fluorodishes (World Precision Instruments, Inc). These dishes were first treated by UV irradiation for 2 minutes, and then with 3-aminopropyltrimethoxysilane (APTMS) for 5 minutes. The dishes were washed thoroughly in distilled water before preparation of the polyacrylamide gels. Hydrophobic coverslips were prepared by incubation in Sigmacote for 3 minutes, followed by thorough washing and drying. A 500 Pa gel was prepared by diluting 40% polyacrylamide and 2% bis-acrylamide solutions to obtain stock solutions of 12% acrylamide/0.1% bis-acrylamide. We sonicated 167 µl of this solution with 10% fluorescent beads, and then added 0.2 µL of TEMED and 10% ammonium persulfate and mixed thoroughly, to initiate polymerization. A volume of 9 µL of the polyacrylamide mixture was immediately pipetted onto the surface of the Fluorodish and a Sigmacote activated coverslip was carefully placed on top. Fluorodishes were immediately inverted, to bring the beads to the surface of the gel. Polymerization was completed in 45 min and the top coverslip was then slowly peeled off and immediately immersed in PBS. Sulfo-SANPAH was used to crosslink antigen to the surface of the gel.It is a surface functionalizing reagent with an amine-binding group that binds to the antigen (HEL, IgG, and IgM) and a photoactivable azide group that binds to the substrate upon activation under UV giving homogeneous distribution of antigen on the surface of PAA gels **(Figure 31)** . We pipetted 150 µl of 0.5 mg/ml sulfo-SANPAH onto the surface and placed the gel under UV light for 2 minutes. The gels were then washed with PBS and the process repeated. The gel was washed thoroughly with PBS and coated with 100 µg/ml antigen, by overnight incubation at 4°C.

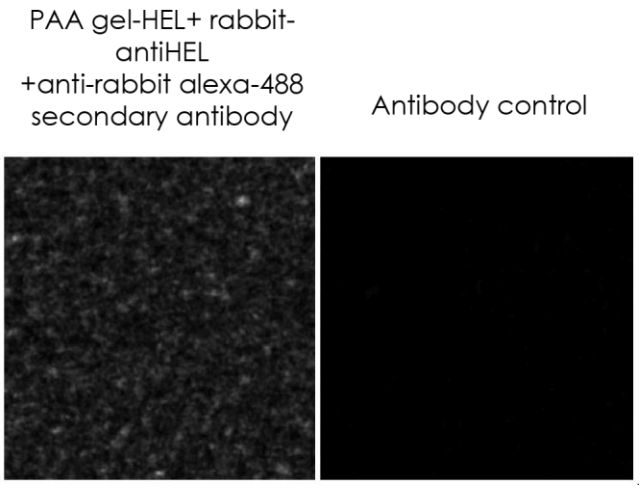

Figure 31. Images showing homogeneous distribution of antigen on PAA gel

Measurement of Young's modulus of PAA gels: The Young's modulus of PAA gel was calculated using a Hertz model for an elastic substrate with finite thickness (Pelham & Wang, 1998) **(Figure 32A)**. Gel height was determined by focussing on the bottom and top of the gel. Glass beads of 0.25 mm radius were deposed on the gel also to different positions of the gel to measure the homogeneity. The force inserted in the Hertz formula was computed theoretically as the weight of the glass bead (density=2.2kg/m^3 and radius 0.25mm) minus the buoyancy in water. PAA gels in our system remains in the range of 400-650 Pa **(Figure 32B).**

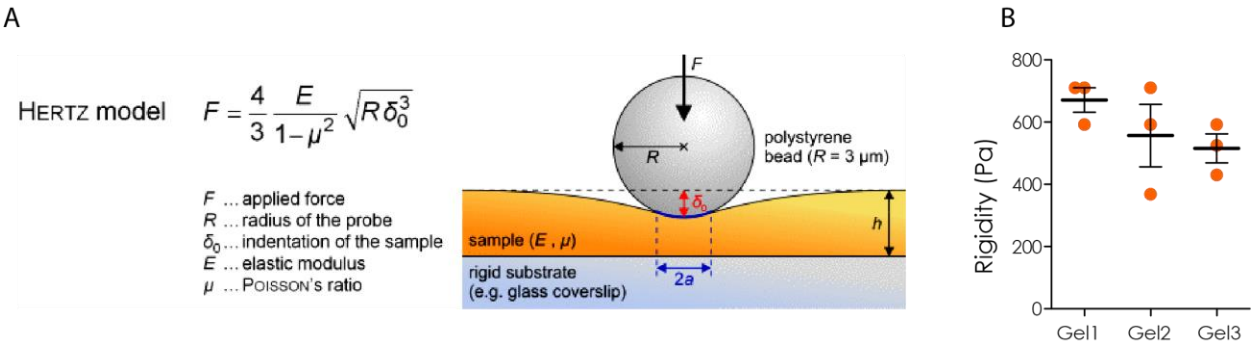

Figure 32. Rigidity measurement of PAA gels:

(A) Schematic of Hertz model (Figure by Steve Pawlizak, 2009). (B) Graph representing rigidity measurement of 3 individual gels at different area of the same gel. Each dot represents a position at the surface of one gel.

Quantification of amount of antigen on PAA gel and glass: To be sure that the difference of spreading on gel and on glass was not due to the amount of antigen coated on different substrates (it is harder to coat gels with protein due to the inherent hydrophobicity of the PAA). We inferred the amount of antigen required for coating the glass with an equivalent concentration of antigen on gel (100µg/ml) by taking images at different concentration on glass and comparing with the fluorescent intensity obtained on the gel of 100µg/ml. Respective glasses and gels were coated with HEL overnight at 4°C and later stained by using rabbit anti-HEL primary antibody at 37°C, eventually staining with anti-rabbit alexa-488 secondary antibody. Images were acquired using laser scanning microscope (Leica) with a 40X 1.4 NA oil immersion objective with 5% 488 laser. Graph representing mean fluorescence intensity at different point fits a logarithmic curve that suggests the equivalent concentration on glass is 0.14 µg/ml **(Figure 33)**.

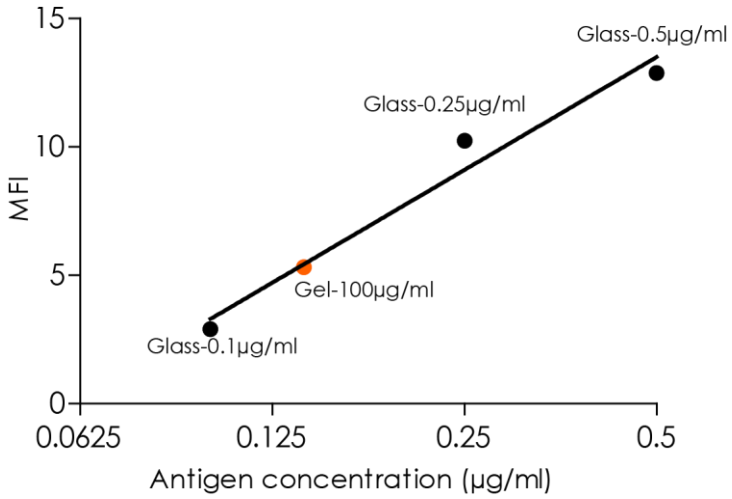

Figure 33.Antigen quantification on coated glass and PAA gels:

Graph representing mean fluorescence intensity of different concentration on glass and PAA gels. Each dot represents the average of 5 points at different position of the substrate

Immunofluorescence: B cells plated on polyacrylamide gels were fixed by incubation in 4% PFA for 10 min at room temperature, and PFA was quenched by incubation in PBS plus 1 mM glycine for 10 min. Fixed cells were incubated with primary antibodies in PBS plus 0.2% BSA and 0.05% saponin, overnight at 4°C. The cells were washed and

incubated with secondary antibodies for 1 hour at room temperature. Immunofluorescence images were acquired on a laser scanning microscope (Leica) with a 40× 1.4 NA oil immersion objective.

Inside-out immunofluorescence: B cells were plated on polyacrylamide gels and incubated for 15 min at 37°C. The cells were then transferred to 4°C and Fc receptors were blocked for 10 min. The cells were washed with PBS and incubated with rabbit anti-HEL antibody at 4°C for one hour and then with Alexa Fluor 488-conjugated anti-rabbit IgG secondary antibody for one hour. The cells were moved to room temperature, fixed by incubation with 4% PFA for 10 minutes and permeablized by incubation with PBS plus 0.2% BSA and 0.05% saponin. The cells were then incubated with rabbit anti-HEL antibodies for one hour, washed with PBS-BSA-SAPONIN, and incubated with the Alexa 546-conjugated anti-rabbit IgG secondary antibody for one hour at room temperature. The cells were washed several times in PBS and then used for imaging. Images were acquired using laser scanning microscope (Leica) with a 40X 1.4 NA oil immersion objective.

SEM Imaging: For SEM analyses, cells were fixed overnight at 4°C in 2.5% glutaraldehyde in phosphate buffer on 0.2µg/ml HEL coated on glass and 100µg/ml HEL coated on PAA gel. They were dehydrated in a graded series of ethanol solutions, then dried by the CO_2 critical-point method, with an EM CPD300 (Leica microsystems). Samples were mounted on an aluminum stub with silver lacquer and sputter-coated with a 5 nm layer of platinum, with an EM ACE600 (Leica Microsystems). Images were acquired with a GeminiSEM 500 (Zeiss). **Coating and imaging was done by San Roman Mabel.**

Electron microcopy: Immunoelectron microscopy was performed by the Tokuyasu method (Slot & Geuze, 2007). Double-immunogold labeling was performed on ultrathin cryosections with protein A-gold conjugates (PAG) (Utrecht University, The Netherlands). Electron micrographs were acquired on a Tecnai Spirit electron microscope (FEI, Eindhoven, The Netherlands) equipped with a Quemesa (SIS) 4k CCD camera (EMSIS GmbH, Mu̇nster, Germany).**Imaging was performed by Danielle Lankar.**

Western blotting: B cells were lysed at 4°C in lysis buffer (10 mM Tris HCL pH 7.4, 150 mM NaCl, 0.5% NP40). Cell lysates were loaded onto mini-PROTEAN TGX SDS–PAGE gels,

which were run at 200 volts and 65 mA. The bands on the gel were transferred onto PVDF membranes (Trans-Blot Turbo Transfer). Membranes were blocked with 5% BSA in 1xTBS–0.05% Tween-20 and incubated overnight at 4°C with primary antibodies and then for 60 min with secondary antibodies. Western blots were developed with Clarity Western ECL substrate, and chemiluminescence was detected with a ChemiDoc imager (all from BioRad).

Density map analysis: On movie reconstruction, individual cells were cropped with ImageJ software. For signal mapping, the images obtained for each individual cell were aligned in a single column. Cell size normalization was applied to each time point, based on mean cell size, with background subtraction. We obtained a mean behaviour for each cell, by projecting every time point onto the average. The mean behaviour of the population was then determined, by projecting the mean signal of every individual cell. This procedure was performed with a custom-designed ImageJ-compatible macro. A similar procedure was used to map forces, except that the real stress value was used, without normalization. For bead density analysis, we smoothed positions with a two-dimensional Gaussian kernel of radius 3 pixels to obtain a density map, as described by (Schauer et al., 2010). These last two analyses were performed in Matlab.

Antigen coated bead presentation experiment: $4x10^7$ 3-mm latex NH2-beads (Polyscience) were activated with 8% glutaraldehyde (Sigma Aldrich) for 2h at room temperature. Beads were washed with PBS 1x and incubated overnight at 4°C with 100µg/ml of HEL ligands. A total of $1x10^5$ myosin II GFP primary B cells were seeded in 35-mm FD35 Fluorodish. HEL coated beads (diluted 100X) were added just before imaging. A single trapped bead was presented to a selected cell and the acquisition in the fluorescence channel started. Images were acquired 0.2Hz at 37°C, under an atmosphere containing 5% CO_2, with an inverted epifluorescence microscope Nikon Eclipse-Ti equipped with a 100X Apo-TIRF, 100×/N.A. 1.45 (Nikon) oil immersion objective and an EM-charge-coupled device camera (Andor iXon 897) driven by Micro-Manager (Edelstein et al 2014). The optical tweezers are made of a 1064 nm laser beam (ytterbium fibre laser, λ = 1064 nm, TEM 00, 5 W, IPG Photonics, Oxford, MA) expanded

and steered (optics and electronics by Elliot Scientific, Harpenden, UK, controlled by Labview) in the back focal plane of the microscope objective.

Antigen-stripping experiments: Round glass coverslips were coated with anti-HEL antibody by overnight incubation. The coverslips were washed with PBS and imaged to obtain the control image. They were then placed on the antigen-coated polyacrylamide gel for 30 seconds to 1 minute. They were stripped off the surface of the gel and imaged as soon as possible using laser scanning microscope (Leica) with a 40× 1.4 NA oil immersion objective. Fluorescence on these images indicated the presence of detached antigen. Absence of fluorescence in stripped gel suggests that quenching is not due to the presence of many layer of antigen.

Traction force Microscopy: energy and flux: The traction force algorithm was based on that used by (Butler et al., 2002) and modified by (Mandal et al., 2014) the custom-developed MATLAB software. Algorithm works in following steps

1. Takes movies of beads
2. Registers whole image
3. Finds the position of the beads in reference image using MTT algorithm (Bertaux & Marguet, 2008)
4. Calculates displacement relative to a reference image
5. Interpolates the displacement to obtain a two-dimensional field on a grid (of mesh grid 4 pixels)
6. Applies Fourier transform
7. Inverts the problem to obtain the stress in Fourier space
8. Back transforms the stress field to obtain the stress at each point of the grid.

Note that the output of the algorithm is the x and y component of the tangential stress on the whole image at each time point with a resolution given by the mesh grid of the interpolation grid. The valus f the force in newton could be extrated at each grid point multiplyin the area of the meshgrid by the stress. With an abuse of language we often used the term "force" instead of stress in a qualitative sense.

Given the size of our cells, the density of beads, the magnitude of displacement we had to optimised some parameters for the analysis. In particular for the detection algorithm (MTT): search window size (5 pixels), particle radius (2.5 pixels) and maximum distance for nearest neighbour (4 pixels). Pixel size of spinning disk confocal microscope is 108 nm (we occasionally used another setup with pixel size 160 nm, but the parameters did not need adjustment). Same parameters were applied for noise detection by measuring force in a non-stressed area not too far from the cell. A quality check of the TFM algorithm is given by the "non equilibrated forces", i.e. by the ratio of the sum of forces vectors (which should be zero) to the sum of magnitude of the forces. Lower ratio signifies higher quality of the analysis. Further calculations based on the output of the algorithm were performed to extract the total strain energy (defined as the sum over the entire cell area of the scalar product force by displacement). Fluxes were calculated by standard vector analysis (Green's theorem): the flux is the integral over the cell area of the divergence of the 2D field (displacement or stresses). An outward flux represents pushing forces and inward flux represents pulling forces.

Note that even if in theory the forces are supposed to be zero outside the cell, we decided not to introduce this constrain to avoid border effects. However when we compute energy and fluxes, we use the mask of the cell extracted by using an imageJ custom made macro. The mask was increased by 10% (dilation of the binary image using Matlab morphometric tools) to avoid excessive cropping of the force/displacement field.

TFM algorithm to analyze coordinated and non-coordinated forces: For coordinated and non-coordinated analysis, we determined whether a bead belongs to the coordinated or non-coordinated group, by calculating the mean correlation between the displacement vector associated with the bead and its nearest neighbours (within 1 µm range). Beads with a correlation coefficient below 0.5 were considered to belong to the non-coordinated pool. Note that we define a correlation that does not depend on the magnitude of the displacement vectors but only of their relative orientation. This implies that beads moving a little or not at all have low correlations coefficient and build up the non-coordinated pool. The scatter plot **(Figure 23B)** based on the correlation was generated based on the correlation coefficient between the entire

time series for total energy and the entire time series for energy associated with coordinated/non-coordinated beads, respectively, for the *x* and *y* axis. **This algorithm was implemented by Paolo Pierobon**

Spectral analysis: To extract a typical timescale of the collective pulsatile dynamics **(Figure 23H)** each signal (flux of displacement, total energy or coordinated energy) was first detrended subtracting a background smoothed using Savitsky-Golay filter (with a window of 500s). The power spectrum was then computed on the detrended signal and the maximum was selected above frequencies of 1/500 Hz (to avoid including effect of the smoothing). **This analysis was done by Paolo Pierobon.**

Statistics: All graphs and statistical analyses were performed with GraphPad Prism 5 (GraphPad Software) and MATLAB. Mann-Whitney tests were used to determine statistical significance unless otherwise stated. Bar graphs show the mean ± SEM. Graphs representing strain energy and displacement flux were aligned to start at time zero, dot plot of strain energy show the average of each cell at each time point at plateau.

References

Arana, E., Vehlow, A., Harwood, N. E., Vigorito, E., Henderson, R., Turner, M., … Batista, F. D. (2008). Activation of the Small GTPase Rac2 via the B Cell Receptor Regulates B Cell Adhesion and Immunological-Synapse Formation. *Immunity*, *28*(1), 88–99. http://doi.org/10.1016/j.immuni.2007.12.003

Bakke, O., & Dobberstein, B. (1990). MHC class II-associated invariant chain contains a sorting signal for endosomal compartments. *Cell*, *63*(4), 707–716. http://doi.org/10.1016/0092-8674(90)90137-4

Bashour, K. T., Gondarenko, A., Chen, H., Shen, K., Liu, X., Huse, M., … Kam, L. C. (2014). CD28 and CD3 have complementary roles in T-cell traction forces. *Proceedings of the National Academy of Sciences of the United States of America*, *111*(6), 2241–6. http://doi.org/10.1073/pnas.1315606111

Basu, R., & Huse, M. (2016). Mechanical Communication at the Immunological Synapse. *Trends in Cell Biology*, xx, 1–14. http://doi.org/10.1016/j.tcb.2016.10.005

Basu, R., Whitlock, B. M., Husson, J., Le Floc'h, A., Jin, W., Oyler-Yaniv, A., … Huse, M. (2016). Cytotoxic T Cells Use Mechanical Force to Potentiate Target Cell Killing. *Cell*, 1–11. http://doi.org/10.1016/j.cell.2016.01.021

Batista, F. D., & Harwood, N. E. (2009). The who, how and where of antigen presentation to B cells. *Nature Reviews. Immunology*, *9*(1), 15–27. http://doi.org/10.1038/nri2454

Bertaux, N., & Marguet, D. (2008). Dynamic multiple-target tracing to probe spatiotemporal cartography of cell membranes, *5*(8), 687–694. http://doi.org/10.1038/NMETH.1233

Bufi, N., Saitakis, M., Dogniaux, S., Buschinger, O., Bohineust, A., Richert, A., … Asnacios, A. (2015). Human Primary Immune Cells Exhibit Distinct Mechanical Properties that Are Modified by Inflammation. *Biophysical Journal*, *108*(9), 2181–2190. http://doi.org/10.1016/j.bpj.2015.03.047

Butler, J. P., Tolić-Nørrelykke, I. M., Fabry, B., & Fredberg, J. J. (2002). Traction fields, moments, and strain energy that cells exert on their surroundings. *American Journal of Physiology. Cell Physiology*, *282*(3), C595-605. http://doi.org/10.1152/ajpcell.00270.2001

Cambier, J. C., Pleiman, C. M., & Clark, M. R. (1994). Signal transduction by the B cell antigen receptor and its coreceptors. *Annu Rev Immunol*, *12*, 457–486. http://doi.org/10.1146/annurev.iy.12.040194.002325

Carrasco, Y. R., & Batista, F. D. (2006). B cell recognition of membrane-bound antigen: an exquisite way of sensing ligands. *Current Opinion in Immunology*, *18*(3), 286–91. http://doi.org/10.1016/j.coi.2006.03.013

Carrasco, Y. R., Fleire, S. J., Cameron, T., Dustin, M. L., & Batista, F. D. (2004). LFA-1/ICAM-1 interaction lowers the threshold of B cell activation by facilitating B cell adhesion and synapse formation. *Immunity*, *20*(5), 589–99. Retrieved from http://www.ncbi.nlm.nih.gov/pubmed/15142527

Champion, J., Walker, A., & Mitragotri, S. (2008). Role of particle size in phagocytosis of polymeric microspheres. *Pharmaceutical Research*, *25*(8), 1815–1821. http://doi.org/10.1007/s11095-008-9562-y.Role

Cheng, J., Grassart, A., & Drubin, D. G. (2012). Myosin 1E coordinates actin assembly and cargo trafficking during clathrin-mediated endocytosis. *Molecular Biology of the Cell*, *23*(15), 2891–904. http://doi.org/10.1091/mbc.E11-04-0383

Clark, K., Langeslag, M., Figdor, C. G., & van Leeuwen, F. N. (2007). Myosin II and mechanotransduction: a balancing act. *Trends in Cell Biology*, *17*(4), 178–186. http://doi.org/10.1016/j.tcb.2007.02.002

Conti, M. A., & Adelstein, R. S. (2008). Nonmuscle myosin II moves in new directions. *Journal of Cell Science*, *121*(Pt 1), 11–18. http://doi.org/121/1/11 [pii]\r10.1242/jcs.007112

Cunningham, A. F., Gaspal, F., Serre, K., Mohr, E., Henderson, I. R., Scott-Tucker, A., … MacLennan, I. C. M. (2007). Salmonella induces a switched antibody response without germinal centers that impedes the extracellular spread of infection. *Journal of Immunology (Baltimore, Md. : 1950)*, *178*(10), 6200–6207. http://doi.org/10.4049/jimmunol.178.10.6200

De Silva, N. S., & Klein, U. (2015). Dynamics of B cells in germinal centres. *Nature Reviews Immunology*, *15*(3), 137–148. http://doi.org/10.1038/nri3804

Delamarre, L., Pack, M., Chang, H., Mellman, I., & Trombetta, E. S. (2005). Differential Lysosomal Proteolysis in Antigen-Presenting Cells Determines Antigen Fate. *Science*, *307*(5715), 1630–1634. http://doi.org/10.1126/science.1108003

Dembo, M., & Wang, Y. L. (1999). Stresses at the cell-to-substrate interface during locomotion of fibroblasts. *Biophysical Journal*, *76*(4), 2307–16. http://doi.org/10.1016/S0006-3495(99)77386-8

Denzin, L. K., & Cresswell, P. (1995). HLA-DM induces clip dissociation from MHC class II αβ dimers and facilitates peptide loading. *Cell*, *82*(1), 155–165. http://doi.org/10.1016/0092-8674(95)90061-6

Denzin, L. K., Sant'Angelo, D. B., Hammond, C., Surman, M. J., & Cresswell, P. (1997). Negative regulation by HLA-DO of MHC class II-restricted antigen processing. *Science (New York, N.Y.)*, *278*(5335), 106–9. Retrieved from http://www.ncbi.nlm.nih.gov/sites/entrez?Db=pubmed&DbFrom=pubmed&Cmd=Link&LinkName=pubmed_pubmed&LinkReadableName=Related Articles&IdsFromResult=9311912&ordinalpos=3&itool=EntrezSystem2.PEntrez.Pubmed.Pubmed_ResultsPanel.Pubmed_RVDocSum

Depoil, D., Weber, M., Treanor, B., Fleire, S. J., Carrasco, Y. R., Harwood, N. E., & Batista, F. D. (2009). Early events of B cell activation by antigen. *Science Signaling*, *2*(63), pt1. http://doi.org/10.1126/scisignal.263pt1

Driessen, C., Bryant, R. A. R., Lennon-Duménil, A. M., Villadangos, J. A., Bryant, P. W., Shi,

G. P., … Ploegh, H. L. (1999). Cathepsin S controls the trafficking and maturation of MHC class II molecules in dendritic cells. *Journal of Cell Biology*, *147*(4), 775–790. http://doi.org/10.1083/jcb.147.4.775

Fleire, S. J., Goldman, J. P., Carrasco, Y. R., Weber, M., Bray, D., & Batista, F. D. (2006). B cell ligand discrimination through a spreading and contraction response. *Science (New York, N.Y.)*, *312*(5774), 738–41. http://doi.org/10.1126/science.1123940

Georgess, D., Machuca-gayet, I., Blangy, A., & Jurdic, P. (2014). Podosome organization drives osteoclast- mediated bone resorption, *8*(3), 192–204. http://doi.org/10.4161/cam.27840

Giannone, G., Dubin-thaler, B., Rossier, O., Cai, Y., Jiang, G., Beaver, W., … Sheetz, M. P. (2017). adhesion site formation, *128*(3), 561–575. http://doi.org/10.1016/j.cell.2006.12.039.Lamellipodial

Gonzalez, S. F., Lukacs-Kornek, V., Kuligowski, M. P., Pitcher, L. a, Degn, S. E., Kim, Y.-A., … Carroll, M. C. (2010). Capture of influenza by medullary dendritic cells via SIGN-R1 is essential for humoral immunity in draining lymph nodes. *Nature Immunology*, *11*(5), 427–434. http://doi.org/10.1038/ni.1856

Goodnow, C. C., Crosbie, J., Adelstein, S., Lavoie, T. B., Smith-Gill, S. J., Brink, R. a, … Raphael, K. (1988). Altered immunoglobulin expression and functional silencing of self-reactive B lymphocytes in transgenic mice. *Nature*, *334*, 676–682. http://doi.org/10.1038/334676a0

Grakoui, a, Bromley, S. K., Sumen, C., Davis, M. M., Shaw, a S., Allen, P. M., & Dustin, M. L. (1999). The immunological synapse: a molecular machine controlling T cell activation. *Science (New York, N.Y.)*, *285*(5425), 221–227. http://doi.org/10.1126/science.285.5425.221

Gupta, M., Sarangi, B. R., Deschamps, J., Nematbakhsh, Y., Callan-Jones, A., Margadant, F., … Ladoux, B. (2015). Adaptive rheology and ordering of cell cytoskeleton govern matrix rigidity sensing. *Nature Communications*, *6*(May), 7525. http://doi.org/10.1038/ncomms8525

Gupta, P., Martin, R., Knö Lker, H.-J., Nihalani, D., & Sinha, D. K. (2017). Myosin-1 inhibition by PCIP affects membrane shape, cortical actin distribution and lipid droplet dynamics in early Zebrafish embryos. *PLoS ONE*, 1–21. http://doi.org/10.1371/journal.pone.0180301

Harris, A. K., Wild, P., & Stopak, D. (1980). Silicone rubber substrata: a new wrinkle in the study of cell locomotion. *Science (New York, N.Y.)*, *208*(4440), 177–9. http://doi.org/10.1126/science.6987736

Hui, K. L., Balagopalan, L., Samelson, L. E., & Upadhyaya, A. (2014). Cytoskeletal forces during signaling activation in Jurkat T cells. *Molecular Biology of the Cell*, *26*, 685–695. http://doi.org/10.1091/mbc.E14-03-0830

Jacobelli, J., Friedman, R. S., Conti, M. A., Lennon-Dumenil, A.-M., Piel, M., Sorensen, C.

M., … Krummel, M. F. (2010). Confinement-optimized three-dimensional T cell amoeboid motility is modulated via myosin IIA-regulated adhesions. *Nature Immunology*, *11*(10), 953–61. http://doi.org/10.1038/ni.1936

Junt, T., Moseman, E. A., Iannacone, M., Massberg, S., Lang, P. a, Boes, M., … von Andrian, U. H. (2007). Subcapsular sinus macrophages in lymph nodes clear lymph-borne viruses and present them to antiviral B cells. *Nature*, *450*(7166), 110–114. http://doi.org/10.1038/nature06287

Kaksonen, M., Toret, C. P., & Drubin, D. G. (2006). Harnessing actin dynamics for clathrin-mediated endocytosis. *Nature Reviews. Molecular Cell Biology*, *7*(6), 404–414. http://doi.org/10.1038/nrm1940

Kasturi, R., Vasulka, C., & Johnson, J. D. (1993). Ca2+, caldesmon, and myosin light chain kinase exchange with calmodulin. *Journal of Biological Chemistry*, *268*(11), 7958–7964.

Kaufmann, S. H. E. (2008). Immunology's foundation: the 100-year anniversary of the Nobel Prize to Paul Ehrlich and Elie Metchnikoff. *Nature Immunology*, *9*(7), 705–712. http://doi.org/10.1038/ni0708-705

Larsson, J., & Karlsson, S. (2005). The role of Smad signaling in hematopoiesis. *Oncogene*, *24*(9), 5676–5692. http://doi.org/10.1038/sj.onc.1208920

Liu, B., Chen, W., Evavold, B. D., & Zhu, C. (2014). Accumulation of dynamic catch bonds between TCR and agonist peptide-MHC triggers T cell signaling. *Cell*, *157*(2), 357–368. http://doi.org/10.1016/j.cell.2014.02.053

Liu, C., Miller, H., Orlowski, G., Hang, H., Upadhyaya, A., & Song, W. (2012). Actin reorganization is required for the formation of polarized B cell receptor signalosomes in response to both soluble and membrane-associated antigens. *Journal of Immunology (Baltimore, Md. : 1950)*, *188*(7), 3237–46. http://doi.org/10.4049/jimmunol.1103065

Liu, C., Miller, H., Sharma, S., Beaven, A., Upadhyaya, A., & Song, W. (2012). Analyzing actin dynamics during the activation of the B cell receptor in live B cells. *Biochemical and Biophysical Research Communications*, *427*(1), 202–6. http://doi.org/10.1016/j.bbrc.2012.09.046

Lotteau, V., Teyton, L., Peleraux, A., Nilsson, T., Karlsson, L., Schmid, S., … Peterson, P. (1990). Lotteau AntiCLIP invariant chain.pdf. *Nature*.

MacLennan, I. C. (1994). From the dark zone to the light. *Curr Biol*, *4*(1), 70–72. http://doi.org/S0960-9822(00)00017-8 [pii]

Mandal, K., Wang, I., Vitiello, E., Orellana, L. A. C., & Balland, M. (2014). Cell dipole behaviour revealed by ECM sub-cellular geometry. *Nature Communications*, *5*, 5749. http://doi.org/10.1038/ncomms6749

Marsh, M., & McMahon, H. T. (1999). The structural era of endocytosis. *Science*, *285*(5425), 215–220. http://doi.org/10.1126/science.285.5425.215

Martinez-Pomares, L., & Gordon, S. (2007). Antigen Presentation the Macrophage Way. *Cell*, *131*(4), 641–643. http://doi.org/10.1016/j.cell.2007.10.046

METZGER, D. W., METZGER, C. A., LING, L. A., HURST, J. S., & VAN CLEAVE, V. H. (1992). Preparative Isolation of Murine CD5 B Cells by Panning and Magnetic Beads. *Annals of the New York Academy of Sciences*, *651*(1), 75–77. http://doi.org/10.1111/j.1749-6632.1992.tb24596.x

Mitchison, N. A. (2004). T-cell–B-cell cooperation. *Nature Reviews Immunology*, *4*(4), 308–312. http://doi.org/10.1038/nri1334

Mostowy, S., & Cossart, P. (2012). Septins: the fourth component of the cytoskeleton. *Nature Reviews. Molecular Cell Biology*, *13*(3), 183–94. http://doi.org/10.1038/nrm3284

Nagasawa, T. (2006). Microenvironmental niches in the bone marrow required for B-cell development. *Nature Reviews. Immunology*, *6*(2), 107–116. http://doi.org/10.1038/nri1780

Natkanski, E., Lee, W.-Y., Mistry, B., Casal, A., Molloy, J. E., & Tolar, P. (2013). B cells use mechanical energy to discriminate antigen affinities. *Science (New York, N.Y.)*, *340*(6140), 1587–90. http://doi.org/10.1126/science.1237572

Needham, D. (1942). The adenosinetriphosphatase activity of myosin preparations. *Biochem J.*, *36*(1–2), 113–120.

Nossal, G. J., Abbot, A., Mitchell, J., & Lummus, Z. (1968). Antigens in immunity. XV. Ultrastructural features of antigen capture in primary and secondary lymphoid follicles. *The Journal of Experimental Medicine*, *127*(2), 277–90. http://doi.org/10.1084/jem.127.2.277

Nutt, S. L., Vambrie, S., Steinlein, P., Kozmik, Z., Rolink, a, Weith, a, & Busslinger, M. (1999). Independent regulation of the two Pax5 alleles during B-cell development. *Nature Genetics*, *21*(4), 390–5. http://doi.org/10.1038/7720

Obino, D., & Lennon-Duménil, A.-M. (2014). A critical role for cell polarity in antigen extraction, processing, and presentation by B lymphocytes. *Advances in Immunology*, *123*, 51–67. http://doi.org/10.1016/B978-0-12-800266-7.00001-7

Okada, T., Miller, M. J., Parker, I., Krummel, M. F., Neighbors, M., Hartley, S. B., … Cyster, J. G. (2005). Antigen-Engaged B Cells Undergo Chemotaxis toward the T Zone and Form Motile Conjugates with Helper T Cells. *PLoS Biology*, *3*(6), e150. http://doi.org/10.1371/journal.pbio.0030150

Pcr, Q. (2006). Extrafollicular Activation of Lymph. *Science*, *312*(June), 1672–1676. http://doi.org/10.1126/science.1125703

Rajewsky, K. (1996). Clonal selection and learning in the antibody system. *Nature*. http://doi.org/10.1038/381751a0

Reif, K., Ekland, E. H., Ohl, L., Nakano, H., Lipp, M., Förster, R., & Cyster, J. G. (2002).

Balanced responsiveness to chemoattractants from adjacent zones determines B-cell position. *Nature*, *416*(6876), 94–99. http://doi.org/10.1038/416094a

Riedl, J., Crevenna, A. H., Kessenbrock, K., Yu, J. H., Neukirchen, D., Bista, M., … Wedlich-Soldner, R. (2008). Lifeact: a versatile marker to visualize F-actin. *Nature Methods*, *5*(7), 605–7. http://doi.org/10.1038/nmeth.1220

Riese, R. J., Wolf, P. R., Brömme, D., Natkin, L. R., Villadangos, J. A., Ploegh, H. L., & Chapman, H. A. (1996). Essential role for cathepsin S in MHC class II - Associated invariant chain processing and peptide loading. *Immunity*, *4*(4), 357–366. http://doi.org/10.1016/S1074-7613(00)80249-6

Roche, P. a, & Cresswell, P. (1991). Proteolysis of the class II-associated invariant chain generates a peptide binding site in intracellular HLA-DR molecules. *Journal of Immunology (Baltimore, Md. : 1950)*, *187*(3), 1076–1080. http://doi.org/10.1073/pnas.88.8.3150

Rock, K. L., Haber, S. I., Liano, D., Benacerraf, B., & Abbas, A. K. (1986). Antigen presentation by hapten???specific B lymphocytes III. Analysis of the immunoglobulin???dependent pathway of antigen presentation to interleukin 1???dependent T lymphocytes. *European Journal of Immunology*, *16*(11), 1407–1412. http://doi.org/10.1002/eji.1830161115

Sabass, B., Gardel, M. L., Waterman, C. M., & Schwarz, U. S. (2008). High resolution traction force microscopy based on experimental and computational advances. *Biophysical Journal*, *94*(1), 207–20. http://doi.org/10.1529/biophysj.107.113670

Saci, A., & Carpenter, C. L. (2005). RhoA GTPase regulates B cell receptor signaling. *Molecular Cell*, *17*(2), 205–214. http://doi.org/10.1016/j.molcel.2004.12.012

Schauer, K., Duong, T., Bleakley, K., Bardin, S., Bornens, M., & Goud, B. (2010). Probabilistic density maps to study global endomembrane organization. *Nature Methods*, *7*(7), 560–566. http://doi.org/10.1038/nmeth.1462

Slot, J. W., & Geuze, H. J. (2007). Cryosectioning and immunolabeling. *Nature Protocols*, *2*(10), 2480–2491. http://doi.org/10.1038/nprot.2007.365

Song, W., Liu, C., & Upadhyaya, A. (2014). The pivotal position of the actin cytoskeleton in the initiation and regulation of B cell receptor activation. *Biochimica et Biophysica Acta*, *1838*(2), 569–78. http://doi.org/10.1016/j.bbamem.2013.07.016

Spillane, K. M., & Tolar, P. (2016). B cell antigen extraction is regulated byphysical properties of antigen presenting cells. *Journal of Cell Biology*, *2*, 1–19.

Stoddart, A., Dykstra, M. L., Brown, B. K., Song, W., Pierce, S. K., & Brodsky, F. M. (2002). Lipid rafts unite signaling cascades with clathrin to regulate BCR internalization. *Immunity*, *17*(4), 451–462. http://doi.org/10.1016/S1074-7613(02)00416-8

Suzuki, K., Grigorova, I., Phan, T. G., Kelly, L. M., & Cyster, J. G. (2009). Visualizing B cell capture of cognate antigen from follicular dendritic cells. *The Journal of Experimental Medicine*, *206*(7), 1485–93. http://doi.org/10.1084/jem.20090209

Tolar, P. (2017). Cytoskeletal control of B cell responses to antigens. *Nature Reviews Immunology*. http://doi.org/10.1038/nri.2017.67

Tolar, P., Hanna, J., Krueger, P. D., & Pierce, S. K. (2009). The constant region of the membrane immunoglobulin mediates B cell-receptor clustering and signaling in response to membrane antigens. *Immunity*, *30*(1), 44–55. http://doi.org/10.1016/j.immuni.2008.11.007

Tolar, P., Sohn, H. W., & Pierce, S. K. (2005). The initiation of antigen-induced B cell antigen receptor signaling viewed in living cells by fluorescence resonance energy transfer. *Nature Immunology*, *6*(11), 1168–1176. http://doi.org/10.1038/ni1262

Tolar, P., Sohn, H. W., & Pierce, S. K. (2008). Viewing the antigen-induced initiation of B-cell activation in living cells. *Immunological Reviews*, *221*, 64–76. http://doi.org/10.1111/j.1600-065X.2008.00583.x

Tolar, P., & Spillane, K. M. (2014). *Force generation in B-cell synapses: mechanisms coupling B-cell receptor binding to antigen internalization and affinity discrimination. Advances in immunology* (1st ed., Vol. 123). Elsevier Inc. http://doi.org/10.1016/B978-0-12-800266-7.00002-9

Treanor, B., Depoil, D., Bruckbauer, A., & Batista, F. D. (2011). Dynamic cortical actin remodeling by ERM proteins controls BCR microcluster organization and integrity. *The Journal of Experimental Medicine*, *208*(5), 1055–68. http://doi.org/10.1084/jem.20101125

Treanor, B., Depoil, D., Gonzalez-Granja, A., Barral, P., Weber, M., Dushek, O., … Batista, F. D. (2010). The membrane skeleton controls diffusion dynamics and signaling through the B cell receptor. *Immunity*, *32*(2), 187–99. http://doi.org/10.1016/j.immuni.2009.12.005

Tsai, F.-C., Kuo, G.-H., Chang, S.-W., & Tsai, P.-J. (2015). Ca²⁺ signaling in cytoskeletal reorganization, cell migration, and cancer metastasis. *BioMed Research International*, *2015*. http://doi.org/10.1155/2015/409245

Tsai, F. C., & Meyer, T. (2012). Ca 2+ pulses control local cycles of lamellipodia retraction and adhesion along the front of migrating cells. *Current Biology*, *22*(9), 837–842. http://doi.org/10.1016/j.cub.2012.03.037

Vascotto, F., Lankar, D., Faure-Andre, G., Vargas, P., Diaz, J., Le Roux, D., … Lennon-Dumenil, A. M. (2007). The actin-based motor protein myosin II regulates MHC class II trafficking and BCR-driven antigen presentation. *J Cell Biol*, *176*(7), 1007–1019. http://doi.org/jcb.200611147 [pii]\r10.1083/jcb.200611147

Vicente-Manzanares, M., Ma, X., Adelstein, R. S., & Horwitz, A. R. (2009). Non-muscle myosin II takes centre stage in cell adhesion and migration. *Nature Reviews. Molecular Cell Biology*, *10*(11), 778–90. http://doi.org/10.1038/nrm2786

Wan, Z., Chen, X., Chen, H., Ji, Q., Chen, Y., Wang, J., … Liu, W. (2015). The activation of IgM- or isotype-switched IgG- and IgE-BCR exhibits distinct mechanical force

sensitivity and threshold. *eLife*, *4*(August), 1–24. http://doi.org/10.7554/eLife.06925

Wan, Z., Zhang, S., Fan, Y., Liu, K., Du, F., Davey, A. M., … Liu, W. (2013). B cell activation is regulated by the stiffness properties of the substrate presenting the antigens. *Journal of Immunology (Baltimore, Md. : 1950)*, *190*(9), 4661–75. http://doi.org/10.4049/jimmunol.1202976

Wang, X., & Ha, T. (2013). Defining single molecular forces required to activate integrin and notch signaling. *Science (New York, N.Y.)*, *340*(6135), 991–4. http://doi.org/10.1126/science.1231041

Weber, M., Treanor, B., Depoil, D., Shinohara, H., Harwood, N. E., Hikida, M., … Batista, F. D. (2008). Phospholipase C-gamma2 and Vav cooperate within signaling microclusters to propagate B cell spreading in response to membrane-bound antigen. *The Journal of Experimental Medicine*, *205*(4), 853–868. http://doi.org/10.1084/jem.20072619

Wickstead, B., & Gull, K. (2011). The evolution of the cytoskeleton. *Journal of Cell Biology*, *194*(4), 513–525. http://doi.org/10.1083/jcb.201102065

Yuseff, M.-I., Reversat, A., Lankar, D., Diaz, J., Fanget, I., Pierobon, P., … Lennon-Duménil, A.-M. (2011). Polarized secretion of lysosomes at the B cell synapse couples antigen extraction to processing and presentation. *Immunity*, *35*(3), 361–74. http://doi.org/10.1016/j.immuni.2011.07.008

Zhang, S., Zhou, X., Lang, R. A., & Guo, F. (2012). RhoA of the Rho family small GTPases is essential for B lymphocyte development. *PLoS ONE*, *7*(3). http://doi.org/10.1371/journal.pone.0033773